Title
Synthesis of Linear Distributed Control and Coupled Oscillators with Multiple Limit Cycles

Author
Ren, Kewei

Publication Date
2021

Peer reviewed|Thesis/dissertation

UNIVERSITY OF CALIFORNIA

Los Angeles

Synthesis of Linear Distributed Control and Coupled Oscillators with Multiple Limit Cycles

A dissertation submitted in partial satisfaction
of the requirements for the degree
Doctor of Philosophy in Aerospace Engineering

by

Kewei Ren

2021

ABSTRACT OF THE DISSERTATION

Synthesis of Linear Distributed Control and
Coupled Oscillators with Multiple Limit Cycles

by

Kewei Ren
Doctor of Philosophy in Aerospace Engineering
University of California, Los Angeles, 2021
Professor Tetsuya Iwasaki, Chair

This dissertation presents a synthesis scheme of distributed controller for continuous time, finite dimensional, linear time-invariant systems. We show that under the assumption that the interconnection of the control units is characterized by a strongly connected directed graph, any centralized controller admits a distributed synthesis with an arbitrary accuracy. This idea applies to a wide variety of control problems such as observer design, stabilizing control, eigenstructure assignment, etc. We further specialize our theories for multi-agent systems with local observability and propose a lower order distributed controller with internal model to achieve eigenstructure assignment. Then by replacing the linear internal model by a nonlinear oscillator network, we show the potential of nonlinear distributed control to achieve pattern formation with the amplitude stabilized. Next, we consider the design of nonlinear oscillator network with linear coupling to have a stable limit cycle with prescribed oscillation profile. We give the sufficient conditions for the orbital stability of the limit cycle. Moreover, we demonstrate that the embedding of multiple limit cycles into the oscillator network is possible. Finally, we consider the design of nonlinear oscillator network with

nonlinear coupling to overcome some limitations of the linearly coupled oscillators. Likewise, conditions for the orbital stability of multiple limit cycles are provided.

The dissertation of Kewei Ren is approved.

Lieven Vandenberghe

Tsu-Chin Tsao

Jason L. Speyer

Tetsuya Iwasaki, Committee Chair

University of California, Los Angeles

2021

TABLE OF CONTENTS

LIST OF FIGURES

ACKNOWLEDGMENTS

I would like to thank my advisor, Professor Iwasaki, for the guidance in my academic life and the training I received during my Ph.D. years. My research achievements are the outcomes of your intellegence, knowledge, patience and understanding. I am grateful for Professor Speyer, Professor Tsao, and Professor Vandenberghe, among other professors, for offering great lectures and imparted to me knowledge about control and optimization, building the foundational block for my research. Special thanks to Professor M'Closkey, for his impeccable teaching as well as for offering me teaching assistantships. I also appreciate for the support from my friends at UCLA with whom I had a great time during my years in Los Angeles. Finally, I must thank my family for the financial and mental support over the Pacific ocean.

VITA

2015 B.S. (Aerospace Engineering), Beihang University.

PUBLICATIONS

Kewei Ren and Tetsuya Iwasaki. "Design of Complex Oscillator Network with multiple Limit Cycles." In *2018 IEEE Conference on Decision and Control (CDC)*, pp. 115–120. IEEE, 2018

Kewei Ren and Tetsuya Iwasaki. "A Network of Nonlinearly Coupled Oscillators with Multiple Limit Cycles." (In Preparation)

Kewei Ren and Tetsuya Iwasaki. "Distributed Synthesis of Linear Controllers." (In Preparation)

CHAPTER 1

Introduction

Our research originates from the study of the control of biological locomotion based on central pattern generators (CPGs). In a nutshell, a CPG is a neuronal network capable of producing periodic signals, which serve as the references for animal locomotion. A CPG interacts with the animal body as well as the environment, adjusting its output accordingly. It is observed that multiple locomotion gaits can be encoded into a CPG. Moreover, the distributed structure of CPGs results in a distributed control strategy. In engineering applications, CPGs are often modeled as coupled oscillators. Our objective is to provide analytical control methods that have all the advantages CPGs possess. To that end, we need to resolve the problem of distributed control for general plants. Also, we would like to have a CPG model convenient for engineering applications. For these reasons, we review the state of the art of several relevant research fields in the coming sections.

1.1 Distributed Control

Over the past few decades we have witnessed a significant growth in complex systems that feature special spatial structures. These systems may comprise spatially distributed units that interact with their neighbors through a communication network. Other scenarios include distributed placement of sensors and/or actuators. Typical examples are autonomous underwater vehicles (AUVs), unmanned aerial vehicles (UAVs), mobile robot swarm, formation flight, constellation satellites, smart grid, automated highway systems, to name a few. For these systems, we seek effective and efficient methods to achieve some desired dynamical

behavior by exploiting their special structure, including, for example, rendering the system stable or embedding periodic motions into the system. Increasing demand in systems with aforementioned features gives rise to the interest in novel control theories that utilize well the distributed nature. We review some of the recent results here.

In [BPD02], the control problems for systems that are described by PDEs are considered. A key property of the systems dealt with in the paper is spatial invariance, which allows designing quadratically optimal controllers for infinite dimensional systems by solving finite dimensional problems for a family of parametrized systems over frequency. The resulting controller admits a localized structure and hence can be implemented in a distributed manner. [DD03] tackles control problems for spatially discrete, interconnected systems that are composed of identical building blocks. Specifically, two types of interconnection are considered: periodic interconnection and infinite interconnection. The controller in the paper is assumed to have the same distributed architecture as the system. Then the well-posedness, stability, performance are analyzed for the closed-loop system. The resulting conditions are given in terms of linear matrix inequalities (LMIs). Following similar ideas and approaches, [LCD04] proposes a convex characterization of controller synthesis for systems of heterogeneous units interconnected over an arbitrary graph. Inspired by dissipativity theory, the results are expressed as a set of coupled LMIs. Again, the controller is assumed to have the same topology as the interconnected subsystems. The notion of "quadratic invariance" introduced in [RL05] indicates that, integrated with Youla parametrization, the constraints on the controller structure can be preserved under feedback and the controller synthesis can be solved via convex programming. This gives a very general framework of decentralized controller synthesis. However, for strongly connected systems, it fails to provide a convex characterization of localized controllers [ADL19]. The System Level Synthesis (SLS) approach [ADL19] formulates a novel parameterization of internally stabilizing controllers by looking at the closed-loop responses of the system rather than the input/output map of the controller itself. Moreover, SLS is able to constrain the closed-loop response to be in arbitrary

sets. And if the constraints admit a convex representation, the resulting system responses will also admit a convex representation. Any constraints on the system response impose a corresponding constraint on the structure of the controller. Specifically, the structural constraints on the system response carries over to the internal realization of the controller. The distributed structure of the resulting controller is achieved by imposing locality constraints on the system response. This method, however, requires selection of basis transfer functions, which may not be trivial. The design of distributed Luenberger observer is considered in [KSC16], where local observers process local measurements and communicate via a undirected, connected graph. They altogether estimate the plant state under the assumption of joint observability. The conditions on the controller gains are derived by an appropriate Lyapunov function. [HTW18] borrows some of the ideas of [KSC16] and considers a strongly connected directed graph instead. The resulting algorithmic procedure to compute a distributed observer is based on solving LMIs. In addition to stabilizing control, there are also works focusing on distributed output regulation of linear multi-agent systems, such as [SH11, SRA16].

As we can see, there are plenty of results for distributed control of multi-agent systems. Also, the control of spatially distributed plants with spatial invariance can be approached in a distributed manner. For general plants not categorized wht special structure, [ADL19] provides a flexible design framework with full parametrization, but the search space is infinite dimensional. A finite dimensional approach for general plants is in demand.

1.2 Central Pattern Generators

An application that inevitably relates itself to distributed control is the control of coordinated periodic motions. Periodic motions are prevalent in nature, e.g., heart beat, respiration, circadian rhythm, animal locomotion, pendulum, waves, etc. Such motions are often coordinated to have a common frequency with specific relative phase pattern for various

spatial parts. Control theories to achieve coordinated oscillations are of great significance and have many potential applications. For example, development of assistive devices would require such control methods to help human with rhythmic activities such as walking, mastication, respiration, etc. Moreover, it may suggest new medical treatments for certain diseases which are pathologically related to some known or unclear coordinated behaviors of neural oscillations, e.g., Parkinson's disease. Many industrial robots operate in coordinated periodic motions, for which control mechanisms to make the production efficient and reliable are desired. Cooperative tasks for multi-agent systems, such as autonomous underwater vehicles (AUVs), unmanned aerial vehicles (UAVs), mobile robot swarm, formation flight, and constellation of satellites, also involve feedback control to achieve coordination.

A representative example of rhythmic behaviors, animal locomotion, has been extensively studied [FK99, BTS00, DFF00, Gri06, HFK06]. Periodic body movements during locomotion are controlled by the Central Pattern Generators (CPGs). CPGs are neuronal networks that can autonomously generate rhythmic coordinated patterns without receiving rhythmic inputs from sensory feedback or higher control center [Ijs08], and function to produce adaptive rhythmic behaviors with sensory feedback [ICF14]. Neural CPG circuits are found in both invertebrates and vertebrates, including lamprey [CW80], salamander [DBD99], leech [JCF05, ZFI07]. CPGs have several features useful for engineering applications. They are capable of producing coordinated oscillation patterns for many variables, and the pattern can be changed by simply tuning several parameters, which greatly reduces complexity/dimensionality of the problem. In fact, it is possible to embed multiple limit cycle oscillations into a single CPG, which is an instrumental property for some behaviors such as gait transition in animal locomotion. Moreover, the rhythmic patterns a CPG generates are stable and robust due to the orbital stability property of the limit cycles. Since a CPG is essentially a network of neurons interconnected with each other, it provides a framework for feedback control with a distributed sensing and actuation. These features make the CPG an excellent platform for control designs to achieve periodic, coordinated movements.

Some CPG models in biology [HGL92, TBL93] are based on the detailed dynamics of neuronal cell membranes using the celebrated Hodgkin-Huxley electrical circuit [HH52]. To simplify the Hodgkin-Huxley model and reduce computational burden, two-variable neuron models have been proposed such as the FitzHugh-Nagumo, the Morris-Lecar, and the Hindmarsh-Rose models [KS98]. Further simplifications are possible when the neuronal interactions are not mediated by action potentials [ZFI07], or the model variable represents the frequency of neural spikes [Mat85]. Based on such simple models, some CPGs with particular connectivity structure are modeled and their oscillation patterns are analyzed by simulations [Mat85, Mat87]. In [Iwa08], CPGs with a general interconnection architecture are analyzed by the multivariable harmonic balance (MHB), analytical insights are provided on how the oscillation profile (frequency, amplitudes, phases) is specified by the eigenstructure of the connectivity matrix.

Another perspective on CPG modeling is somewhat more abstract, based on the framework of coupled nonlinear oscillators. The focus of this type of modeling is on how the coupling topology determines the coordination pattern for populations of neurons [GS03]. Extensively studied models include the phase coupled oscillators [BI04a, CHR82, KEW91, SJK90], which provide a powerful tool for analyses, but have not been found useful for designs. On the other hand, networks of Andronov-Hopf oscillators (AHOs) [PS07] and their variations [LI17] have been found useful for engineering design applications. For instance, an adaptive frequency AHO is proposed [BI04b, RBI06] to learn the frequency of a periodic input signal, and is used to design a programmable CPG for bipedal locomotion [RI06]. The AHO has also been used as a basic control unit with sensory feedback to achieve synchronization [SCS10] and natural oscillations [ZI17].

Despite the progress made in the past decades, there are still many shortcomings among the existing CPG models. The theory on the relationship between the oscillation pattern and neuronal connectivity is incomplete for the simple oscillators in [Mat85, Mat87] due to the lack of generality in the network architecture. The MHB analysis in [IZ06] provides a

practically effective method for designing CPGs, but stability of the oscillation cannot be guaranteed due to the approximate nature of the analysis. In [PS07], global convergence to synchronized oscillations is proved for AHOs with diffusive coupling based on the contraction theory, which is an interesting result. However, when one desires to embed multiple limit cycles in a CPG for a variety of behaviors, convergence has to be local. Most of the CPG models in the literature have a fixed temporal waveform, e.g., a sinusoid as in AHOs. A general method for achieving an arbitrary temporal shape is developed in [RI06] by superposing outputs of multiple AHOs to form a Fourier series. While the idea is interesting and the method is effective, this CPG model lacks a rigorous stability proof, and its complexity grows with the number of Fourier terms. Thus, there is no single CPG model that encompasses the issues of multiple limit cycles, temporal waveform, and rigorous stability proof.

1.3 Coupled Oscillators

To achieve periodic motions for a physical system, one could design a feedback regulator to track an oscillatory command. The oscillatory command can be generated by an oscillator since oscillators naturally embed periodic patterns. Also, it is desirable to be able to switch to a different pattern when the environment or task changes. For example, a locomotive robot switches between different gaits. Moreover, a distributed structure is preferred since in some cases spatial constraints are present. Thus, a multi-pattern oscillator with distributed structure is of great interest.

In the mathematical language, the problem is to design a dynamical system, $\dot{\mathbf{x}}(t) = f(\mathbf{x}(t), t),\ \mathbf{x} \in \mathbb{R}^n,\ f : \mathbb{R}^n \times \mathbb{R} \mapsto \mathbb{R}^n$, that has a periodic solution of desired properties. For analyzing the periodic solutions of generic oscillatory systems, general methods include Floquet theory, Poincaré maps, etc., can be exploited, and the existence as well as the stability can be proved either numerically or analytically if possible. When $f(\mathbf{x}(t), t)$ exhibits weak nonlinearity, the method of harmonic balance is helpful by approximating the system

to be a linear system [Iwa08]. This approach establishes the correspondence between the structure of the coupled oscillator network and the resulting oscillation profile. However, the stability is not guaranteed and the oscillation profile cannot be achieved accurately due to the nature of harmonic approximation. These theories are mainly for ensuring the stability of limit cycles. In order to implement a distributed architecture, we need additional ideas such as a network structure, and the associated theories to cope with them.

The network of coupled subsystems is a good framework for distributed architecture. The advances in the consensus/synchronization problems of multi-agent systems offer some great instructions on the distributed structure using graph theory. In this framework, each agent has its own dynamics, while receiving signals from neighboring agents. The communication between agents is defined by a graph. Based on the dynamics of individual agents and the connectivity across agents, various theories are developed for specific models. For example, the agents can be homogeneous with identical dynamics [OM04, Ren08, SS09]; also they can be heterogeneous with dynamics differing from agent to agent [WSA11, KSS10]. The agents can be oscillators [BRI06], which are able to produce periodic signals without the inputs from other agents. Also, agents can be non-oscillatory, but may start to show rhythmic motion if coupled properly with others [ZCM15]. The coupling between agents may be linear [SAJ13] or nonlinear [PPS18], and the coupling strength may be strong or weak. Moreover, the topology may be structured or unstructured. Some of these properties can be exploited, as will be explained in the paragraphs that follow.

When the agents are homogeneous, the method of master stability equation can be employed to ensure local stability [PC98, HTI14]. Master stability equation is developed as a general method for the synchronization of homogeneous dynamical systems for which a common function is used to form the coupling term with neighboring systems. It linearizes the coupled system around the synchronization manifold, and shows the linearized dynamics can be decoupled into separated linear systems of smaller dimension, each of which has one parameter determined by the connectivity matrix. Therefore the stability of the syn-

chronization manifold boils down to the stability of these low dimensional linear systems. This method is powerful for synchronization and also for coordination with a coordinate transformation if the system exhibits flow invariance. The limitation, nonetheless, is that the coupling between the variables of different oscillators is assumed to be uniform. This limitation reduces the design freedom which is important when one explores the possibilities for multiple limit cycles.

If the coupling is weak, the coupled oscillators can be reduced to phase-coupled oscillators. Approaches developed for phase-coupled oscillators can be utilized for synchronization/coordination [Kur75, EK84, IK06, DB14]. While the framework of phase-coupled oscillators is powerful for analysis of various models in many engineering and science fields, there lacks a good paradigm for design given desired oscillation profiles. Another drawback of this architecture is that the frequencies of the oscillators converge to a common value. Thus it is not possible to have multiple limit cycles with various frequencies.

When the coupling is strong, the theory of contraction/semi-passivity can be adopted to obtain conditions for global stability [PN01, PSN02, LS98, WS05, PS07]. This theory extends Lyapunov theory to the case of convergence to a flow-invariant subspace. Unfortunately the global stability to a limit cycle ensured by this approach eliminates the existence of extra limit cycles.

Having capability of generating multiple patterns and transition between them is desired in many applications such as the gait transition in robotics. There are several ways to achieve multiple gaits. Most of the methods in the literature define the gait in terms of duty ratio of the swing/stance phases of limbs and phase differences between limbs [SM11]. The duration of swing and stance phases is controlled by the period of the oscillation of the same oscillator network with different configuration or different oscillator networks. To define a new gait, simply the duty ratio of stance/swing phases is modified and the timing of the onset to the swing/stance phases for different limbs during a cycle is changed as well. However, this approach involves a lot of heuristics and manual parameter tuning hence no stability

is guaranteed. Another strategy is to have multiple limit cycles embedded in one oscillator network, using additional structure to impose the convergence to a specific limit cycle. For a linear system with multiple oscillatory modes, a potential function can be designed to control which mode it exhibits based on the 'energy' of that mode [IYA03]. But the design of the potential function is case-by-case and heuristic. The stability is not proved either. Having multiple limit cycles embedded in a single system may be advantageous for achieving adaptive gait transition based on the environmental change in an autonomous manner. Switching the parameter values for gait transition may create some stability problem and convergence may not be guaranteed. But having multiple stable limit cycles would avoid this instability issue.

The review on existing methods indicates that we have to carefully pick the coupling strength between oscillators to accommodate our needs. The coupling cannot be too strong because the theory of contraction suggests it would result in global stability which disables multiple limit cycles. The coupling cannot be too weak either since the study on phase coupled oscillators suggests that the frequency of the oscillators will synchronize.

The problem of distributed structure for multiple patterns has not been addressed, although the solution to distributed structure problem has been well established for a single limit cycle case using graph Laplacian. But the idea does not apply to multiple limit cycle case. The only eigenvalue at the origin along with the corresponding eigenvector essentially specifies the synchronization condition. When there is an additional pattern to be achieved, an extra eigenvalue at the origin with a different eigenvector is imposed. Then this will violate the spanning tree structure which is the key to the stability of the synchronization.

1.4 Notations

We use the following notations. $\mathbb{I}_n$ is defined as the integer set modulo n, $\mathbb{I}_n := \{1, 2, \ldots, n\}$. The imaginary unit is denoted by $j := \sqrt{-1}$. $\Re[\cdot], \Im[\cdot]$ denote the real and imaginary parts of a complex number, respectively. Vectors are denoted by boldface, lowercase letters, while

uppercase letters are used for matrices. For a vector $\mathbf{v} \in \mathbb{C}^n$, v_i denotes the i^{th} entry. The transpose and complex conjugate of $\mathbf{x}$ are denoted by $\mathbf{v}^\mathsf{T}$ and $\bar{\mathbf{v}}$, respectively, and define $\mathbf{v}^* := \bar{\mathbf{v}}^\mathsf{T}$. $\text{col}(\cdot)$ means a vertical concatenation of the entries. The diagonal matrix with entries v_i is denoted by $\text{diag}(v_1, \ldots, v_n)$ or $\text{diag}(\mathbf{v})$. For a scalar x and vector $\mathbf{y}$, the notation $\mathbf{z} = x + \mathbf{y}$ means that $z_i = x + y_i$. For vectors $\mathbf{x}$ and $\mathbf{y}$, the notation $\mathbf{z} = \mathbf{x} \cdot \mathbf{y}$ means elementwise multiplication, i.e., $z_i = x_i y_i$. $\mathbf{1}$ is the vector with all entries being 1. The Kronecker product is denoted by $\otimes$. Functions sin, cos, exp, and absolute value $|\cdot|$ act on the argument elementwise, e.g. $|\mathbf{z}|$ is a vector with entries $|z_i|$. $L = [\ell_{ij}]$ represents the matrix L with ℓ_{ij} being the $(i,j)^{\text{th}}$ entry. The Moore-Penrose inverse of a matrix X is denoted by $X^\dagger$. $\text{eig}(X)$ is the set of eigenvalues of X. For a transfer function $P(s)$, $\|P\|_{H_2}$, $\|P\|_{H_\infty}$, $\|P\|_{L_\infty}$ are its H_2 norm, H_∞ norm, L_∞ norm, respectively. For a matrix X, $X \prec 0$, $X \preceq 0$, $X \succ 0$, $X \succeq 0$ indicate that X is negative definite, negative semidefinite, positive definite, positive semidefinite, respectively. We also use the set $\mathbb{R}^n_{++}$ to imply an $n \times n$ matrix in this set is positive definite whenever convenient.

CHAPTER 2

Distributed Synthesis of Linear Control for Stability and Performance

2.1 Problem Formulation

2.1.1 Problem Statement

In this chapter, we discuss the problem of synthesizing a linear stabilizing control in a distributed fashion. Given a generalized LTI plant,

$$\begin{bmatrix} \mathbf{z} \\ \mathbf{y} \end{bmatrix} = G(s) \begin{bmatrix} \mathbf{w} \\ \mathbf{u} \end{bmatrix}, \tag{2.1}$$

where $\mathbf{z}$ is the performance output, $\mathbf{y}$ the measured output, $\mathbf{w}$ the exogenous input containing disturbance, reference, etc, $\mathbf{u}$ the control input, and $G(s)$ the transfer function. Oftentimes the measured output of the plant is partitioned into several channels and so is the control input,

$$\mathbf{y} = \mathrm{col}(\mathbf{y}_1, \ldots, \mathbf{y}_q), \quad \mathbf{u} = \mathrm{col}(\mathbf{u}_1, \ldots \mathbf{u}_q), \tag{2.2}$$

where the local actuation $\mathbf{u}_i$ and the local measurements $\mathbf{y}_i$ are vectors or scalars and q is the number of channels. If the partition of input and output is ignored, a stabilizing output feedback controller can be synthesized using various existing control methods,

$$\mathbf{u} = K(s)\mathbf{y}. \tag{2.3}$$

Let the closed-loop system be denoted by $\mathbf{z} = H(s)\mathbf{w}$ and assume that $H(s)$ is stable. Now we must take into consideration the constraints on the input and output structure and thereby seek a distributed synthesis of the controller in the following form

$$\begin{bmatrix} \mathbf{u}_i \\ \mathbf{v}_i \end{bmatrix} = K_i(s) \begin{bmatrix} \mathbf{y}_i \\ \mathbf{h}_i \end{bmatrix}, \quad \mathbf{h}_i = \eta \sum_{j \in \mathbb{N}_i} \ell_{ij} \mathbf{v}_j, \tag{2.4}$$

where $\mathbb{N}_i$ is the set of indices specifying the "neighbors" of the i^{th} control unit. Each control unit only picks up local information from the plant, and generates local control input. The communication between neighboring control units is reflected in the signals $\mathbf{v}_i$. The i^{th} control unit receives from neighbors a weighted sum of $\mathbf{v}_j$. Also we make explicit the coupling strength η, which is a common parameter, for convenience. Let the closed-loop system of this controller and the generalized plant $G(s)$ be denoted by $\mathbf{z} = H_\eta(s)\mathbf{w}$. Figure 2.1 shows the schematics for closed-loop systems. We would naturally wonder if we are able to find such a distributed controller that performs similarly to the controller (2.3) which is yielded without any consideration of distributed structure. The formal statement of the problem is given as follows.

Problem 1. Let $G(s)$ in (2.1) and $K(s)$ in (2.3) be given such that the closed-loop system $\mathbf{z} = H(s)\mathbf{w}$ is stable. Let the control input $\mathbf{u}$ and measured output $\mathbf{y}$ be partitioned as in (2.2), and consider the sets $\mathbb{N}_i$ with $i \in \mathbb{I}_q$. For a given scalar $\varepsilon > 0$, find a distributed controller of the form (2.4) such that the resulting closed-loop system $\mathbf{z} = H_\eta(s)\mathbf{w}$ is stable and satisfies $\|H - H_\eta\|_\infty < \varepsilon$. □

We assume that the sets of neighbors $\mathbb{N}_i$ are given such that the corresponding network graph, as we will define in a later section, is strongly connected. Under this assumption, the problem turns out to be feasible for an arbitrary $\varepsilon > 0$ as we show later.

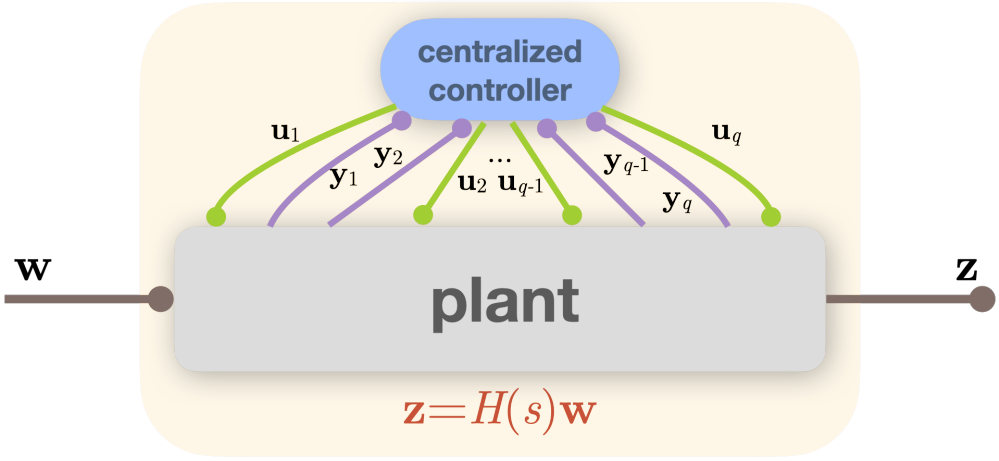

(a)

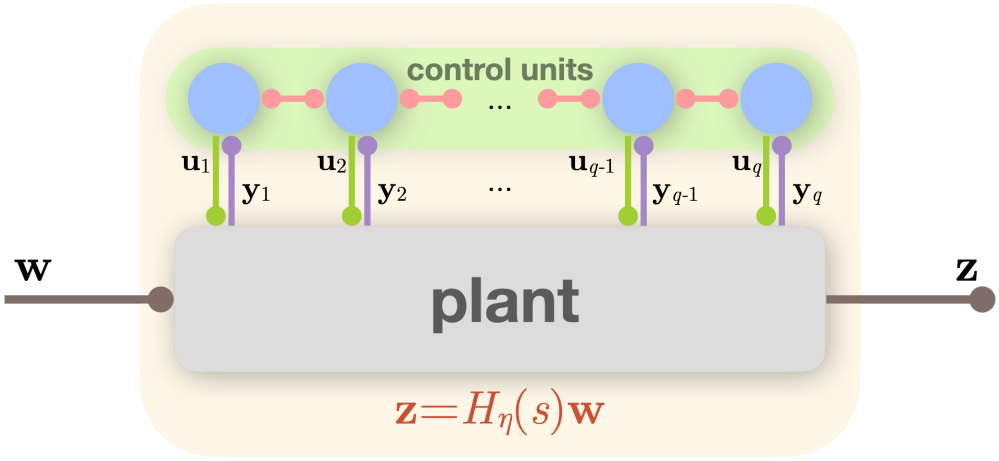

(b)

Figure 2.1: Schematics for the closed-loop systems: (a) centralized control; (b) distributed control.

2.1.2 Controller Architecture

As a special class of the distributed controller in (2.4), we consider the following state space model,

$$\begin{aligned}\dot{\hat{\mathbf{x}}}_i &= A_i\hat{\mathbf{x}}_i + qF_i\mathbf{y}_i + G_i\mathbf{z}_i, \quad i \in \mathbb{I}_q,\\ \mathbf{z}_i &= \eta\sum_{j\in\mathbb{N}_i}\ell_{ij}(\hat{\mathbf{x}}_j - \hat{\mathbf{x}}_i),\\ \mathbf{u}_i &= K_i\hat{\mathbf{x}}_i.\end{aligned} \tag{2.5}$$

Let us define a matrix L by specifying its $(i,j)^{\text{th}}$ entry as ℓ_{ij}. The above model is independent of the diagonal entries ℓ_{ii} but we choose them so that $L\mathbf{1} = 0$ for technical convenience. The matrix L then represents a directed graph, which is defined in the subsequent section, that specifies the distributed structure of the control units. The i^{th} control unit has state $\hat{\mathbf{x}}_i$, takes in the input $\mathbf{y}_i$, communicates with neighboring subsystems through a network whose topology is characterized by L and coupling strength by η, and outputs $\mathbf{u}_i$.

Taking the Laplace transform for a control unit (2.5),

$$\hat{\mathbf{x}}_i = qM_i(s)F_i\mathbf{y}_i + M_i(s)G_i\mathbf{z}_i, \quad M_i(s) := (sI - A_i)^{-1}.$$

Here with a slight abuse of notation we denote by the same letter both the signal in time and s-domain. The structure of a control unit in s-domain can be illustrated by the block diagram in Figure 2.2.

In the matrix form,

$$\begin{aligned}\hat{\mathbf{x}} &= q\mathsf{M}(s)\mathsf{F}\mathbf{y} + \mathsf{M}(s)\mathsf{G}\mathbf{z},\\ \mathbf{z} &= \eta\mathsf{L}\hat{\mathbf{x}},\\ \mathbf{u} &= \mathsf{K}\hat{\mathbf{x}},\end{aligned} \tag{2.6}$$

where $\mathsf{M}(s)$, F, G, and K are block diagonal matrices with $M_i(s)$, F_i, G_i, and K_i on the diagonal, and

$$\mathsf{L} := L \otimes I.$$

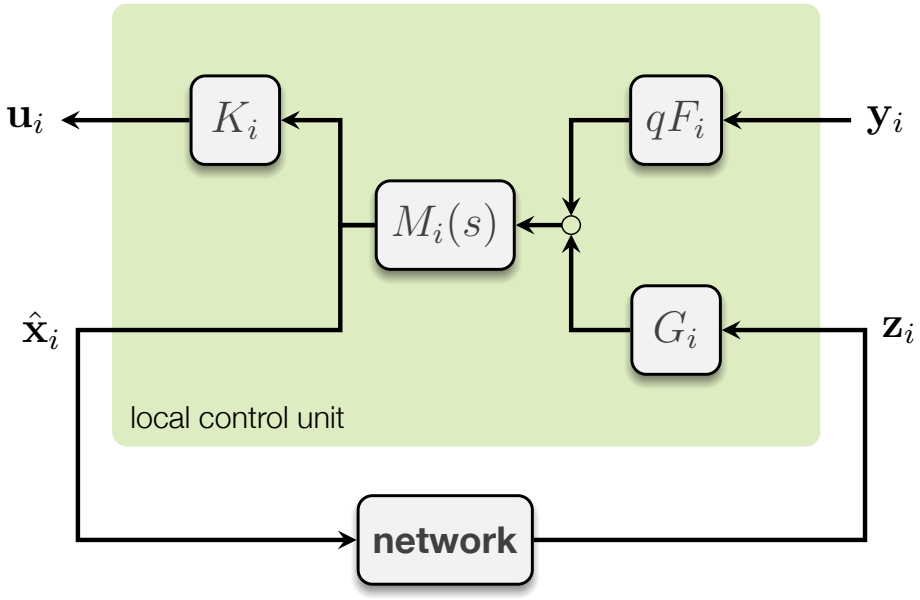

Figure 2.2: Block diagram of the local control unit.

Subsequently, we obtain the mapping from $\mathbf{y}$ to $\mathbf{u}$,

$$\mathbf{u} = q\mathsf{K}\left(I - \eta\mathsf{M}(s)\mathsf{GL}\right)^{-1}\mathsf{M}(s)\mathsf{F}\mathbf{y}. \tag{2.7}$$

2.2 Approach

2.2.1 Review of Graph Theory

A natural and convenient tool to describe the interconnection between distributed control units is a graph. A graph $\mathcal{G}$ of q interconnected vertices is defined as an ordered pair of two sets, $\mathcal{G} = (\mathcal{V}, \mathcal{E})$, where $\mathcal{V} = \{\, v_i \mid i \in \mathbb{I}_q \,\}$ is the set of vertices and $\mathcal{E} \subseteq \{\, e_{ij} = (v_i, v_j) \mid (v_i, v_j) \in \mathcal{V} \times \mathcal{V}, v_i \neq v_j \,\}$ is the set of edges. An edge e_{ij} belongs to $\mathcal{E}$ only when v_i and v_j are connected. To further examine the connection between edges, we define a directed graph. A directed graph is defined as a graph in which edges have directions. An edge e_{ij} belongs to $\mathcal{E}$ of a directed graph only when there is an edge pointing from v_j to v_i [1].

[1] This may not align with the conventional definition, but serves out purposes in the sequel.

A path from a vertex $v_0 \in \mathcal{V}$ to another vertex $v_k \in \mathcal{V}$ is a sequence of vertices $(v_0, \ldots, v_k)$ such that the edge $(v_i, v_{i+1}) \in \mathcal{E}$ for all $0 \leq i \leq k-1$. The graph $\mathcal{G}$ is said to be strongly connected if for any two distinct vertices $v_i, v_j \in \mathcal{V}$, there is a path from v_i to v_j and a path from v_j to v_i. We further associate each edge e_{ij} with a weight a_{ij}. And in this dissertation, we restrict a_{ij} to be positive. Define the Laplacian matrix $L = [\ell_{ij}] \in \mathbb{R}^{q \times q}$ of the graph $\mathcal{G}$ as follows,

$$\ell_{ij} = \begin{cases} -a_{ij} & i \neq j, \\ \sum_{j=1}^{q} a_{ij} & i = j. \end{cases}$$

We immediately see that $L\mathbf{1} = 0$.

Lemma 1 ([OM04, RBM05, YCC09])**.** *Consider a network with a directed graph specified by Laplacian matrix $L \in \mathbb{R}^{q \times q}$. Suppose the network is strongly connected with positive weights (i.e., $\ell_{ij} < 0$ for connected edges). Then there exists a vector $\mathbf{r} \in \mathbb{R}^q$ such that $\mathbf{r}^\mathsf{T} L = 0$ and $r_i > 0$ for all $i \in \mathbb{I}_q$. Moreover, we have*

$$Q := RL + (RL)^\mathsf{T} \succeq 0, \quad Q\mathbf{1} = 0, \quad R := \operatorname{diag}(\mathbf{r}),$$

with the dimension of the null space of Q being one. □

Remark 1. As noted in [HTW18], RL is the Laplacian matrix of the balanced directed graph obtained by adjusting the weights of the original graph. While the matrix Q is the Laplacian matrix of the undirected graph obtained by uniting the edges of a vertex pair in this balanced directed graph. This undirected graph is called the mirror of the balanced graph [OM04]. □

Define

$$J := \operatorname{col}(I, \ldots, I), \tag{2.8}$$

and N is such that the columns form an orthonormal basis for the null space of J^T. We have

$$\begin{bmatrix} \frac{1}{q} J^\mathsf{T} \\ N^\mathsf{T} \end{bmatrix} \begin{bmatrix} J & N \end{bmatrix} = I. \tag{2.9}$$

J and N will be used frequently in this dissertation for a coordinate transformation, so that the average dynamics of the connected systems can be isolated.

Lemma 2. *Suppose L is the Laplacian matrix of a strongly connected directed graph with positive weights and $\mathsf{L} := L \otimes I$, where I is an $n \times n$ identity matrix. Let $\mathbf{r}$ be a positive vector such that $\mathbf{r}^\mathsf{T} L = 0$, and r_i be the i^{th} entry of $\mathbf{r}$. Given a positive definite matrix $X \in \mathbb{R}^n_{++}$. Define $G_i = r_i X$ for $i \in \mathbb{I}_q$, and G to be the block diagonal matrix with G_i on the diagonal. Let J and N be defined as in (2.8) and (2.9). Then $\mathcal{H} := -N^\mathsf{T} \mathsf{G}\mathsf{L} N$ is Hurwitz.* □

Proof. Since $G_i := r_i X$ and $\mathsf{L} := L \otimes I$, we have

$$\mathsf{G}\mathsf{L} = (R \otimes X)(L \otimes I) = (RL) \otimes X,$$

where $R := \operatorname{diag}(\mathbf{r})$. This indicates that the eigenvalues of $\mathsf{G}\mathsf{L}$ are $\lambda_i \mu_j$, where $\lambda_i, i \in \mathbb{I}_q$ are the eigenvalues of RL and $\mu_j, j \in \mathbb{I}_n$ are the eigenvalues of X. Therefore $-\mathsf{G}\mathsf{L}$ has the eigenvalue decomposition

$$(-\mathsf{G}\mathsf{L}) \begin{bmatrix} J & N \end{bmatrix} = \begin{bmatrix} J & N \end{bmatrix} \begin{bmatrix} 0 & \\ & \mathcal{H} \end{bmatrix}, \quad \mathcal{H} := -N^\mathsf{T} \mathsf{G}\mathsf{L} N.$$

The fact $L\mathbf{1} = 0$ implies that $\mathcal{H}$ is Hurwitz. ■

2.2.2 Basic Idea for Distributed Synthesis

We are interested in the mapping from $\mathbf{y}$ to $\mathbf{u}$ of the distributed controller as in (2.7) where each control unit in general is a dynamical system, i.e., $M_i(s)$ are transfer functions. It is, however, a good practice to start off investigating the case where the mapping is static. As such, we assume $M_i(s) = M_i$ are constant matrices for all $i \in \mathbb{I}_q$. The static mapping from $\mathbf{y}$ to $\mathbf{u}$ then is characterized as

$$\begin{bmatrix} \mathbf{u}_i \\ \mathbf{x}_i \end{bmatrix} = \begin{bmatrix} qK_iM_iF_i & K_iM_iG_i \\ qM_iF_i & M_iG_i \end{bmatrix} \begin{bmatrix} \mathbf{y}_i \\ \mathbf{z}_i \end{bmatrix}, \quad \mathbf{z}_i = \eta \sum \ell_{ij}(\mathbf{x}_j - \mathbf{x}_i). \tag{2.10}$$

In matrix form

$$\mathbf{u} = \mathsf{K}\hat{\mathbf{x}}, \quad \hat{\mathbf{x}} = q\mathsf{M}\mathsf{F}\mathbf{y} + \mathsf{M}\mathsf{G}\mathbf{z}, \quad \mathbf{z} = \eta\mathsf{L}\hat{\mathbf{x}},$$

where M, F, G, and K are block diagonal matrices with M_i, F_i, G_i, and K_i on the diagonal, and $\mathsf{L} := L \otimes I$. Therefore the mapping from $\mathbf{y}$ to $\mathbf{u}$ is

$$\mathbf{u} = q\mathsf{K}\left(I - \eta\mathsf{M}\mathsf{G}\mathsf{L}\right)^{-1}\mathsf{M}\mathsf{F}\mathbf{y}. \tag{2.11}$$

We would like to examine the limiting case when $\eta \to \infty$. The following lemma provides a useful result that comes handy later.

Lemma 3. *Let a square matrix M be given and suppose it has a possibly repeated semisimple eigenvalue at the origin. Let J and W be matrices whose columns and rows form bases for the right and left null spaces of M, respectively ($MJ = 0$ and $WM = 0$), normalized such that $WJ = I$. Then*

$$\lim_{\eta\to\infty}(I - \eta M)^{-1} = JW.$$

□

Proof. From a standard linear algebra result, there exists a similarity transformation that block diagonalizes M as

$$\begin{bmatrix} W \\ V \end{bmatrix} M \begin{bmatrix} J & N \end{bmatrix} = \begin{bmatrix} 0 & 0 \\ 0 & \Lambda \end{bmatrix}, \quad \begin{bmatrix} W \\ V \end{bmatrix} \begin{bmatrix} J & N \end{bmatrix} = I,$$

with appropriate matrices J, N, W, and V, where $\Lambda \in \mathbb{R}^{(n-m)\times(n-m)}$ is nonsingular. Then

$$\begin{aligned}(I - \eta M)^{-1} &= \left(I - \eta \begin{bmatrix} J & N \end{bmatrix} \begin{bmatrix} W \\ V \end{bmatrix} M \begin{bmatrix} J & N \end{bmatrix} \begin{bmatrix} W \\ V \end{bmatrix}\right)^{-1} \\ &= \begin{bmatrix} J & N \end{bmatrix} \begin{bmatrix} I & 0 \\ 0 & I - \eta\Lambda \end{bmatrix}^{-1} \begin{bmatrix} W \\ V \end{bmatrix}, \\ &= JW + N(I - \eta\Lambda)^{-1}V \to JW.\end{aligned}$$

■

We show the convergence of the static mapping from $\mathbf{y}$ to $\mathbf{u}$ specified by (2.10) in the following lemma.

Lemma 4 (static mapping)**.** *Let $\Phi := K\Psi F$ be given where Ψ is nonsingular. Let L be the Laplacian matrix of a strongly connected directed graph with positive weights. Let $\mathbf{r}$ be a vector with positive entries such that $\mathbf{r}^{\mathsf{T}} L = 0$, and r_i be the i^{th} entry of $\mathbf{r}$. Partition K and F such that*

$$K = \operatorname{col}(K_1, \ldots, K_q), \quad F = \operatorname{row}(F_1, \ldots, F_q).$$

Define $G_i = r_i X$ with an arbitrary nonsingular X, and choose nonsingular matrices M_i such that

$$\Psi = \left(\frac{1}{q} \sum_{i=1}^{q} M_i^{-1} \right)^{-1}.$$

Then the static mapping $\mathbf{u} = H_\eta \mathbf{y}$ specified by (2.10) is a distributed synthesis of Ψ in the sense that

$$\lim_{\eta \to \infty} H_\eta = K\Psi F.$$

□

Proof. The static mapping $\mathbf{u} = H_\eta \mathbf{y}$ is equivalent to (2.11). Note that

$$\mathsf{L} J = 0, \quad J^{\mathsf{T}} \mathsf{G} \mathsf{L} = 0, \quad J := \operatorname{col}(I, \ldots, I).$$

Thus

$$(\mathsf{M}\mathsf{G}\mathsf{L})\, J \left(J^{\mathsf{T}} \mathsf{M}^{-1} J \right)^{-1} = 0, \quad J^{\mathsf{T}} \mathsf{M}^{-1} (\mathsf{M}\mathsf{G}\mathsf{L}) = 0.$$

Applying Lemma 3,

$$\lim_{\eta \to \infty} (I - \eta \mathsf{M}\mathsf{G}\mathsf{L})^{-1} = J \left(J^{\mathsf{T}} \mathsf{M}^{-1} J \right)^{-1} J^{\mathsf{T}} \mathsf{M}^{-1}.$$

Further,

$$\lim_{\eta\to\infty} \mathbf{u} = \lim_{\eta\to\infty} q\mathsf{K}\left(I - \eta\mathsf{MGL}\right)^{-1}\mathsf{MF}\mathbf{y} = q\mathsf{K}J\left(J^{\mathsf{T}}\mathsf{M}^{-1}J\right)^{-1}J^{\mathsf{T}}\mathsf{F}\mathbf{y}.$$

Finally

$$\lim_{\eta\to\infty} \mathbf{u} = K\Psi F\mathbf{y}$$

by noticing that

$$\mathsf{K}J = K, \quad (J^{\mathsf{T}}\mathsf{M}^{-1}J)^{-1} = \frac{1}{q}\Psi, \quad J^{\mathsf{T}}\mathsf{F} = F.$$

■

Remark 2. Lemma 4 is the basis for the developments in the sequel. It shows how a communication network with a strong coupling strength approaches a central mapping. Conversely, it gives guidelines as for how a given centralized mapping can be synthesized as a distributed network mapping. As the theoretical convergence happens with sufficiently large coupling strength, strong connectivity is crucial for the distributed synthesis. □

2.3 Distributed Control Synthesis

2.3.1 Controller Approximation

This section shows that an arbitrary centralized controller $K(s)$ admits a distributed synthesis $K_\eta(s)$ with an arbitrary accuracy, i.e. $\|K - K_\eta\|_{L_\infty}$ can be arbitrarily small.

As the previous section suggests, the distributed synthesis of a static mapping comprises of three parts. The first (K) and third components (F) correspond to the input and output coefficient matrices of the individual control units, respectively. While the middle component (Ψ) is determined in terms of the "average" of M_i^{-1}. This motivates us to study the average dynamics of the control units. We present a coordinate transformation result in the following lemma which gives insights to the distributed synthesis of an arbitrary centralized controller.

Lemma 5 (coordinate transformation)**.** *Consider the distributed controller parametrized by (2.5). Let J and N be defined as in (2.8) and (2.9). Define $\bar{A} := \frac{1}{q}\sum_{i=1}^{q} A_i$, $K := \mathrm{col}(K_1, \ldots, K_q)$, $F := \mathrm{row}(F_1, \ldots, F_q)$. Let A, G, F, and K be block diagonal matrices with A_i, G_i, F_i, and K_i on the diagonal, and $\mathsf{L} := L \otimes I$, $\mathcal{H} := -N^{\mathsf{T}}\mathsf{G}\mathsf{L}N$. Then the controller has a state space realization*

$$\begin{bmatrix} \dot{\mathbf{x}}_1 \\ \dot{\mathbf{x}}_2 \\ \mathbf{u} \end{bmatrix} = \begin{bmatrix} \bar{A} & \frac{1}{q}J^{\mathsf{T}}\mathsf{A}N & F \\ N^{\mathsf{T}}\mathsf{A}J & N^{\mathsf{T}}\mathsf{A}N + \eta\mathcal{H} & N^{\mathsf{T}}\mathsf{F} \\ K & \mathsf{K}N & 0 \end{bmatrix} \begin{bmatrix} \mathbf{x}_1 \\ \mathbf{x}_2 \\ \mathbf{y} \end{bmatrix}. \tag{2.12}$$

□

Proof. The distributed controller (2.5) can be written in the matrix form

$$\dot{\hat{\mathbf{x}}} = (\mathsf{A} + \eta\mathsf{G}\mathsf{L})\hat{\mathbf{x}} + q\mathsf{F}\mathbf{y},$$
$$\mathbf{u} = \mathsf{K}\mathbf{x},$$

Consider the coordinate transformation

$$\mathbf{x} = \begin{bmatrix} \mathbf{x}_1 \\ \mathbf{x}_2 \end{bmatrix} = \begin{bmatrix} \frac{1}{q}J^{\mathsf{T}} \\ N^{\mathsf{T}} \end{bmatrix} \hat{\mathbf{x}}.$$

Note that $\mathbf{x}_1 = \frac{1}{q}J^{\mathsf{T}}\hat{\mathbf{x}} = \frac{1}{q}\sum_{i=1}^{q}\hat{\mathbf{x}}_i$ is the average state of the distributed control units. Then

$$\begin{bmatrix} \dot{\mathbf{x}}_1 \\ \dot{\mathbf{x}}_2 \end{bmatrix} = \begin{bmatrix} \frac{1}{q}J^{\mathsf{T}}\left(\mathsf{A} + \eta\mathsf{G}\mathsf{L}\right)J & \frac{1}{q}J^{\mathsf{T}}\left(\mathsf{A} + \eta\mathsf{G}\mathsf{L}\right)N \\ N^{\mathsf{T}}\left(\mathsf{A} + \eta\mathsf{G}\mathsf{L}\right)J & N^{\mathsf{T}}\left(\mathsf{A} + \eta\mathsf{G}\mathsf{L}\right)N \end{bmatrix} \begin{bmatrix} \mathbf{x}_1 \\ \mathbf{x}_2 \end{bmatrix} + \begin{bmatrix} J^{\mathsf{T}} \\ N^{\mathsf{T}} \end{bmatrix} \mathsf{F}\mathbf{y}.$$

Using the fact that

$$\mathsf{L}J = 0, \quad J^{\mathsf{T}}\mathsf{G}\mathsf{L} = 0, \quad J := \mathrm{col}(I, \ldots, I),$$

and

$$\frac{1}{q}J^{\mathsf{T}}\mathsf{A}J = \bar{A}, \quad J^{\mathsf{T}}\mathsf{F} = F,$$

we have

$$\begin{bmatrix} \dot{\mathbf{x}}_1 \\ \dot{\mathbf{x}}_2 \end{bmatrix} = \begin{bmatrix} \bar{A} & \frac{1}{q} J^{\mathsf{T}} \mathsf{A} N \\ N^{\mathsf{T}} \mathsf{A} J & N^{\mathsf{T}} \mathsf{A} N + \eta N^{\mathsf{T}} \mathsf{G} \mathsf{L} N \end{bmatrix} \begin{bmatrix} \mathbf{x}_1 \\ \mathbf{x}_2 \end{bmatrix} + \begin{bmatrix} F \\ N^{\mathsf{T}} \mathsf{F} \end{bmatrix} \mathbf{y}. \tag{2.13}$$

The control input can be expressed as

$$\mathbf{u} = \mathsf{K} \hat{\mathbf{x}} = \mathsf{K} \begin{bmatrix} J & N \end{bmatrix} \mathbf{x} = \begin{bmatrix} K & \mathsf{K} N \end{bmatrix} \mathbf{x}. \tag{2.14}$$

Putting (2.13) and (2.14) together yields (2.12). ■

The next lemma demonstrates how the input-output relationship evolves for a system parametrized by a coupling strength like (2.12).

Lemma 6. *Consider an LTI system parametrized by $\eta \in \mathbb{R}$:*

$$\begin{bmatrix} \dot{\boldsymbol{\xi}} \\ \dot{\boldsymbol{\zeta}} \\ \mathbf{z} \end{bmatrix} = \begin{bmatrix} A & N & B \\ M & \mho + \eta \mathcal{H} & J \\ C & H & D \end{bmatrix} \begin{bmatrix} \boldsymbol{\xi} \\ \boldsymbol{\zeta} \\ \mathbf{w} \end{bmatrix}. \tag{2.15}$$

Denote the transfer function from $\mathbf{w}$ to $\mathbf{z}$ by $R_\eta(s)$ and define $P(s) := C(sI - A)^{-1}B + D$. The following statements are true.

- *If neither A nor $\mathcal{H}$ has eigenvalues on the imaginary axis, then $\lim_{\eta \to \infty} \|R_\eta - P\|_{L_\infty} = 0$, where $\|\cdot\|_{L_\infty}$ is the L_∞ norm.*
- *If A and $\mathcal{H}$ are Hurwitz, then $\lim_{\eta \to \infty} \|R_\eta - P\|_{H_\infty} = 0$, where $\|\cdot\|_{H_\infty}$ is the H_∞ norm.*

□

Proof. Taking the Laplace transform of (2.15),

$$\boldsymbol{\zeta} = \Gamma_\eta(s)(M\boldsymbol{\xi} + J\mathbf{w}), \quad \Gamma_\eta(s) := (sI - \mho - \eta\mathcal{H})^{-1},$$
$$\boldsymbol{\xi} = \Phi(s)(N\boldsymbol{\zeta} + B\mathbf{w}), \quad \Phi_(s) := (sI - A)^{-1}.$$

Rearranging,

$$\begin{bmatrix} I & -\Gamma_\eta(s)M \\ -\Phi(s)N & I \end{bmatrix} \begin{bmatrix} \boldsymbol{\zeta} \\ \boldsymbol{\xi} \end{bmatrix} = \begin{bmatrix} \Gamma_\eta(s)J \\ \Phi(s)B \end{bmatrix} w.$$

Then

$$R_\eta(s) = \begin{bmatrix} H & C \end{bmatrix} \begin{bmatrix} I & -\Gamma_\eta(s)M \\ -\Phi(s)N & I \end{bmatrix}^{-1} \begin{bmatrix} \Gamma_\eta(s)J \\ \Phi(s)B \end{bmatrix} + D.$$

Using the matrix inversion formula,

$$\begin{bmatrix} A & B \\ C & D \end{bmatrix}^{-1} = \begin{bmatrix} E & -EBD^{-1} \\ -D^{-1}CE & D^{-1} + D^{-1}CEBD^{-1} \end{bmatrix}, \quad E := (A - BD^{-1}C)^{-1},$$

the transfer function can be written as

$$R_\eta(s) = C\Phi(s)B + D + \Delta_\eta(s) = P(s) + \Delta_\eta(s),$$

where $\Delta_\eta(s)$ is defined as

$$\Delta_\eta(s) := (H + C\Phi(s)N)\, E(s)\Gamma_\eta(s)\, (J + M\Phi(s)B), \quad E(s) := (I - \Gamma_\eta(s)M\Phi(s)N)^{-1}.$$

Define $\varpi = \frac{1}{\eta}\omega$. Then the L_∞ norm of $\eta\Gamma_\eta$ is

$$\|\eta\Gamma_\eta\|_{L_\infty} = \sup_{\varpi} \left\| \left(j\varpi I - \frac{1}{\eta}\mho - \mathcal{H} \right)^{-1} \right\|_2.$$

We now prove the first statement given that $\mathcal{H}$ has no eigenvalues on the imaginary axis. There exists η_0 such that $\frac{1}{\eta}\mho + \mathcal{H}$ has no eigenvalues on the imaginary axis for $\eta > \eta_0$ due to continuity. Thus for each $\eta > \eta_0$, $\|\eta\Gamma_\eta\|_{L_\infty}$ is well defined and finite. As η approaches infinity, $\|\eta\Gamma_\eta\|_{L_\infty}$ is bounded and approaches the L_∞ norm of $(sI - \mathcal{H})^{-1}$, i.e.,

$$\lim_{\eta\to\infty} \|\eta\Gamma_\eta\|_{L_\infty} = \left\|(sI - \mathcal{H})^{-1}\right\|_{L_\infty},$$

which is finite. Therefore, $\lim_{\eta\to\infty} \|\Gamma_\eta\|_{L_\infty} = \lim_{\eta\to\infty} \frac{1}{\eta} \|\eta\Gamma_\eta\|_{L_\infty} = 0$. When $\|\Gamma_\eta\|_{L_\infty}$ gets sufficiently small as $\eta \to \infty$, $\det(I - \Gamma_\eta(s)M\Phi(s)N) \neq 0$ due to the small gain theorem. Hence $E(s) = (I - \Gamma_\eta(s)M\Phi(s)N)^{-1}$ is well defined and $\|E\|_{L_\infty}$ is finite. We finally have

$$\begin{aligned}
\lim_{\eta\to\infty} \|R_\eta - P\|_{L_\infty} &= \lim_{\eta\to\infty} \|\Delta_\eta\|_{L_\infty} \\
&\leq \lim_{\eta\to\infty} \|H + C\Phi N\|_{L_\infty} \|E\|_\infty \|\Gamma_\eta\|_{L_\infty} \|J + M\Phi B\|_{L_\infty} \\
&= 0.
\end{aligned}$$

The proof for the second statement can be done in a similar manner. Note that $\|\Delta_\eta\|_{H_\infty}$ becomes finite with large η. $\|R_\eta\|_{H_\infty}$ is thereby finite for sufficiently large η. The rest of the proof is done with the fact that there exists η_0 such that $\frac{1}{\eta}\mathcal{O} + \mathcal{H}$ becomes Hurwitz for $\eta > \eta_0$ given that $\mathcal{H}$ is Hurwitz. ■

We build upon Lemmas 5 and 6 to show that a distributed control can approximate a centralized control arbitrarily closely and state the result in the following theorem.

Theorem 1 (controller approximation)**.** *Consider the mapping from* $\mathbf{y}$ *to* $\mathbf{u}$ *specified by* (2.5) *and denote it as* $R_\eta(s)$*. Suppose* L *is the Laplacian matrix of a strongly connected directed graph with positive weights. Let* $\mathbf{r}$ *be a positive vector such that* $\mathbf{r}^\mathsf{T} L = 0$*, and* r_i *be the* i^{th} *entry of* $\mathbf{r}$*. Define* $\bar{A} := \frac{1}{q}\sum_{i=1}^{q} A_i$*,* $K := \text{col}(K_1, \ldots, K_q)$*,* $F := \text{row}(F_1, \ldots, F_q)$*, and* $P(s) := K(sI - \bar{A})^{-1}F$*. Then*

$$\lim_{\eta\to\infty} \|R_\eta - P\|_{L_\infty} = 0$$

where $\|\cdot\|_{L_\infty}$ *is the* L_∞ *norm, if* $G_i = r_i X$ *where* $X = X^\mathsf{T} \succ 0$*, and* $\bar{A}$ *has no eigenvalues on the imaginary axis. Further, if* $\bar{A}$ *is Hurwitz, then*

$$\lim_{\eta\to\infty} \|R_\eta - P\|_{H_\infty} = 0$$

where $\|\cdot\|_{H_\infty}$ *is the* H_∞ *norm.* □

Proof. The distributed controller (2.5) has a state space realization (2.12) due to Lemma 5, where $\mathcal{H} := -N^{\mathsf{T}}\mathsf{GL}N$ is Hurwitz by Lemma 2. Then the proof is completed by applying Lemma 6. ■

Theorem 1 shows that under certain conditions a distributed control can be made arbitrarily close to a centralized control by increasing the coupling strength. Moreover, it also shows how one can synthesize a distributed controller given a centralized one.

Example 1. Let a centralized controller $P(s) = K(sI - A)^{-1}F$ be given with

$$A = \begin{pmatrix} 1 & 0 & 0 & 0 & 0 & 0 \\ -1 & 1 & 1 & 0 & 0 & 0 \\ 1 & -2 & -1 & -1 & 1 & 1 \\ 0 & 0 & 0 & -1 & 0 & 0 \\ -8 & 1 & -1 & -1 & -2 & 0 \\ 4 & -1 & 1 & 0 & 0 & -4 \end{pmatrix}, \quad K = \left(\begin{array}{cccccc} 1 & 0 & 0 & 2 & 0 & 0 \\ 2 & 0 & 0 & 1 & 0 & 0 \\ \hline 2 & 0 & 1 & 0 & 0 & 1 \\ \hline 0 & 0 & 0 & 2 & 0 & 0 \\ \hline 1 & 0 & 2 & 0 & 0 & 0 \\ 2 & 0 & 4 & 0 & 0 & 0 \end{array}\right) = \begin{pmatrix} K_1 \\ K_2 \\ K_3 \\ K_4 \end{pmatrix}.$$

F is given by $F = \mathrm{row}(F_1, F_2, F_3, F_4)$ with

$$F_i = K_i^{\mathsf{T}}, \quad i = 1, 2, 3, 4.$$

We construct a distributed controller composed of 4 control units as in (2.5) with $A_i = A$ and the connectivity of the control units is described by a graph with Laplacian

$$L = \begin{pmatrix} 2 & -1 & 0 & -1 \\ 0 & 1 & -1 & 0 \\ -1 & -1 & 2 & 0 \\ -1 & 0 & 0 & 1 \end{pmatrix}.$$

The left eigenvector of L associated with 0 is $\mathbf{r}^{\mathsf{T}} = \begin{bmatrix} 1 & 2 & 1 & 1 \end{bmatrix}$ and G_i are then chosen to be $G_i = r_i I$. Denote by $R_\eta(s)$ the transfer function of the distributed controller. Figure 2.4 shows the spectral norm of $P(s)$ and $R_\eta(s)$ with various η. The difference between $P(s)$ and $R_\eta(s)$ gets diminished as η becomes larger. □

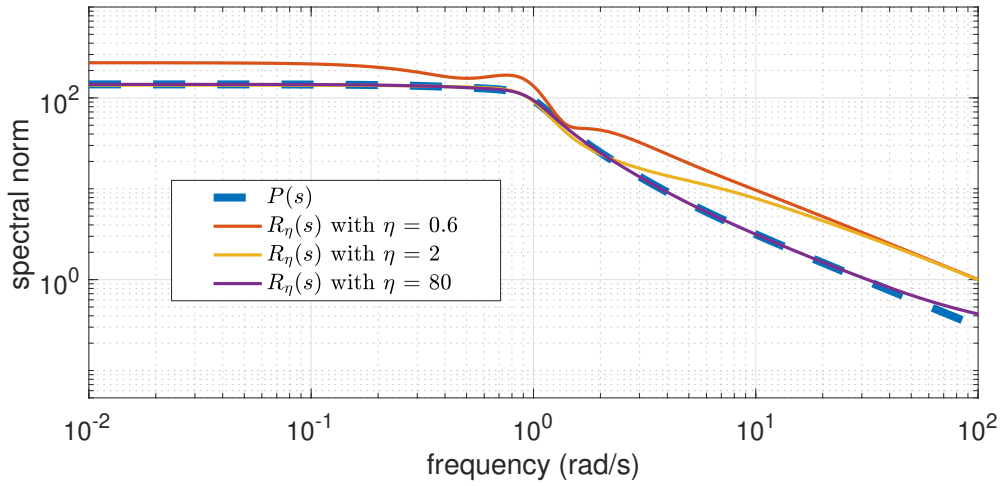

Figure 2.3: Spectral norm of $P(s)$ and $R_\eta(s)$ with various η.

2.3.2 Closed-Loop Performance

This section shows that the closed-loop performance of the central controller can be recovered by the distributed synthesis with an arbitrary accuracy. Since the controller transfer function can be exactly recovered in the limit $\eta \to \infty$, the closed-loop transfer function can also be recovered exactly. However, for practical purposes, the limiting property is not enough since the limit may be approached by a sequence of the unstable closed-loop systems. We will show that for sufficiently large $\eta > 0$, the closed-loop system is internally stable, justifying the approximate distributed synthesis with a finite value of η.

Consider the generalized plant

$$\begin{aligned} \dot{\mathbf{x}} &= A\mathbf{x} + B_1\mathbf{w} + B_2\mathbf{u}, \\ \mathbf{z} &= C_1\mathbf{x} + D_{11}\mathbf{w} + D_{12}\mathbf{u}, \\ \mathbf{y} &= C_2\mathbf{x} + D_{21}\mathbf{w}. \end{aligned} \tag{2.16}$$

Let a centralized controller be given by

$$\begin{aligned} \dot{\hat{\mathbf{x}}} &= \bar{A}\hat{\mathbf{x}} + F\mathbf{y}, \\ \mathbf{u} &= K\hat{\mathbf{x}}. \end{aligned} \tag{2.17}$$

Theorem 2 (closed-loop approximation)**.** *Consider the generalized plant (2.16). Denote by $P(s)$ the transfer function from $\mathbf{w}$ to $\mathbf{z}$ of the closed-loop system formed by the plant and the centralized controller (2.17). Likewise, denote by $R_\eta(s)$ the transfer function from $\mathbf{w}$ to $\mathbf{z}$ of the closed-loop system formed by the plant and the distributed controller (2.5). Suppose G_i are determined according to Theorem 1 and the centralized controller (2.17) stabilizes the generalized plant (2.16). Then*

$$\lim_{\eta\to\infty} \|R_\eta - P\|_{H_\infty} = 0$$

where $\|\cdot\|_{H_\infty}$ is the H_∞ norm. □

Proof. The closed-loop system formed by the generalized plant (2.16) and the centralized controller (2.17) can be written as

$$\begin{bmatrix} \dot{\mathbf{x}} \\ \dot{\hat{\mathbf{x}}} \\ \mathbf{z} \end{bmatrix} = \left[\begin{array}{cc|c} A & B_2K & B_1 \\ FC_2 & \bar{A} & FD_{21} \\ \hline C_1 & D_{12}K & D_{11} \end{array}\right] \begin{bmatrix} \mathbf{x} \\ \hat{\mathbf{x}} \\ \mathbf{w} \end{bmatrix}. \tag{2.18}$$

Since the distributed controller (2.5) is equivalent to (2.12) through a coordinate transformation, the closed-loop system formed by the plant and the distributed controller can be written as

$$\begin{bmatrix} \dot{\mathbf{x}} \\ \dot{\boldsymbol{\chi}}_1 \\ \dot{\boldsymbol{\chi}}_2 \\ \mathbf{z} \end{bmatrix} = \left[\begin{array}{cc|c|c} A & B_2K & B_2\mathsf{K}N & B_1 \\ FC_2 & \bar{A} & \frac{1}{q}J^\mathsf{T}\mathsf{A}N & FD_{21} \\ \hline N^\mathsf{T}\mathsf{F}C_2 & N^\mathsf{T}\mathsf{A}JC_2 & N^\mathsf{T}\mathsf{A}N + \eta\mathcal{H} & N^\mathsf{T}\mathsf{F}D_{21} \\ \hline C_1 & D_{12}K & D_{12}\mathsf{K}N & D_{11} \end{array}\right] \begin{bmatrix} \mathbf{x} \\ \boldsymbol{\chi}_1 \\ \boldsymbol{\chi}_2 \\ \mathbf{w} \end{bmatrix}, \tag{2.19}$$

where $\mathcal{H} := -N^\mathsf{T}\mathsf{G}\mathsf{L}N$ is Hurwitz by Lemma 2. The proof is completed by applying Lemma 6. ■

Theorem 2 indicates that an optimal control with respect to an arbitrary optimality criterion on the closed-loop transfer function can be approximately implemented in a distributed manner with an arbitrarily close performance. We apply this result to LQG controllers as an example in the subsequent section.

2.4 Application to H_2 Optimal Control

2.4.1 Distributed Observer

In the framework of a generalized plant, the plant with a state observer can be formulated as

$$\begin{aligned}\dot{\mathbf{x}} &= A\mathbf{x} + B\mathbf{w},\\ \mathbf{z} &= \mathbf{x} - \hat{\mathbf{x}},\\ \mathbf{y} &= C\mathbf{x} + D\mathbf{w},\end{aligned} \quad \Longleftrightarrow \quad \begin{bmatrix}\dot{\mathbf{x}}\\ \mathbf{z}\\ \mathbf{y}\end{bmatrix} = \left[\begin{array}{c|cc} A & B & 0\\ \hline I & 0 & -I\\ C & D & 0\end{array}\right] \begin{bmatrix}\mathbf{x}\\ \mathbf{w}\\ \hat{\mathbf{x}}\end{bmatrix},$$

and the state observer is given by

$$\dot{\hat{\mathbf{x}}} = A\hat{\mathbf{x}} + F(\mathbf{y} - C\hat{\mathbf{x}})$$

with $A - FC$ being Hurwitz. Motivated by Theorem 1, we consider a distributed observer of the form

$$\dot{\hat{\mathbf{x}}}_i = A\hat{\mathbf{x}}_i + qF_i(\mathbf{y}_i - C_i\hat{\mathbf{x}}_i) + \eta G_i \sum_{j\in\mathbb{N}_i} \ell_{ij}(\hat{\mathbf{x}}_j - \hat{\mathbf{x}}_i), \quad i \in \mathbb{I}_q. \tag{2.20}$$

Lemma 7. *Consider the matrix*

$$\mathcal{A} = \begin{bmatrix} A & N\\ M & \mho + \eta\mathcal{H}\end{bmatrix}.$$

Suppose A and $\mathcal{H}$ are Hurwitz. Then $\mathcal{A}$ becomes Hurwitz with sufficiently large η. □

Proof. Since A and $\mathcal{H}$ are Hurwitz, there exist $P_1 = P_1^\mathsf{T} \succ 0$ and $P_2 = P_2^\mathsf{T} \succ 0$ such that

$$P_1A + A^\mathsf{T}P_1 \prec 0, \quad P_2\mathcal{H} + \mathcal{H}^\mathsf{T}P_2 \prec 0.$$

And there exists a factorization

$$-(P_2\mathcal{H} + \mathcal{H}^\mathsf{T}P_2) = EE^\mathsf{T}$$

where E has the same dimension as $\mathcal{H}$ and is full rank. Define $P := \text{diag}(P_1, P_2)$ and

$$\begin{aligned}\Phi &:= P\mathcal{A} + \mathcal{A}^\mathsf{T} P \\ &= \begin{bmatrix} P_1 A + A^\mathsf{T} P_1 & P_1 N + M^\mathsf{T} P_2 \\ P_2 M + N^\mathsf{T} P_1 & P_2 \mathcal{U} + \mathcal{U}^\mathsf{T} P_2 + \eta(P_2 \mathcal{H} + \mathcal{H}^\mathsf{T} P_2) \end{bmatrix} \\ &= \begin{bmatrix} P_1 A + A^\mathsf{T} P_1 & P_1 N + M^\mathsf{T} P_2 \\ P_2 M + N^\mathsf{T} P_1 & P_2 \mathcal{U} + \mathcal{U}^\mathsf{T} P_2 \end{bmatrix} - \eta \begin{bmatrix} 0 \\ E \end{bmatrix} \begin{bmatrix} 0 & E^\mathsf{T} \end{bmatrix}.\end{aligned}$$

Note that one option for the orthogonal complement of $\begin{bmatrix} 0 \\ E \end{bmatrix}$ is $\begin{bmatrix} I & 0 \end{bmatrix}$. It follows from Finsler's lemma that there exists $\eta > 0$ such that $\Phi \prec 0$ if and only if

$$\begin{bmatrix} I & 0 \end{bmatrix} \begin{bmatrix} P_1 A + A^\mathsf{T} P_1 & P_1 N + M^\mathsf{T} P_2 \\ P_2 M + N^\mathsf{T} P_1 & P_2 \mathcal{U} + \mathcal{U}^\mathsf{T} P_2 \end{bmatrix} \begin{bmatrix} I \\ 0 \end{bmatrix} = P_1 A + A^\mathsf{T} P_1 \prec 0,$$

which is true by assumption. Finally, $\Phi \prec 0$ indicates $\mathcal{A}$ is Hurwitz. ■

Theorem 3. *Consider the plant*

$$\begin{aligned} \dot{\mathbf{x}} &= A\mathbf{x}, \quad \mathbf{x} \in \mathbb{R}^n, \\ \mathbf{y} &= C\mathbf{x}, \quad \mathbf{y} \in \mathbb{R}^m, \end{aligned} \tag{2.21}$$

where (C, A) is observable. Let the output $\mathbf{y}(t) \in \mathbb{R}^m$ be partitioned into vectors $\mathbf{y}_i(t) \in \mathbb{R}^{m_i}$ so that $\mathbf{y} = \text{col}(\mathbf{y}_1, \dots \mathbf{y}_q)$, and partition $C = \text{col}(C_1, \dots, C_q)$ accordingly. Let a distributed observer be of the form (2.20) where the index set $\mathbb{N}_i$ specifies the neighbors of the node i, and the parameters are chosen as follows.

(a) Let L be the Laplacian matrix of a strongly connected directed graph with positive weights, and ℓ_{ij} be the $(i,j)^{\text{th}}$ entry of L. Let $\mathbf{r}$ be a positive vector such that $\mathbf{r}^\mathsf{T} L = 0$.

(b) Let $P = P^\mathsf{T} \succ 0$ and F be such that $A - FC$ is Hurwitz, and define F_i and G_i by

$$G_i = r_i P, \quad F =: \text{row}(F_1, \dots, F_q).$$

Then the state estimation $||\mathbf{x}(t) - \hat{\mathbf{x}}_i(t)|| \to 0$ *as* $t \to \infty$ *is achieved for all initial condition* $\mathbf{x}(0)$ *and* $\hat{\mathbf{x}}(0)$ *if* $\eta > 0$ *is sufficiently large.* □

Proof. Define the local estimation error of the i^{th} observer as

$$\mathbf{e}_i := \hat{\mathbf{x}}_i - \mathbf{x},$$

and let $\mathbf{e} := \text{col}(\mathbf{e}_1, \dots, \mathbf{e}_q)$. Then the error dynamics is given by

$$\dot{\mathbf{e}} = (\mathsf{A} - q\mathsf{FC} + \eta\mathsf{GL})\mathbf{e},$$

where F, C, and G are block diagonal matrices with F_i, C_i, and G_i on the diagonal, and

$$\mathsf{A} := I \otimes A, \quad \mathsf{L} := L \otimes I.$$

A similarity transformation yields

$$\begin{bmatrix} \frac{1}{q}J^{\mathsf{T}} \\ N^{\mathsf{T}} \end{bmatrix} (\mathsf{A} - q\mathsf{FC} + \eta\mathsf{GL}) \begin{bmatrix} J & N \end{bmatrix} = \begin{bmatrix} A - FC & \frac{1}{q}J^{\mathsf{T}}(\mathsf{A} - q\mathsf{FC})N \\ N^{\mathsf{T}}(\mathsf{A} - q\mathsf{FC})J & N^{\mathsf{T}}(\mathsf{A} - q\mathsf{FC})N + \eta N^{\mathsf{T}}\mathsf{GL}N \end{bmatrix}.$$

Since $A - FC$ and $N^{\mathsf{T}}\mathsf{GL}N$ are Hurwitz by Lemma 2, it follows from Lemma 7 that $\mathsf{A} - q\mathsf{FC} + \eta\mathsf{GL}$ becomes Hurwitz with sufficiently large η. ■

Remark 3. When F is chosen to be the Kalman gain to make $A - FC$ Hurwitz, Theorem 3 gives a distributed synthesis of the Kalman filter with an arbitrary accuracy. □

2.4.2 LQG Control

We apply the general result Theorem 2 to the LQG control.

Corollary 1. *Consider the generalized plant* (2.16) *with the partition*

$$\mathbf{y} = \text{col}(\mathbf{y}_1, \dots \mathbf{y}_q), \quad C = \text{col}(C_{2,1}, \dots, C_{2,q}).$$

Denote by $P(s)$ the transfer function from $\mathbf{w}$ to $\mathbf{z}$ of the closed-loop system formed by the plant and the centralized LQG controller

$$\begin{aligned}\dot{\hat{\mathbf{x}}} &= (A + B_2K - FC_2)\hat{\mathbf{x}} + F\mathbf{y},\\ \mathbf{u} &= K\hat{\mathbf{x}}.\end{aligned} \tag{2.22}$$

Likewise, denote by $R_\eta(s)$ the transfer function from $\mathbf{w}$ to $\mathbf{z}$ of the closed-loop system formed by the plant and the distributed controller

$$\begin{aligned}\dot{\hat{\mathbf{x}}}_i &= (A + B_2K - qF_iC_{2,i})\hat{\mathbf{x}}_i + F_i\mathbf{y}_i + G_i\mathbf{z}_i, \quad i \in \mathbb{I}_q,\\ \mathbf{z}_i &= \eta \sum_{j\in\mathbb{N}_i} \ell_{ij}(\hat{\mathbf{x}}_j - \hat{\mathbf{x}}_i),\\ \mathbf{u}_i &= K_i\hat{\mathbf{x}}_i,\end{aligned} \tag{2.23}$$

where

$$K =: \operatorname{col}(K_1, \ldots, K_q), \quad F =: \operatorname{row}(F_1, \ldots, F_q).$$

Suppose G_i are determined according to Theorem 1. Then given an arbitrarily small $\varepsilon > 0$, there exists $\eta > 0$ such that

$$\|R_\eta\|_{H_2} < \gamma_{\text{opt}} + \varepsilon,$$

where γ_{opt} is the optimal H_2 norm of $P(s)$. □

Proof. The result is obtained directly by applying Theorem 2 when the given centralized controller is a LQG controller. ■

Example 2. We apply the theorem to a plant described by

$$\begin{aligned}\dot{\mathbf{x}} &= A\mathbf{x} + B\mathbf{u},\\ \mathbf{y} &= C\mathbf{x},\end{aligned}$$

with

$$A = \begin{pmatrix} 1 & 0 & 0 & 0 & 0 & 0 \\ -1 & 1 & 1 & 0 & 0 & 0 \\ 1 & -2 & -1 & -1 & 1 & 1 \\ 0 & 0 & 0 & -1 & 0 & 0 \\ -8 & 1 & -1 & -1 & -2 & 0 \\ 4 & -0.5 & 0.5 & 0 & 0 & -4 \end{pmatrix}, \quad C = \left(\begin{array}{cccccc} 1 & 0 & 0 & 2 & 0 & 0 \\ 2 & 0 & 0 & 1 & 0 & 0 \\ \hline 2 & 0 & 1 & 0 & 0 & 1 \\ \hline 0 & 0 & 0 & 2 & 0 & 0 \\ \hline 1 & 0 & 2 & 0 & 0 & 0 \\ 2 & 0 & 4 & 0 & 0 & 0 \end{array}\right) = \begin{pmatrix} C_1 \\ C_2 \\ C_3 \\ C_4 \end{pmatrix}.$$

B_i are given by

$$B_i = C_i^{\mathsf{T}}, \quad i = 1, 2, 3, 4.$$

The connectivity of the control units is described by a graph with Laplacian

$$L = \begin{pmatrix} 2 & -1 & 0 & -1 \\ 0 & 1 & -1 & 0 \\ -1 & -1 & 2 & 0 \\ -1 & 0 & 0 & 1 \end{pmatrix}.$$

The left eigenvector of L associated with 0 is $\mathbf{r}^{\mathsf{T}} = \begin{bmatrix} 1 & 2 & 1 & 1 \end{bmatrix}$ and G_i are then chosen to be $G_i = r_i I$. We first obtain the LQG controller with proper weighting matrices and synthesize the distributed controller accordingly. Figure 2.4 shows the spectral norm of $P(s)$ and $R_\eta(s)$ with various η. The difference between $P(s)$ and $R_\eta(s)$ gets diminished as η becomes larger. Figure 2.5 shows the closed-loop eigenvalues on the complex plane with a centralized LQG controller, as well as with a distributed controller with various η. As can be seen, the closed-loop eigenvalues with the distributed controller approach those with the centralized controller as η gets larger. □

2.4.3 Reduction of Communication over Network

Without specifying the structure of G_i in (2.5), the neighboring control units may have to exchange information via all the state variables since G_i in general is full rank. In this

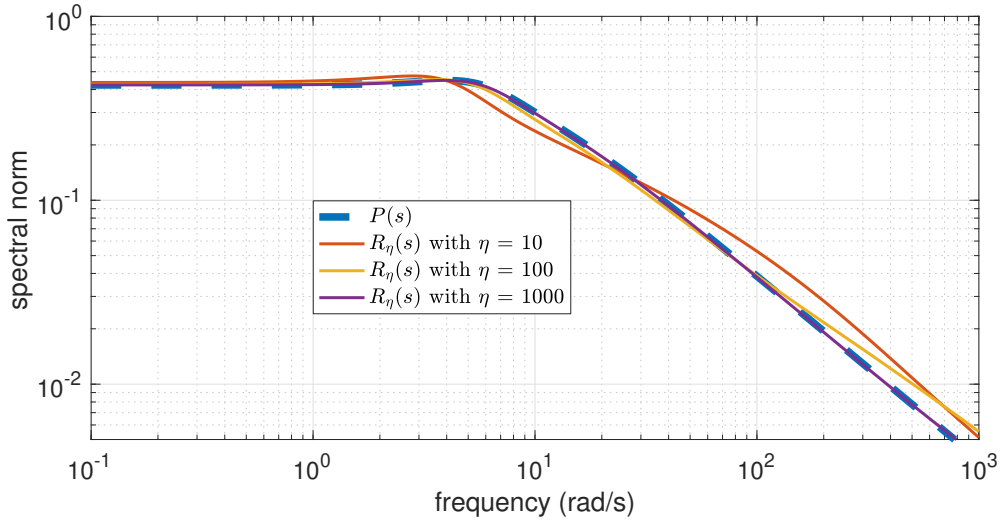

Figure 2.4: Spectral norm of $P(s)$ and $R_\eta(s)$ with various η.

subsection, we consider the problem of reducing the rank of G_i to diminish the coupling between control units. First we have $G_i = r_i X, X \in \mathbb{R}^n_{++}$ by Theorem 1. Then it is equivalent to minimize the rank of X. To see how the rank reduction of X leads to reduction of communication, we assume the rank of X is reduced to $r < n$. Then X can be factored as

$$X = ST, \quad S \in \mathbb{R}^{n\times r}, \quad T \in \mathbb{R}^{r\times n}.$$

By (2.5), we have

$$\dot{\hat{\mathbf{x}}}_i = A_i\hat{\mathbf{x}}_i + qF_i\mathbf{y}_i + r_iS\boldsymbol{\zeta}_i, \quad i \in \mathbb{I}_q,$$

where

$$\boldsymbol{\zeta}_i := T\mathbf{z}_i = \eta \sum_{j\in\mathbb{N}_i} \ell_{ij}(\boldsymbol{\xi}_j - \boldsymbol{\xi}_i), \quad \boldsymbol{\xi}_i := T\hat{\mathbf{x}}_i.$$

The communication between control units is taken care of by $\boldsymbol{\zeta}_i$ and $\boldsymbol{\xi}_i$, which have dimension $r < n$.

We show the rank minimization of X can be achieve through an example of H_2 optimal control where X is treated as decision variables. Consider the closed-loop system with a

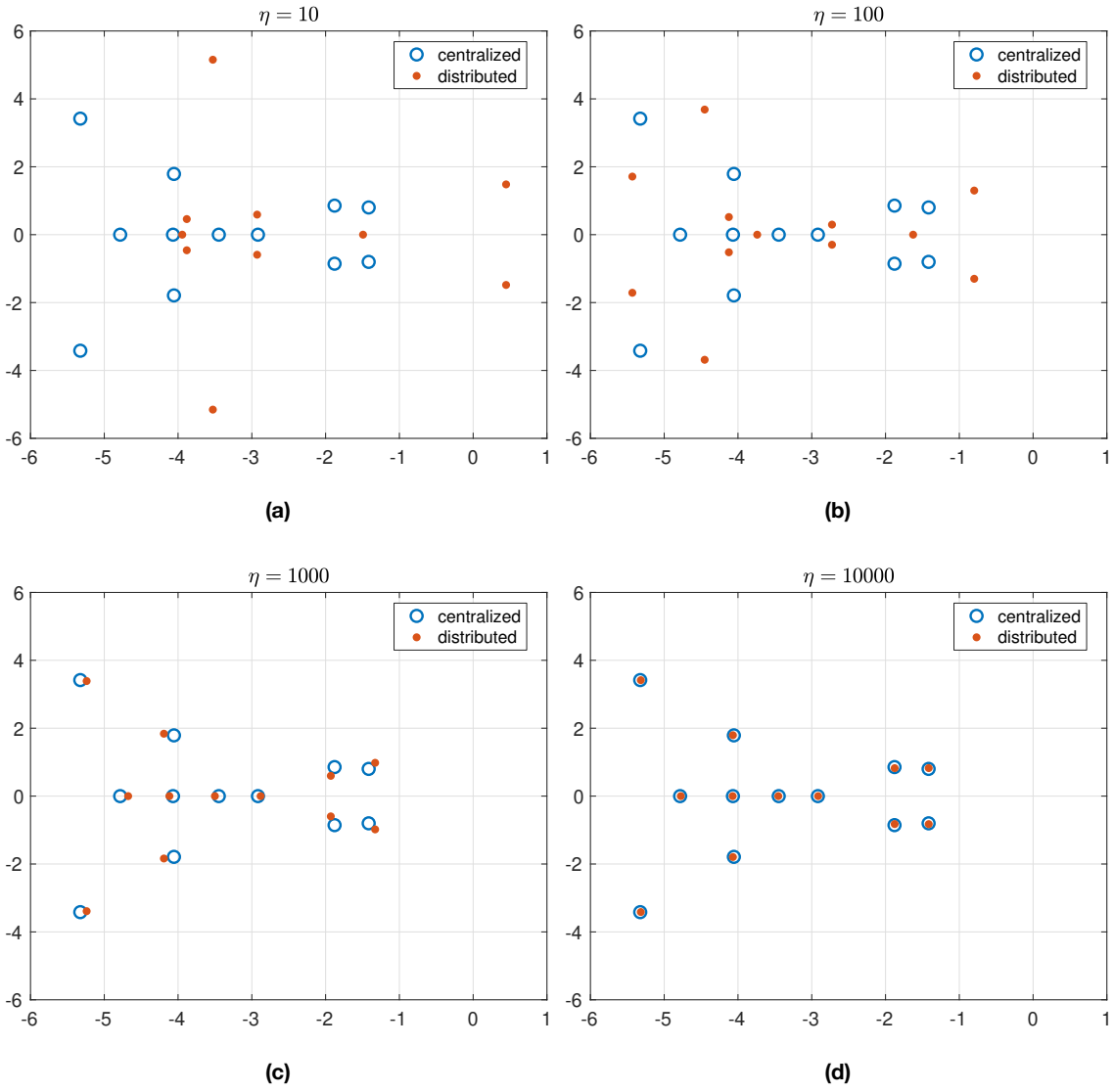

Figure 2.5: The closed-loop eigenvalues.

centralized controller (2.18), and the closed-loop system with a distributed controller (2.19). Assume $D_{11} = 0$ and that the optimal H_2 norm of (2.18) is γ_*. It is equivalent to say that, for an arbitrary $\gamma > \gamma_*$, there exists $P_0 = P_0^\mathsf{T} \succ 0$ such that

$$P_0 A_0 + A_0^\mathsf{T} P_0 + C_0^\mathsf{T} C_0 \prec 0, \quad \mathrm{tr}(B_0 P_0 B_0) < \gamma^2, \tag{2.24}$$

where

$$A_0 := \begin{bmatrix} A & B_2 K \\ F C_2 & \bar{A} \end{bmatrix}, \quad B_0 := \begin{bmatrix} B_1 \\ F D_{21} \end{bmatrix}, \quad C_0 := \begin{bmatrix} C_1 & D_{12} K \end{bmatrix}.$$

Given γ larger than γ_*, we will provide a convex characterization of X that yields a distributed controller such that the closed-loop system (2.19) has the H_2 norm less than γ. Let

$$\begin{aligned} \Phi &:= \begin{bmatrix} B_2 \mathsf{K} N \\ \frac{1}{q} J^\mathsf{T} \mathsf{A} N \end{bmatrix}, \quad \Psi := \begin{bmatrix} N^\mathsf{T} \mathsf{F} C_2 & N^\mathsf{T} \mathsf{A} J C_2 \end{bmatrix}, \quad E := N^\mathsf{T} \mathsf{A} N, \\ B &:= \begin{bmatrix} B_0 \\ B_H \end{bmatrix}, \quad B_H := N^\mathsf{T} \mathsf{F} D_{21}, \\ C &:= \begin{bmatrix} C_0 & C_H \end{bmatrix}, \quad C_H := D_{12} \mathsf{K} N, \end{aligned} \tag{2.25}$$

and $H(X) = \eta \mathcal{H}$ be a matrix-valued function of matrix X,

$$H(X) := -\eta N^\mathsf{T} \mathsf{G} \mathsf{L} N, \quad \mathsf{G} := \mathrm{blkdiag}(G_i), \quad G_i := r_i X. \tag{2.26}$$

We formulate an LMI (also known as SDP) problem to express the H_2 norm constraint. To this end, a proper LMI is derived in the following theorem.

Theorem 4. *Consider the closed-loop system (2.18) with a centralized LQG controller and its optimal H_2 cost γ_*. Let $\gamma > \gamma_*$ be given. Assume (2.24) holds. Let Φ, Ψ, B, C, $H(X)$ be defined as in (2.25) and (2.26). Define*

$$P_\varepsilon := \begin{bmatrix} P_0 & 0 \\ 0 & \varepsilon I \end{bmatrix}, \quad P := \begin{bmatrix} P_0 & 0 \\ 0 & I \end{bmatrix}, \quad A_\varepsilon := \begin{bmatrix} A_0 & \Phi \\ \varepsilon \Psi & H_\varepsilon(X_\varepsilon) + \varepsilon E \end{bmatrix}, \quad \begin{aligned} X_\varepsilon &:= \varepsilon X, \\ H_\varepsilon(X_\varepsilon) &:= \varepsilon H(X). \end{aligned}$$

Then there exist X_ε and $\varepsilon > 0$ such that the following LMIs which are linear in X_ε and ε hold,

$$PA_\varepsilon + A_\varepsilon^\mathsf{T} P + C^\mathsf{T} C \prec 0, \quad \mathrm{tr}\left(B^\mathsf{T} P_\varepsilon B\right) < \gamma^2, \quad X_\varepsilon \succ 0. \tag{2.27}$$

With this X, the distributed controller in (2.5) yields the closed-loop system with H_2 norm less than γ. □

Proof. A direct calculation gives

$$\begin{aligned}
&PA_\varepsilon + A_\varepsilon^\mathsf{T} P + C^\mathsf{T} C \\
&= \begin{bmatrix} P_0 & 0 \\ 0 & I \end{bmatrix} \begin{bmatrix} A_0 & \Phi \\ \varepsilon\Psi & H_\varepsilon(X_\varepsilon) + \varepsilon E \end{bmatrix} + \begin{bmatrix} A_0^\mathsf{T} & \varepsilon\Psi^\mathsf{T} \\ \Phi^\mathsf{T} & H_\varepsilon(X_\varepsilon)^\mathsf{T} + \varepsilon E^\mathsf{T} \end{bmatrix} \begin{bmatrix} P_0 & 0 \\ 0 & I \end{bmatrix} + \begin{bmatrix} C_0^\mathsf{T} \\ C_H^\mathsf{T} \end{bmatrix} \begin{bmatrix} C_0 & C_H \end{bmatrix} \\
&= \begin{bmatrix} P_0 A_0 + A_0^\mathsf{T} P + C_0^\mathsf{T} C_0 & P_0\Phi + \varepsilon\Psi^\mathsf{T} + C_0^\mathsf{T} C_H \\ \Phi^\mathsf{T} P_0 + \varepsilon\Psi + C_H^\mathsf{T} C_0 & \left(H_\varepsilon(X_\varepsilon) + H_\varepsilon(X_\varepsilon)^\mathsf{T}\right) + \varepsilon\left(E + E^\mathsf{T}\right) + C_H^\mathsf{T} C_H \end{bmatrix}.
\end{aligned}$$

We notice that $P_0 A_0 + A_0^\mathsf{T} P + C_0^\mathsf{T} C_0 \prec 0$ by assumption. And

$$\mathsf{GL} = (R \otimes X)(L \otimes I) = (RL) \otimes X, \quad R := \mathrm{diag}(r_1, \ldots, r_q).$$

Further, defining $\tilde{N}$ such that $N = \tilde{N} \otimes I$,

$$\begin{aligned}
H_\varepsilon(X_\varepsilon) + H_\varepsilon(X_\varepsilon)^\mathsf{T} &= \varepsilon\left(H(X) + H(X)^\mathsf{T}\right) \\
&= -\eta\varepsilon N^\mathsf{T}\left(\mathsf{GL} + (\mathsf{GL})^\mathsf{T}\right) N \\
&= -\eta\varepsilon N^\mathsf{T}\left(\left(RL + (RL)^\mathsf{T}\right) \otimes X\right) N \\
&= -\eta\left(\tilde{N}^\mathsf{T}\left(RL + (RL)^\mathsf{T}\right)\tilde{N}\right) \otimes X_\varepsilon.
\end{aligned}$$

This indicates that the eigenvalues of $H_\varepsilon(X_\varepsilon) + H_\varepsilon(X_\varepsilon)^\mathsf{T}$ are $-\eta\lambda_i\mu_j$, where $\lambda_i, i \in \mathbb{I}_q$ are the eigenvalues of $\tilde{N}^\mathsf{T}\left(RL + (RL)^\mathsf{T}\right)\tilde{N}$ and $\mu_j, j \in \mathbb{I}_n$ are the eigenvalues of X_ε. It follows from Lemmas 1 and 2 that $\tilde{N}^\mathsf{T}\left(RL + (RL)^\mathsf{T}\right)\tilde{N} \succ 0$. Therefore $H_\varepsilon(X_\varepsilon) + H_\varepsilon(X_\varepsilon)^\mathsf{T} \prec 0$. Applying Lemma 7, we have $PA_\varepsilon + A_\varepsilon^\mathsf{T} P + C^\mathsf{T} C \prec 0$ for sufficiently large η. Also

$$B^\mathsf{T} P_\varepsilon B = \begin{bmatrix} B_0^\mathsf{T} & B_H^\mathsf{T} \end{bmatrix} \begin{bmatrix} P_0 & 0 \\ 0 & \varepsilon I \end{bmatrix} \begin{bmatrix} B_0 \\ B_H \end{bmatrix} = B_0^\mathsf{T} P_0 B_0 + \varepsilon B_H^\mathsf{T} B_H,$$

$$\implies \mathrm{tr}\left(B^\mathsf{T} P_\varepsilon B\right) = \mathrm{tr}\left(B_0^\mathsf{T} P_0 B_0\right) + \varepsilon\,\mathrm{tr}\left(B_H^\mathsf{T} B_H\right).$$

Thus $\operatorname{tr}\left(B^{\mathsf{T}}PB\right) < \gamma^2$ if ε is sufficiently small. ■

We adopt a log-det heuristic for positive semidefinite matrices [FHB01] to iteratively reduce the rank,

$$\begin{aligned} X_{k+1} &= \arg\min_{X \in \mathcal{C}} \operatorname{tr}(W_k X), \\ W_k &= (X_k + \delta I)^{-1}, \end{aligned}$$

where $\delta > 0$ is a small constant for regularization and $\mathcal{C}$ is the feasible set determined by the LMI constraints (2.27) along with other applicable constraints. In each iteration a convex problem is formulated and hence can be efficiently solved. X_k is expected to converge to a rank deficient positive semidefinite matrix.

Example 3. Consider the generalized plant (2.16). We first generate random matrices $A \in \mathbb{R}^{5\times 5}$, $B_2 \in \mathbb{R}^{5\times 2}$, $C_2 \in \mathbb{R}^{2\times 5}$. Then we generate weighting matrices $Q \in \mathbb{R}^{5\times 5}_{++}$ and $R \in \mathbb{R}^{2\times 2}_{++}$ randomly, and set

$$B_1 = \begin{bmatrix} B_2 & 0 \end{bmatrix}, \quad C_1 = \begin{bmatrix} Q^{\frac{1}{2}} \\ 0 \end{bmatrix}, \quad D_{11} = 0, \quad D_{12} = \begin{bmatrix} 0 \\ R^{\frac{1}{2}} \end{bmatrix}, \quad D_{21} = \begin{bmatrix} 0 & I \end{bmatrix}.$$

An LQG controller is obtained of the form (2.17). The corresponding closed-loop system has H_2 norm $\|P_{\text{centralized}}\|_{H_2} = 22.0881$. We then synthesize a distributed controller having two control units given the partition $B_2 = \operatorname{row}(B_{2,1}, B_{2,2})$ and $C_2 = \operatorname{col}(C_{2,1}, C_{2,2})$. Let the associated graph Laplacian be

$$L = \begin{bmatrix} 1 & -1 \\ -1 & 1 \end{bmatrix}.$$

For all the control units we choose $A_i = \bar{A}$. Through the above log-det heuristic we get the

singular values of X

$$\sigma(X) = 10^3 \times \begin{bmatrix} 2.70717 \\ 0.02681 \\ 0 \\ 0 \\ 0 \end{bmatrix}$$

and the corresponding H_2 norm $\|P_{\text{distributed}}\|_{H_2} = 22.3467$. The difference is computed as $\|P_{\text{distributed}}\|_{H_2} - \|P_{\text{centralized}}\|_{H_2} = 0.2586$. It is seen that the rank of X is reduced while the controller performance is preserved. □

CHAPTER 3

Distributed Synthesis of Linear Control for Eigenstructure Assignment

The previous chapter shows how a linear stabilizing controller can be recovered through a distributed synthesis. This chapter focuses on a special class of control problem in which a subset of eigenvectors and eigenvalues are assigned to the closed-loop system.

3.1 General Synthesis

3.1.1 Problem Formulation

We start by defining a convenient notation for linear systems. $\mathring{P}$ is a state space system and P is the associated matrix:

$$\mathbf{y} = \mathring{P}\mathbf{u}, \quad \mathring{P} = \left[\begin{array}{c|c} A & B \\ \hline C & D \end{array}\right] \iff \begin{bmatrix} \dot{\mathbf{x}} \\ \mathbf{y} \end{bmatrix} = P \begin{bmatrix} \mathbf{x} \\ \mathbf{u} \end{bmatrix}, \quad P := \begin{bmatrix} A & B \\ C & D \end{bmatrix},$$

where $(\mathbf{x}, \mathbf{u}, \mathbf{y})$ are the state, input, and output of $\mathring{P}$, respectively.

The model of plant we consider for eigenstructure assignment problems is described by

$$\begin{aligned} \dot{\mathbf{x}} &= A\mathbf{x} + B_1\mathbf{w} + B_2\mathbf{u}, \\ \mathbf{z} &= C_1\mathbf{x} + D_{11}\mathbf{w} + D_{12}\mathbf{u}, \\ \mathbf{y} &= C_2\mathbf{x} + D_{21}\mathbf{w}, \\ \mathbf{p} &= C_p\mathbf{x} + D_p\mathbf{u}, \end{aligned} \tag{3.1}$$

where $\mathbf{x}(t) \in \mathbb{R}^n$ is the state, $\mathbf{u}(t) \in \mathbb{R}^{n_\mathbf{u}}$ the control input, $\mathbf{w}(t) \in \mathbb{R}^{n_\mathbf{w}}$ the exogenous input containing disturbance, reference, etc, $\mathbf{y}(t) \in \mathbb{R}^{n_\mathbf{y}}$ the measured output, $\mathbf{z}(t) \in \mathbb{R}^{n_\mathbf{z}}$ the performance output, $\mathbf{p}(t) \in \mathbb{R}^{n_\mathbf{p}}$ the pattern output for examining the steady state.

The objective of eigenstructure assignment is to embed prescribed eigenvalues and eigenvectors to the closed-loop system, while placing the unassigned eigenvalues in the open left half plane. We now formally define the set of controllers that achieve the design objective as follows.

Definition 1. Consider the plant (3.1), target eigenstructure $(\Pi, \Lambda) \in \mathbb{R}^{n_\mathbf{z} \times r} \times \mathbb{R}^{r \times r}$, and controller $\mathbf{u} = \mathring{K}\mathbf{y}$. Let the closed-loop system with $\mathbf{w}(t) \equiv 0$ be described by $\dot{\mathbf{x}} = \mathsf{A}_{c\ell}\mathbf{x}$ and $\mathbf{p} = \mathsf{H}_{c\ell}\mathbf{x}$ with $\mathbf{x} = \mathrm{col}(\mathbf{x}, \mathbf{x}_c)$ where $\mathbf{x}_c$ is the controller state. The controller is said to be **admissible** if the following conditions hold.

$$\Pi = \mathsf{H}_{c\ell}\mathsf{X}, \quad \mathsf{A}_{c\ell}\mathsf{X} = \mathsf{X}\Lambda, \quad \mathrm{eig}(\mathsf{A}_{c\ell}) \setminus \mathrm{eig}(\Lambda) \in \mathbb{C}_- \tag{3.2}$$

for some full column rank X. The set of admissible controllers is denoted by $\mathbb{A}$. □

The first two equalities in (3.2) basically mean that the output $\mathbf{p}(t)$ of the plant (3.1) converges to $\Pi e^{\Lambda t}\mathbf{p}_0$ for some vector $\mathbf{p}_0$, starting with an arbitrary initial state $\mathbf{x}(0)$ when $\mathbf{w}(t) \equiv 0$. Since (Π, Λ) specifies the steady state behavior of $\mathbf{p}(t)$, any eigenvalues of Λ in the open left half plane would not have any influence, and for this reason, we make the following assumption.

Assumption 1. All the eigenvalues of Λ have nonnegative real parts. □

Depending on the choice of (Π, Λ), the steady state behavior can be any combination of sinusoidal oscillations and constants. For example, the sinusoidal oscillation $\sin \omega t$ can be specified by $\Pi e^{\Lambda t}\mathbf{p}_0$ with $\Pi = \begin{bmatrix} 1 & 0 \end{bmatrix}$, $\Lambda = \begin{bmatrix} 0 & \omega \\ -\omega & 0 \end{bmatrix}$, $\mathbf{p}_0 = \begin{bmatrix} 0 \\ 1 \end{bmatrix}$. The eigenstructure assignment formalism captures control design problems for autonomous pattern formation and output regulation to reject disturbances and/or track command signals.

In addition to the admissibility, we search for controllers of distributed architecture like in the previous chapter. The formal problem statement is given below.

Problem 2. Consider the plant (3.1) and let the control input $\mathbf{u}$ and measured output $\mathbf{y}$ be partitioned as

$$\mathbf{y} = \mathrm{col}(\mathbf{y}_1, \dots, \mathbf{y}_q), \quad \mathbf{u} = \mathrm{col}(\mathbf{u}_1, \dots \mathbf{u}_q),$$

where $\mathbf{u}_i$ and $\mathbf{y}_i$ are vectors or scalars and q is the number of channels. Given the target eigenstructure $(\Pi, \Lambda) \in \mathbb{R}^{n_{\mathbf{z}} \times r} \times \mathbb{R}^{r \times r}$ and assume Assumption 1 holds. Find a distributed controller of the form (2.4) that is admissible as defined in Definition 1. □

3.1.2 Distributed Control Synthesis

The results in last chapter indicate that a distributed linear stabilizing controller can be synthesized from a centralized linear stabilizing controller. Therefore we first review the general theoretical result that solves the eigenstructure assignment problem without the requirement on the controller architecture.

Lemma 8 ([WI17, Theorem 3])**.** *Consider the plant (3.1) and target dynamics (Π, Λ), where Assumption 1 holds and (C_2, A) is detectable. The set of admissible controllers $\mathbb{A}$ in Definition 1 is nonempty if and only if there exists (X, U) such that the following regulator equation is satisfied*

$$AX + B_2U = X\Lambda, \quad \Pi = C_pX + D_pU, \tag{3.3}$$

and $(A, \hat{B}_2)$ is stabilizable, where $\hat{B}_2 := \begin{bmatrix} B_2 & -X \end{bmatrix}$. Such a controller is parametrized by

$$\begin{bmatrix} \mathbf{u} \\ \dot{\boldsymbol{\xi}} \end{bmatrix} = \begin{bmatrix} U \\ \Lambda \end{bmatrix} \boldsymbol{\xi} + \mathring{\Theta}(\mathbf{y} - C_2X\boldsymbol{\xi}) \tag{3.4}$$

for some $\mathring{\Theta}$ that stabilizes the augmented plant $(A, \hat{B}_2, C_2)$ and for some (X, U) satisfying (3.3). For this controller, the unforced ($\mathbf{w} = 0$) closed-loop trajectory satisfies

$$\mathbf{x}(t) \to Xe^{\Lambda t}\boldsymbol{\rho}_0, \quad \mathbf{u}(t) \to Ue^{\Lambda t}\boldsymbol{\rho}_0, \quad \mathbf{z}(t) \to Ze^{\Lambda t}\boldsymbol{\rho}_0, \quad \mathbf{p}(t) \to \Pi e^{\Lambda t}\boldsymbol{\rho}_0,$$

for some $\boldsymbol{\rho}_0 \in \mathbb{R}^r$ *depending on the initial state, where*

$$Z := C_1 X + D_{12} U.$$

□

We then derive a distributed controller by direct application of the results in Section 2.3 to the controller synthesis in Lemma 8. Suppose $\mathring{\Theta}$ in (3.4) is parametrized by

$$\mathring{\Theta} := \left[\begin{array}{c|c} A_q & B_q \\ \hline C_{q1} & D_{q1} \\ C_{q2} & D_{q2} \end{array}\right]. \tag{3.5}$$

The controller (3.4) is equivalent to

$$\begin{aligned} \dot{\boldsymbol{\xi}} &= \Lambda \boldsymbol{\xi} + C_{q2}\mathbf{z} + D_{q2}(\mathbf{y} - C_2 X \boldsymbol{\xi}), \\ \dot{\mathbf{z}} &= A_q \mathbf{z} + B_q(\mathbf{y} - C_2 X \boldsymbol{\xi}), \\ \mathbf{u} &= U\boldsymbol{\xi} + C_{q1}\mathbf{z} + D_{q1}(\mathbf{y} - C_2 X \boldsymbol{\xi}), \end{aligned} \quad \Longleftrightarrow \quad \begin{bmatrix} \dot{\boldsymbol{\xi}} \\ \dot{\mathbf{z}} \\ \mathbf{u} \end{bmatrix} = \left[\begin{array}{cc|c} \Lambda - D_{q2}C_2X & C_{q2} & D_{q2} \\ -B_qC_2X & A_q & B_q \\ \hline U - D_{q1}C_2X & C_{q1} & D_{q1} \end{array}\right] \begin{bmatrix} \boldsymbol{\xi} \\ \mathbf{z} \\ \mathbf{y} \end{bmatrix}. \tag{3.6}$$

Assume the output is partitioned as

$$\mathbf{y} = \mathrm{col}(\mathbf{y}_1, \dots \mathbf{y}_q), \quad C_2 = \mathrm{col}(C_{2,1}, \dots, C_{2,q}).$$

We subsequently construct a distributed controller composed of q control units. We reuse the notations $\boldsymbol{\xi}$, $\mathbf{z}$ and $\mathbf{u}$ to denote the state and output of the distributed controller. Consider the following partitions

$$\begin{aligned} B_q &= \begin{bmatrix} B_{q,1} & \dots & B_{q,q} \end{bmatrix}, & C_{q1} &= \mathrm{col}(C_{q1,1}, \dots, C_{q1,q}), \\ D_{q2} &= \begin{bmatrix} D_{q2,1} & \dots & D_{q2,q} \end{bmatrix}, & U &= \mathrm{col}(U_1, \dots, U_q), \end{aligned}$$

and assume $D_{q1} = 0$. The connectivity of the control units is described by a strongly connected directed graph with Laplacian matrix L. Let $\mathbf{r}$ be a positive vector such that $\mathbf{r}^{\mathsf{T}} L = 0$, and r_i be the i^{th} entry of $\mathbf{r}$. We construct the control units as follows.

$$\begin{aligned} \dot{\mathbf{x}}_i &= \mathcal{F}\mathbf{x}_i + \mathcal{G}_i(\mathbf{y}_i - \mathcal{C}_i\mathbf{x}_i) - \eta r_i P \sum_{j \in \mathbb{N}_i} \ell_{ij}(\mathbf{x}_j - \mathbf{x}_i), \quad \mathbf{x}_i := \mathrm{col}(\boldsymbol{\xi}_i, \mathbf{z}_i), \\ \mathbf{u}_i &= \mathcal{K}_i \mathbf{x}_i, \end{aligned} \tag{3.7}$$

where

$$\mathcal{F} := \begin{bmatrix} \Lambda & C_{q2} \\ 0 & A_q \end{bmatrix}, \quad \mathcal{G}_i := q \begin{bmatrix} D_{q2,i} \\ B_{q,i} \end{bmatrix}, \quad \mathcal{C}_i := \begin{bmatrix} C_{2,i}X & 0 \end{bmatrix}, \quad \mathcal{K}_i := \begin{bmatrix} U_i & C_{q1,i} \end{bmatrix},$$

and $P = P^{\mathsf{T}} \succ 0$.

Moreover, we show that the distributed control with a finite coupling strength η satisfies the eigenstructure condition in addition to the stability requirement. The following theorem formally proves our claim.

Theorem 5. *Consider the plant (3.1). Suppose the regulator equation (3.3) is satisfied, and $\mathring{\Theta}$ defined in (3.5) stabilizes the augmented plant $(A, \hat{B}_2, C_2)$ with $\hat{B}_2 := \begin{bmatrix} B_2 & -X \end{bmatrix}$. Then the distributed controller (3.7) is admissible as defined in Definition 1 for sufficiently large η.* □

Proof. Let the closed-loop system be denoted by

$$\dot{\mathbf{x}} = \mathcal{A}\mathbf{x}, \quad \mathbf{z} = \mathcal{H}\mathbf{x}. \tag{3.8}$$

$\mathcal{A}$ can be expressed as

$$\mathcal{A} = \begin{bmatrix} A & B_2\mathsf{K} \\ \mathsf{G}C_2 & \mathsf{F} - \mathsf{G}\mathsf{C}_2 - \eta\mathsf{P}\mathsf{L} \end{bmatrix},$$

where G, C_2, K, P are block diagonal matrices with $\mathcal{G}_i$, $\mathcal{C}_i$, $\mathcal{K}_i$, r_iP on the diagonal, respectively, and $\mathsf{F} := I \otimes \mathcal{F}$, $\mathsf{L} := L \otimes I$. Let J and N be defined as in (2.8) and (2.9). It then follows from direct calculation that

$$\mathcal{A}\mathcal{V} = \mathcal{V}\Lambda, \quad \mathcal{H}\mathcal{V} = R, \quad \mathcal{V} := \begin{bmatrix} X \\ J_1 \end{bmatrix},$$

where J_1 is formed by the first r columns of J, rendering $\mathcal{V}$ full column rank. Apply a

similarity transformation on $\mathcal{A}$,

$$\tilde{\mathcal{A}} = \left[\begin{array}{c|c} I & 0 \\ \hline 0 & \begin{array}{c} \frac{1}{q}J^\mathsf{T} \\ N^\mathsf{T} \end{array} \end{array}\right] \mathcal{A} \left[\begin{array}{c|cc} I & 0 & \\ \hline 0 & J & N \end{array}\right] = \begin{bmatrix} A & B_2U & B_2C_{q1} & * \\ D_{q2}C_2 & \Lambda - D_{q2}C_2X & C_{q2} & * \\ B_qC_2 & -B_qC_2X & A_q & * \\ * & * & * & M + \eta\mathcal{H} \end{bmatrix},$$

where $*$ denotes some matrix and $\mathcal{H} := -N^\mathsf{T}\mathsf{P}\mathsf{L}N$. Define

$$\Omega := \begin{bmatrix} A + \hat{B}_2D_qC_2 & \hat{B}_2C_q \\ B_qC_2 & A_q \end{bmatrix}, \quad \begin{aligned} \hat{B}_2 &:= \begin{bmatrix} B_2 & -X \end{bmatrix}, \\ C_q &:= \mathrm{col}(C_{q1}, C_{q2}), \\ D_q &:= \mathrm{col}(D_{q1}, D_{q2}). \end{aligned}$$

Then,

$$\tilde{\mathcal{A}} \begin{bmatrix} X & I & 0 & 0 \\ I & 0 & 0 & 0 \\ 0 & 0 & I & 0 \\ 0 & 0 & 0 & I \end{bmatrix} = \begin{bmatrix} X & I & 0 & 0 \\ I & 0 & 0 & 0 \\ 0 & 0 & I & 0 \\ 0 & 0 & 0 & I \end{bmatrix} \left[\begin{array}{c|ccc} \Lambda & * & * & * \\ \hline 0 & \multicolumn{3}{c}{\multirow{2}{*}{Ω}} & * \\ & & & & * \\ & * & * & M + \eta\mathcal{H} \end{array}\right].$$

Since

$$\mathring{\Theta} = \left[\begin{array}{c|c} A_q & B_q \\ \hline C_{q1} & D_{q1} \\ C_{q2} & D_{q2} \end{array}\right] = \left[\begin{array}{c|c} A_q & B_q \\ \hline C_q & D_q \end{array}\right]$$

stabilizes the augmented plant $(A, \hat{B}_2, C_2)$ with $\hat{B}_2 := \begin{bmatrix} B_2 & -X \end{bmatrix}$, Ω is Hurwitz. Also, $\mathcal{H}$ is Hurwitz due to Lemma 2. Finally, with the fact that $\mathrm{eig}(\mathcal{A}) = \mathrm{eig}(\tilde{\mathcal{A}})$, it follows from Lemma 7 that $\mathrm{eig}(\mathcal{A}) \setminus \mathrm{eig}(\Lambda) \subset \mathbb{C}_-$ if η is sufficiently large. ■

Example 4. We apply Theorem 5 to a flipper locomotor [Iwa12] whose equations of motion are given by

$$\begin{aligned} J\ddot{\boldsymbol{\theta}} + D\dot{\boldsymbol{\theta}} + v\Lambda\boldsymbol{\theta} &= B\mathbf{u}, \\ m\dot{v} + d(\boldsymbol{\theta})v + \dot{\boldsymbol{\theta}}^\mathsf{T}\Lambda\boldsymbol{\theta} &= 0, \end{aligned} \tag{3.9}$$

where $\boldsymbol{\theta}(t) \in \mathbb{R}^5$ are the tail joint angles, $v(t) \in \mathbb{R}$ is the velocity of the center of mass. J, D, Λ, B are constant matrices of appropriate size, and m is the total mass of the flipper. $d(\boldsymbol{\theta})$ is a linear function of $\boldsymbol{\theta}$. Define the relative joint angles

$$\boldsymbol{\phi} := B^{\mathsf{T}}\boldsymbol{\theta}.$$

Assuming constant velocity $v(t) \equiv v_0$, we obtain a LTI system in terms of $\boldsymbol{\phi}$,

$$J_0\ddot{\boldsymbol{\phi}} + D_0\dot{\boldsymbol{\phi}} + v_0\Lambda_0\boldsymbol{\phi} = \mathbf{u}, \qquad J_0 := EJE^{\mathsf{T}}, \quad D_0 := EDE^{\mathsf{T}}, \quad \Lambda_0 := E\Lambda E^{\mathsf{T}}, \quad E := B^{-1}.$$

Then the state space realization yields

$$\begin{aligned}
&\dot{\mathbf{x}} = \mathsf{A}\mathbf{x} + \mathsf{B}\mathbf{u}, \quad \mathbf{y} = \mathsf{C}\mathbf{x}, \\
&\mathbf{x} := \begin{bmatrix} \boldsymbol{\phi} \\ \dot{\boldsymbol{\phi}} \end{bmatrix}, \quad \mathsf{A} := \begin{bmatrix} 0 & I \\ -J_0^{-1}(v_0\Lambda_0) & -J_0^{-1}D_0 \end{bmatrix}, \quad \mathsf{B} := \begin{bmatrix} 0 \\ J_0^{-1} \end{bmatrix}, \quad \mathsf{C} := \begin{bmatrix} I & 0 \end{bmatrix}.
\end{aligned}$$

Let the permutation matrix be defined by

$$P := \begin{bmatrix} \mathbf{e}_1 & \mathbf{e}_3 & \mathbf{e}_5 & \mathbf{e}_7 & \mathbf{e}_9 & \mathbf{e}_2 & \mathbf{e}_4 & \mathbf{e}_6 & \mathbf{e}_8 & \mathbf{e}_{10} \end{bmatrix}$$

where $\mathbf{e}_k \in \mathbb{R}^{10}$ is the i^{th} column of the 10×10 identity matrix. Define the new state vector

$$\mathbf{x} := P\mathbf{x} = \operatorname{col}(\mathsf{x}_1, \mathsf{x}_6, \mathsf{x}_2, \mathsf{x}_7, \mathsf{x}_3, \mathsf{x}_8, \mathsf{x}_4, \mathsf{x}_9, \mathsf{x}_5, \mathsf{x}_{10}) = \operatorname{col}(\boldsymbol{\zeta}_1, \ldots, \boldsymbol{\zeta}_5), \quad \boldsymbol{\zeta}_k := \operatorname{col}(\phi_k, \dot{\phi}_k).$$

In the new coordinates,

$$\begin{aligned}
&\dot{\mathbf{x}} = \mathcal{A}\mathbf{x} + \mathcal{B}\mathbf{u}, \quad \mathbf{y} = \mathcal{C}\mathbf{x}, \\
&\mathcal{A} := P\mathsf{A}P^{\mathsf{T}}, \quad \mathcal{B} := P\mathsf{B}, \quad \mathcal{C} := \mathsf{C}P^{\mathsf{T}}.
\end{aligned} \tag{3.10}$$

The target optimal gait is given by $\boldsymbol{\phi}(t) = \Im[\hat{\boldsymbol{\phi}}e^{j\omega t}]$ where $\hat{\boldsymbol{\phi}} \in \mathbb{C}^5$ is a given phasor defining the relative phases/amplitudes of the state $\boldsymbol{\phi}$ in steady state, and ω is the frequency of the oscillations in steady state. The values are given to be

$$\hat{\boldsymbol{\phi}} = \begin{bmatrix} 4.9 + j10.2 \\ 11.7 - j21.0 \\ -26.8 - j16.0 \\ -25.1 + j28.9 \\ 24.7 + j35.4 \end{bmatrix}, \quad \omega = 21.4 \text{ rad/s}.$$

In real form

$$\boldsymbol{\phi}(t) = \begin{bmatrix} 11.3\sin(21.4t) \\ 24.1\sin(21.4t - 125.1^\circ) \\ 31.2\sin(21.4t - 146.5^\circ) \\ 38.3\sin(21.4t + 66.7^\circ) \\ 43.1\sin(21.4t + 9.2^\circ) \end{bmatrix}.$$

Consequently, the phasor of the target gait in terms of the state vector is

$$\hat{\mathbf{x}} = P\hat{\mathbf{x}}, \quad \hat{\mathbf{x}} = \begin{bmatrix} \hat{\boldsymbol{\phi}} \\ j\omega\hat{\boldsymbol{\phi}} \end{bmatrix}.$$

The state trajectory corresponding to this gait can be expressed in the real form as

$$\mathbf{x}(t) = Xe^{\Omega t}\boldsymbol{\eta} \quad X := \begin{bmatrix} \Re[\hat{\mathbf{x}}] & \Im[\hat{\mathbf{x}}] \end{bmatrix}, \quad \Omega := \begin{bmatrix} 0 & \omega \\ -\omega & 0 \end{bmatrix}, \quad \boldsymbol{\eta} := \begin{bmatrix} 0 \\ 1 \end{bmatrix}. \tag{3.11}$$

We then solve the regulator equation (3.3) for U and synthesize a controller in the form of (3.4) by applying Lemma 8. Given the centralized controller, we are about to construct a distributed controller composed of 5 control units. Assume $\mathcal{B}$ and $\mathcal{C}$ are partitioned as

$$\mathcal{B} =: \text{row}(\mathcal{B}_1, \mathcal{B}_2, \mathcal{B}_3, \mathcal{B}_4, \mathcal{B}_5), \quad \mathcal{B}_i \in \mathbb{R}^{10\times 1}\ \forall i \in \mathbb{I}_5,$$

$$\mathcal{C} =: \text{col}(\mathcal{C}_1, \mathcal{C}_2, \mathcal{C}_3, \mathcal{C}_4, \mathcal{C}_5), \quad \mathcal{C}_i \in \mathbb{R}^{1\times 10}\ \forall i \in \mathbb{I}_5.$$

The control units are connected through a nearest neighbor coupling with the graph Laplacian

$$L = \begin{bmatrix} 1 & -1 & 0 & 0 & 0 \\ -1 & 2 & -1 & 0 & 0 \\ 0 & -1 & 2 & -1 & 0 \\ 0 & 0 & -1 & 2 & -1 \\ 0 & 0 & 0 & -1 & 1 \end{bmatrix}.$$

The distributed controller is constructed by application of Theorem 5. We simulate the closed-loop system with the linearized plant (3.10) and generate randomly the initial conditions. $\phi_i(t), i \in \mathbb{I}_5$ are illustrated in Figure 3.1. The frequency and relative phases/amplitudes are exactly the same as specified by the target optimal gait.

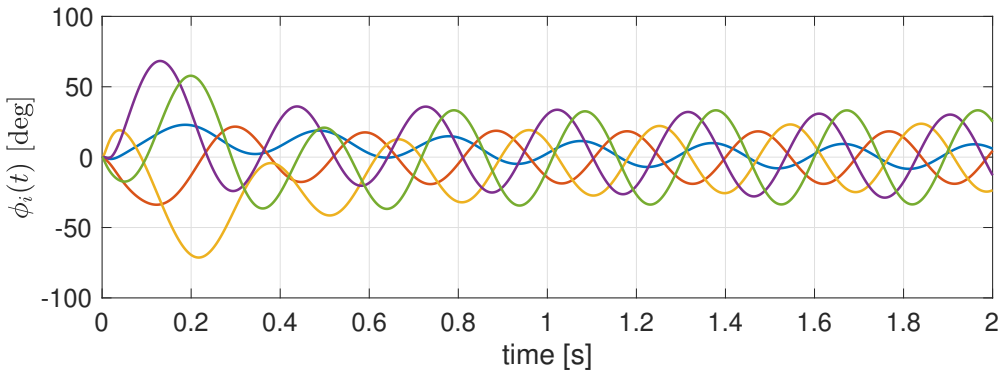

Figure 3.1: Pattern formation via a distributed controller.

The centralized controller we start with has the dimension of 10, which is of the same order as the linearized plant (3.10). By construction, each control unit specified by (3.7) has the dimension of the sum of the centralized plant and Ω. Hence the total order of the distributed controller sums up to 60. The high order of the controller may introduce complexity in implementation. We will show that the order reduction is possible when the plant has special structures such as multi-agent systems.

Though we have achieved the desired frequency and relative phase/amplitude of the target optimal gait, it is impossible to stabilize the absolute amplitude within the linear control framework. This is shown by another simulation with different initial conditions as in Figure 3.2. We will show in Section 3.2.2 that the stabilization of amplitude is made possible with a nonlinear controller. □

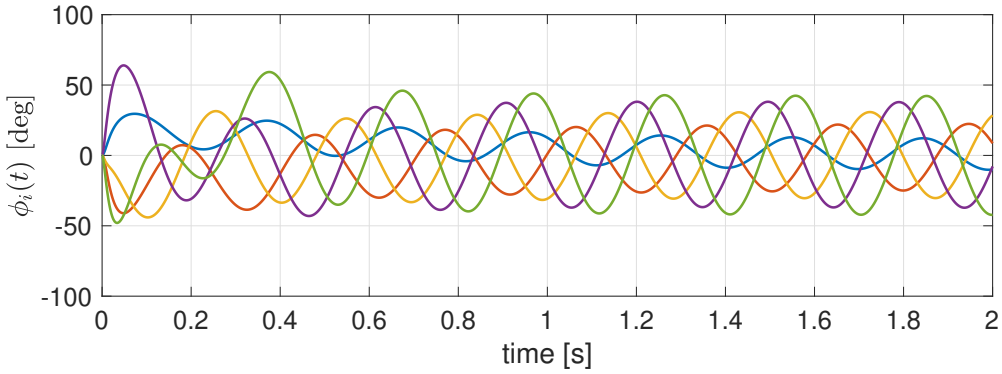

Figure 3.2: Pattern formation via a distributed controller with different initial conditions.

3.2 Synthesis for Multi-Agent Systems

3.2.1 Autonomous Pattern Formation

In this section, we consider the eigenstructure assignment problem when the plant (3.1) is a multi-agent system,

$$\dot{\mathbf{x}}_i = A_i\mathbf{x}_i + B_{2,i}\mathbf{u}_i, \quad i \in \mathbb{I}_q,$$

$$\mathbf{y}_i = C_{2,i}\mathbf{x},$$

where we assume $\mathbf{w} \equiv 0$. This is equivalent to say A, B_2, C_2 are block diagonal,

$$A = \begin{bmatrix} A_1 & & \\ & \ddots & \\ & & A_q \end{bmatrix}, \quad B_2 = \begin{bmatrix} B_{2,1} & & \\ & \ddots & \\ & & B_{2,q} \end{bmatrix}, \quad C_2 = \begin{bmatrix} C_{2,1} & & \\ & \ddots & \\ & & C_{2,q} \end{bmatrix}. \tag{3.12}$$

Theorem 5 gives a solution to the distributed control problem for multi-agent systems. However, each control unit has the state dimension equal to the dimension of Λ plus $\mathring{\Theta}$. Since $\mathring{\Theta}$ is supposed to stabilize the augmented plant which has a dimension of the sum of the dimensions of all agents, the dimension of $\mathring{\Theta}$ is often about the same as the entire plant. This may exhibit difficulty in implementation due to the controller's large complexity. Nonetheless, the complexity may be reduced by exploiting the fact that the plant is a collection of multiple agents without direct interactions. We will show that the complexity

reduction is possible under the assumption that each agent is detectable utilizing observers. To this end, we first give an observer-based centralized control solution to the eigenstructure problem, which is a special case of Lemma 8.

Lemma 9. *Consider the plant (3.1) and target dynamics (Π, Λ). Assume Assumption 1 holds and (C_2, A) is detectable. The set of admissible controllers $\mathbb{A}$ in Definition 1 is nonempty if and only if there exists (X, U) such that the regulator equation (3.3) holds and $(A, \hat{B}_2)$ is stabilizable, where $\hat{B}_2 := \begin{bmatrix} B_2 & -X \end{bmatrix}$. Then an observer-based controller $\mathring{K} \in \mathbb{A}$ is given by*

$$\begin{aligned} \dot{\hat{\mathbf{x}}} &= A\hat{\mathbf{x}} + B_2\mathbf{u} + \mathsf{F}(C_2\hat{\mathbf{x}} - \mathbf{y}), \\ \dot{\boldsymbol{\xi}} &= \Lambda\boldsymbol{\xi} + E(C_2\hat{\mathbf{x}} - \mathbf{y}), \\ \mathbf{u} &= (U - \mathsf{K}X)\boldsymbol{\xi} + \mathsf{K}\hat{\mathbf{x}}, \end{aligned} \tag{3.13}$$

for some E, F, and K such that $A + B_2\mathsf{K}$ and $A + \mathsf{F}C_2$ are Hurwitz. □

Proof. Define $\mathbf{e} := \mathbf{x} - \hat{\mathbf{x}}$, $\hat{\mathbf{e}} := \hat{\mathbf{x}} - X\boldsymbol{\xi}$. We have

$$\begin{aligned} \dot{\mathbf{e}} &= \dot{\mathbf{x}} - \dot{\hat{\mathbf{x}}} \\ &= A\mathbf{x} + B_2\mathbf{u} - (A\hat{\mathbf{x}} + B_2\mathbf{u} + \mathsf{F}(C_2\hat{\mathbf{x}} - \mathbf{y})) \\ &= (A + \mathsf{F}C_2)\mathbf{e}, && (\mathbf{y} = C_2\mathbf{x}) \end{aligned}$$

$$\dot{\boldsymbol{\xi}} = \Lambda\boldsymbol{\xi} + E(C_2\hat{\mathbf{x}} - \mathbf{y}) = \Lambda\boldsymbol{\xi} - EC_2\mathbf{e},$$

$$\begin{aligned} \dot{\hat{\mathbf{e}}} &= \dot{\hat{\mathbf{x}}} - X\dot{\boldsymbol{\xi}} \\ &= A\hat{\mathbf{x}} + B_2\mathbf{u} + \mathsf{F}(C_2\hat{\mathbf{x}} - \mathbf{y}) - X\left(\Lambda\boldsymbol{\xi} + E(C_2\hat{\mathbf{x}} - \mathbf{y})\right) \\ &= A\left(\hat{\mathbf{e}} + X\boldsymbol{\xi}\right) + B_2(U\boldsymbol{\xi} + \mathsf{K}\hat{\mathbf{e}}) - X\Lambda\boldsymbol{\xi} + (XE - \mathsf{F})C_2\mathbf{e} \\ &\qquad\qquad (\mathbf{u} = (U - \mathsf{K}X)\boldsymbol{\xi} + \mathsf{K}\hat{\mathbf{x}} = U\boldsymbol{\xi} + \mathsf{K}\hat{\mathbf{e}}) \\ &= (A + B_2\mathsf{K})\hat{\mathbf{e}} + (XE - \mathsf{F})C_2\mathbf{e}. && (AX + B_2U = X\Lambda) \end{aligned}$$

Thus the closed-loop system is given by

$$\dot{\mathbf{x}} = \mathsf{A}_{c\ell}\mathbf{x}$$

where $\boldsymbol{\chi} = \mathrm{col}(\boldsymbol{\xi}, \hat{\mathbf{e}}, \mathbf{e})$ and

$$\mathsf{A}_{c\ell} = \begin{bmatrix} \Lambda & 0 & -EC_2 \\ 0 & A + B_2\mathsf{K} & (XE - \mathsf{F})C_2 \\ 0 & 0 & A + \mathsf{F}C_2 \end{bmatrix}.$$

Clearly

$$\mathsf{A}_{c\ell} \begin{bmatrix} I \\ 0 \\ 0 \end{bmatrix} = \begin{bmatrix} I \\ 0 \\ 0 \end{bmatrix} \Lambda$$

and $\mathrm{eig}(\mathsf{A}_{c\ell}) \setminus \mathrm{eig}(\Lambda) \in \mathbb{C}_-$ since $A + B_2\mathsf{K}$ and $A + \mathsf{F}C_2$ are Hurwitz, rendering the observer-based controller (3.13) admissible. ■

Consider applying Lemma 9 and Theorem 5 to a multi-agent system with the state space matrices (3.12). Each control unit would have an observer of the entire plant. However, if $(C_{2,i}, A_i)$ is observable, then the observer dynamics of the entire controller in (3.13) do not need to be repeated in each control unit, and this leads to the order reduction of the controller.

For multi-agent systems, K, F in Lemma 9 can be made block diagonal,

$$\mathsf{K} = \begin{bmatrix} K_1 & & \\ & \ddots & \\ & & K_q \end{bmatrix}, \quad \mathsf{F} = \begin{bmatrix} F_1 & & \\ & \ddots & \\ & & F_q \end{bmatrix},$$

such that $A_i + B_{2,i}K_i$ and $A_i + F_iC_{2,i}$ are Hurwitz for all $i \in \mathbb{I}_q$. We also make the partition $E = \mathrm{row}(E_1, \ldots, E_q)$, $U = \mathrm{col}(U_1, \ldots, U_q)$, $X = \mathrm{col}(X_1, \ldots, X_q)$. The distributed controller

is proposed to be

$$\begin{aligned}
\dot{\hat{\mathbf{x}}}_i &= A_i\hat{\mathbf{x}}_i + B_{2,i}\mathbf{u}_i + F_i(C_{2,i}\hat{\mathbf{x}}_i - \mathbf{y}_i), \quad i \in \mathbb{I}_q,\\
\dot{\boldsymbol{\xi}}_i &= \Lambda\boldsymbol{\xi}_i + E_i(C_{2,i}\hat{\mathbf{x}}_i - \mathbf{y}_i) + G_i\mathbf{z}_i,\\
\mathbf{z}_i &= \eta\sum_{j\in\mathbb{N}_i}\ell_{ij}(\boldsymbol{\xi}_j - \boldsymbol{\xi}_i),\\
\mathbf{u}_i &= (U_i - K_iX_i)\boldsymbol{\xi}_i + K_i\hat{\mathbf{x}}_i,
\end{aligned} \tag{3.14}$$

where $L := [\ell_{ij}]$ is the Laplacian matrix associated with the graph that depicts the interconnection of the control units, G_i are design parameters to be defined later, $\mathbb{N}_i$ is the set of the neighbors of i^{th} control unit, and $\eta > 0$ is the coupling strength. Each control unit has an observer over the local agent only, and the interaction across control units is done through $\boldsymbol{\xi}_i, i \in \mathbb{I}_q$. We prove that the proposed distributed controller (3.14) is indeed admissible in the theorem that follows.

Theorem 6. *Suppose L is the Laplacian matrix of a strongly connected directed graph with positive weights. Let $\mathbf{r}$ be a positive vector such that $\mathbf{r}^{\mathsf{T}}L = 0$, and r_i be the i^{th} entry of $\mathbf{r}$. The distributed controller (3.14) is admissible with sufficiently large η if the centralized controller (3.13) is admissible and $G_i = r_iP$ where $P = P^{\mathsf{T}} \succ 0$.* □

Proof. The distributed controller (3.14) in matrix form is expressed as

$$\begin{bmatrix}\dot{\hat{\mathbf{x}}}\\ \dot{\boldsymbol{\xi}}\\ \mathbf{u}\end{bmatrix} = \begin{bmatrix}A + B_2\mathsf{K} + \mathsf{F}C_2 & B_2(\mathsf{U} - \mathsf{K}\mathsf{X}) & -\mathsf{F}\\ \mathsf{E}C_2 & \Lambda & -\mathsf{E}\\ \mathsf{K} & \mathsf{U} - \mathsf{K}\mathsf{X} & 0\end{bmatrix}\begin{bmatrix}\hat{\mathbf{x}}\\ \boldsymbol{\xi}\\ \mathbf{y}\end{bmatrix}, \quad \begin{aligned}\mathbf{x} &:= \operatorname{col}(\mathbf{x}_1,\dots,\mathbf{x}_q),\\ \boldsymbol{\xi} &:= \operatorname{col}(\boldsymbol{\xi}_1,\dots,\boldsymbol{\xi}_q),\\ \mathbf{u} &:= \operatorname{col}(\mathbf{u}_1,\dots,\mathbf{u}_q),\\ \mathbf{y} &:= \operatorname{col}(\mathbf{y}_1,\dots,\mathbf{y}_q),\end{aligned} \tag{3.15}$$

where

$$\mathsf{E} := \begin{bmatrix}E_1 & & \\ & \ddots & \\ & & E_q\end{bmatrix}, \quad \mathsf{U} := \begin{bmatrix}U_1 & & \\ & \ddots & \\ & & U_q\end{bmatrix}, \quad \mathsf{X} := \begin{bmatrix}X_1 & & \\ & \ddots & \\ & & X_q\end{bmatrix}.$$

Let J and N be defined as in (2.8) and (2.9) and define the coordinate transformation

$$\begin{bmatrix} \boldsymbol{\varphi} \\ \boldsymbol{\phi} \end{bmatrix} := \begin{bmatrix} \frac{1}{q} J^{\mathsf{T}} \\ N^{\mathsf{T}} \end{bmatrix} \boldsymbol{\xi} \iff \boldsymbol{\xi} = \begin{bmatrix} J & N \end{bmatrix} \begin{bmatrix} \boldsymbol{\varphi} \\ \boldsymbol{\phi} \end{bmatrix}.$$

Then the controller in the new coordinate is expressed as,

$$\begin{bmatrix} \dot{\hat{\mathbf{x}}} \\ \dot{\boldsymbol{\varphi}} \\ \dot{\boldsymbol{\phi}} \\ \mathbf{u} \end{bmatrix} = \begin{bmatrix} A + B_2\mathsf{K} + \mathsf{F}C_2 & B_2(U - \mathsf{K}X) & B_2(\mathsf{U} - \mathsf{K}\mathsf{X}) & -\mathsf{F} \\ EC_2 & \Lambda & \frac{1}{q} J^{\mathsf{T}} \Lambda N & -E \\ N^{\mathsf{T}}\mathsf{E}C_2 & N^{\mathsf{T}}\Lambda J & N^{\mathsf{T}}\Lambda N + \eta N^{\mathsf{T}}\mathsf{G}\mathsf{L}N & -N^{\mathsf{T}}\mathsf{E} \\ \mathsf{K} & U - \mathsf{K}X & (\mathsf{U} - \mathsf{K}\mathsf{X})N & 0 \end{bmatrix} \begin{bmatrix} \hat{\mathbf{x}} \\ \boldsymbol{\varphi} \\ \boldsymbol{\phi} \\ \mathbf{y} \end{bmatrix}, \tag{3.16}$$

where

$$\mathsf{G} := \begin{bmatrix} G_1 & & \\ & \ddots & \\ & & G_m \end{bmatrix}, \quad \mathsf{L} := L \otimes I, \quad \Lambda := I \otimes \Lambda.$$

The closed-loop system composed of the multi-agent system and the centralized controller (3.13) is

$$\begin{bmatrix} \dot{\mathbf{x}} \\ \dot{\hat{\mathbf{x}}} \\ \dot{\boldsymbol{\xi}} \end{bmatrix} = \begin{bmatrix} A & B_2\mathsf{K} & B_2(U - \mathsf{K}X) \\ -\mathsf{F}C_2 & A + B_2\mathsf{K} + \mathsf{F}C_2 & B_2(U - \mathsf{K}X) \\ -EC_2 & EC_2 & \Lambda \end{bmatrix} \begin{bmatrix} \mathbf{x} \\ \hat{\mathbf{x}} \\ \boldsymbol{\xi} \end{bmatrix}. \tag{3.17}$$

While the closed-loop system composed of the multi-agent system and the distributed controller in the new coordinate (3.16) is

$$\begin{bmatrix} \dot{\mathbf{x}} \\ \dot{\hat{\mathbf{x}}} \\ \dot{\boldsymbol{\varphi}} \\ \dot{\boldsymbol{\phi}} \end{bmatrix} = \begin{bmatrix} A & B_2\mathsf{K} & B_2(U - \mathsf{K}X) & B_2(\mathsf{U} - \mathsf{K}\mathsf{X})N \\ -\mathsf{F}C_2 & A + B_2\mathsf{K} + \mathsf{F}C_2 & B_2(U - \mathsf{K}X) & B_2(\mathsf{U} - \mathsf{K}\mathsf{X}) \\ -EC_2 & EC_2 & \Lambda & \frac{1}{q} J^{\mathsf{T}} \Lambda N \\ -N^{\mathsf{T}}\mathsf{E}C_2 & N^{\mathsf{T}}\mathsf{E}C_2 & N^{\mathsf{T}}\Lambda J & N^{\mathsf{T}}\Lambda N + \eta N^{\mathsf{T}}\mathsf{G}\mathsf{L}N \end{bmatrix} \begin{bmatrix} \mathbf{x} \\ \hat{\mathbf{x}} \\ \boldsymbol{\varphi} \\ \boldsymbol{\phi} \end{bmatrix}. \tag{3.18}$$

We first show that the eigenstructure is satisfied,

$$\begin{bmatrix} A & B_2\mathsf{K} & B_2(U-\mathsf{K}X) & B_2(\mathsf{U}-\mathsf{K}\mathsf{X})N \\ -\mathsf{F}C_2 & A+B_2\mathsf{K}+\mathsf{F}C_2 & B_2(U-\mathsf{K}X) & B_2(\mathsf{U}-\mathsf{K}\mathsf{X}) \\ -EC_2 & EC_2 & \Lambda & \frac{1}{q}J^{\mathsf{T}}\Lambda N \\ -N^{\mathsf{T}}\mathsf{E}C_2 & N^{\mathsf{T}}\mathsf{E}C_2 & N^{\mathsf{T}}\Lambda J & N^{\mathsf{T}}\Lambda N+\eta N^{\mathsf{T}}\mathsf{G}\mathsf{L}N \end{bmatrix} \begin{bmatrix} X \\ X \\ I \\ 0 \end{bmatrix} = \begin{bmatrix} X \\ X \\ I \\ 0 \end{bmatrix} \Lambda. \quad (3.19)$$

Then we examine the eigenvalues. Define $\mathbf{e} := \mathbf{x} - \hat{\mathbf{x}}$, we have

$$\begin{bmatrix} \dot{\hat{\mathbf{x}}} \\ \dot{\boldsymbol{\varphi}} \\ \dot{\boldsymbol{\phi}} \\ \dot{\mathbf{e}} \end{bmatrix} = \begin{bmatrix} A+B_2\mathsf{K} & B_2(U-\mathsf{K}X) & B_2(\mathsf{U}-\mathsf{K}\mathsf{X})N & -\mathsf{F}C_2 \\ 0 & \Lambda & \frac{1}{q}J^{\mathsf{T}}\Lambda N & -EC_2 \\ 0 & 0 & N^{\mathsf{T}}\Lambda N+\eta N^{\mathsf{T}}\mathsf{G}\mathsf{L}N & -N^{\mathsf{T}}\mathsf{E}C_2 \\ 0 & 0 & 0 & A+\mathsf{F}C_2 \end{bmatrix} \begin{bmatrix} \hat{\mathbf{x}} \\ \boldsymbol{\varphi} \\ \boldsymbol{\phi} \\ \mathbf{e} \end{bmatrix}. \quad (3.20)$$

Therefore the stability of the closed-loop system is determined by $A+B_2\mathsf{K}$, $A+\mathsf{F}C_2$, which are Hurwitz by assumption, and $N^{\mathsf{T}}\Lambda N+\eta N^{\mathsf{T}}\mathsf{G}\mathsf{L}N$, which is Hurwitz for sufficiently large η by Lemma 2. This completes the proof. ■

Remark 4. Theorem 6 implies that by exploiting the structure of a multi-agent system and the local observability, a pattern formation can be achieved by a distributed controller based on local observers. Subsequently each control unit for a local agent has a dimension of a local observer plus that of the pattern generator whose dynamics is captured by Λ. This greatly reduces the controller complexity compared to the general distributed control synthesis presented in Theorem 5. □

3.2.2 Potential for Extension to Nonlinear Control

The controller that achieves eigenstructure assignment given in (3.4) can be illustrated by the block diagram in Figure 3.3, where

$$Q_1(s) := \left[\begin{array}{c|c} A_q & B_q \\ \hline C_{q1} & D_{q1} \end{array}\right], \quad Q_2(s) := \left[\begin{array}{c|c} A_q & B_q \\ \hline C_{q2} & D_{q2} \end{array}\right], \quad \mathring{\Theta} := \left[\begin{array}{c|c} A_q & B_q \\ \hline C_{q1} & D_{q1} \\ C_{q2} & D_{q2} \end{array}\right],$$

and the pattern generator is a linear internal model with the transfer function

$$P(s) = (sI - \Lambda)^{-1}.$$

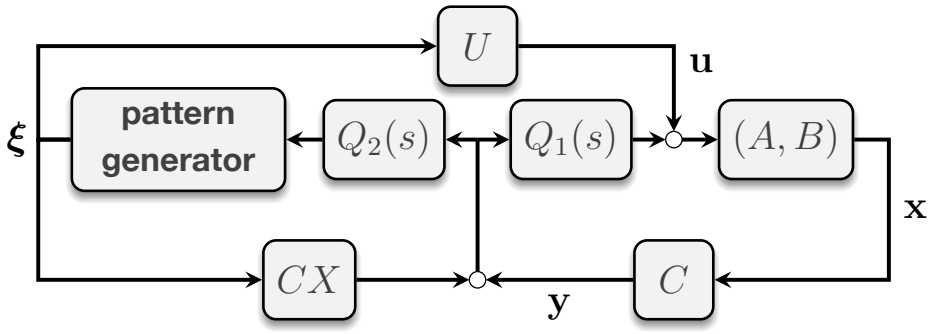

Figure 3.3: Block diagram of the control system for eigenstructure assignment problems.

When the plant is a multi-agent system, we apply Theorem 6 to synthesize a distributed controller of the form (3.14). Hence the pattern generator in the block diagram becomes a distributed network of control units. Unfortunately, within the linear framework the oscillation is not structurally stable and lacks convergence of the oscillation amplitude to prescribed values. A stable limit cycle may be achieved by replacing the linear internal model (Λ dynamics) by a nonlinear oscillator. We demonstrate the potential extension to nonlinear control by the following example.

Example 5. We consider the flipper locomotor (3.9) in Example 4. In the solution we present in Example 4, each control unit has a copy of Λ dynamics as a pattern generator. Now we seek to replace it by a nonlinear oscillator. Note that the target optimal gait is given by $\boldsymbol{\phi}(t) = \Im[\hat{\boldsymbol{\phi}} e^{j\omega t}]$ where $\hat{\boldsymbol{\phi}} \in \mathbb{C}^5$ is a given phasor and ω is the frequency. To correctly generate the reference signals for the state variable, we need 5 oscillators that have the target oscillation $\boldsymbol{\phi}(t)$ as the limit cycle. To this end, we first introduce the Andronov-Hopf oscillator (AHO) parametrized by

$$\dot{\boldsymbol{\xi}} = \begin{bmatrix} \sigma(\boldsymbol{\xi}) & \omega \\ -\omega & \sigma(\boldsymbol{\xi}) \end{bmatrix} \boldsymbol{\xi}, \quad \sigma(\boldsymbol{\xi}) := \mu(1 - \|\boldsymbol{\xi}\|_2^2), \tag{3.21}$$

where $\boldsymbol{\xi} \in \mathbb{R}^2$ is the oscillator state, ω is the frequency of the periodic signal $\boldsymbol{\xi}$ converges to, $\mu > 0$ is a design parameter. It is known that

$$\boldsymbol{\xi}(t) \to \begin{bmatrix} \sin \omega t \\ \cos \omega t \end{bmatrix}$$

with orbital stability[1]. We continue to consider a network of coupled AHOs described by

$$\dot{\boldsymbol{\xi}}_i = \begin{bmatrix} \sigma(\boldsymbol{\xi}_i) & \omega \\ -\omega & \sigma(\boldsymbol{\xi}_i) \end{bmatrix} \boldsymbol{\xi}_i + \sum_{j=1}^{n} \delta_{ij}(\boldsymbol{\xi}_i - \mho_{ij}\boldsymbol{\xi}_j), \quad i \in \mathbb{I}_5, \tag{3.22}$$

to achieve the target oscillation

$$\mathbf{h}_i(t) = \begin{bmatrix} \sin(\omega t + \beta_i) \\ \cos(\omega t + \beta_i) \end{bmatrix}, \quad \beta_i := \angle \hat{\phi}_i,$$

where $\mho_{ij}$ is chosen by

$$\mho_{ij} := \mho_i \mho_j^{\mathsf{T}}, \quad \mho_i := \begin{bmatrix} \cos \beta_i & \sin \beta_i \\ -\sin \beta_i & \cos \beta_i \end{bmatrix}.$$

The coupling $\Delta := [\delta_{ij}]$ should be chosen such that $\Delta \mathbf{1} = 0$ for the target to be a solution, and $-\Delta \in \mathbb{H}_o$ for orbital stability[2] [PN01, PSN02, PS07, LI17]. These conditions, together with the nearest neighbor coupling requirement, can be met by choosing

$$\Delta = \begin{bmatrix} \delta_1 & -\delta_1 & 0 & 0 & 0 \\ -\delta_2 & 2\delta_2 & -\delta_2 & 0 & 0 \\ 0 & -\delta_3 & 2\delta_3 & -\delta_3 & 0 \\ 0 & 0 & -\delta_4 & 2\delta_4 & -\delta_4 \\ 0 & 0 & 0 & -\delta_5 & \delta_5 \end{bmatrix}, \quad \delta_i > 0.$$

We choose $\delta_i = 1$ for all i.

Figure 3.4 shows one simulation example of the AHO network. The top figure illustrates the first entry of $\boldsymbol{\xi}_i$ for $i \in \mathbb{I}_5$, while the state of the 5^{th} oscillator is shown in the bottom figure. We see that in addition to the pattern, the amplitude is stabilized as well.

[1] The definition of orbital stability is introduced in Definition 2 in a later chapter.

[2] The definition of $\mathbb{H}_o$ is presented in Definition 3 in a later chapter.

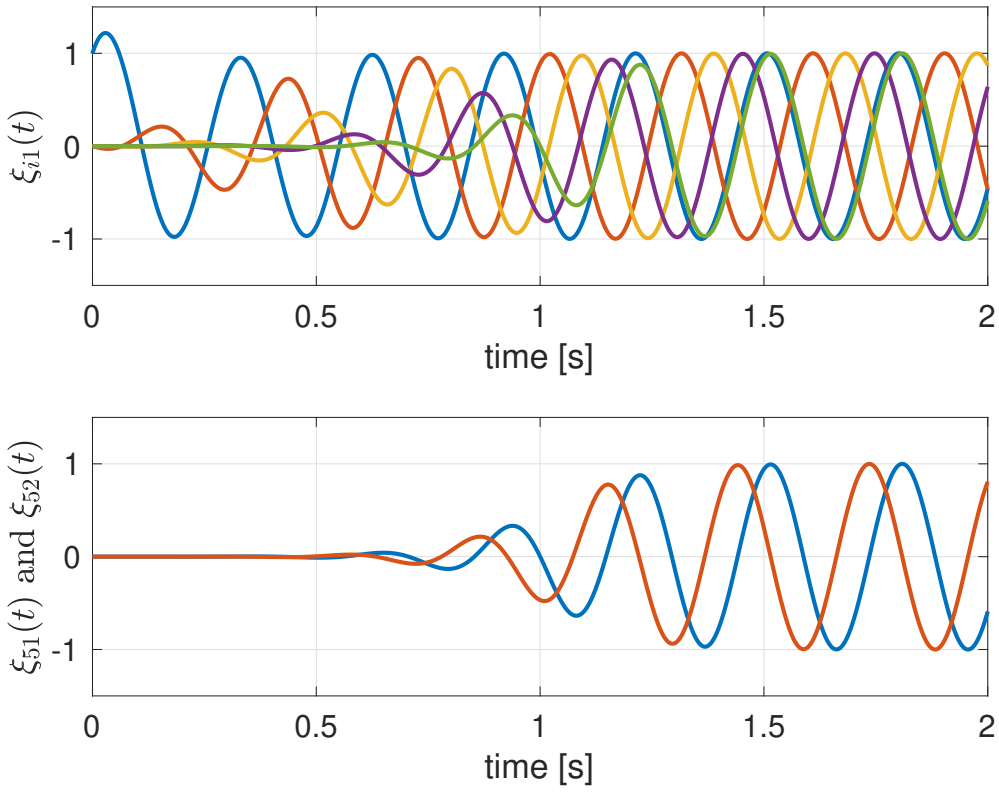

Figure 3.4: Coupled Andronov-Hopf oscillators.

Consider a decentralized output regulator of the form

$$\mathbf{u} = \mathsf{U}\boldsymbol{\xi} + Q(\mathbf{y} - \mathcal{C}\mathsf{X}\boldsymbol{\xi}), \quad \dot{\boldsymbol{\xi}} = \varphi(\boldsymbol{\xi}),$$

to achieve convergence to the optimal gait defined in (3.11), where $\dot{\boldsymbol{\xi}} = \varphi(\boldsymbol{\xi})$ is the network oscillator constructed by (3.22), Q is a constant matrix. The controller structure is decentralized in the sense that $\mathbf{u}_i$ depends only on $\mathbf{y}_i$ and $\boldsymbol{\xi}_i$. This requires U, X, Q to be block diagonal. (3.11) defines X, and we solve the regulator equation (3.3) for U. Then X and U are partitioned as

$$X =: \mathrm{col}(X_1, \ldots, X_5), \quad U =: \mathrm{col}(U_1, \ldots, U_5).$$

Note that

$$\mathbf{h}(t) = He^{\Omega t}\boldsymbol{\eta}, \quad H = \mathrm{col}(H_1, \ldots, H_5), \quad H_i := \begin{bmatrix} \cos\beta_i & \sin\beta_i \\ -\sin\beta_i & \cos\beta_i \end{bmatrix} = \mathcal{O}_i, \quad \boldsymbol{\eta} := \begin{bmatrix} 0 \\ 1 \end{bmatrix}.$$

The matrix pair (X, U) can be chosen as

$$\mathsf{X} = \mathrm{diag}(\mathsf{X}_1, \ldots, \mathsf{X}_5), \quad \mathsf{U} = \mathrm{diag}(\mathsf{U}_1, \ldots, \mathsf{U}_5), \quad \mathsf{X}_i := X_i H_i^{-1}, \quad \mathsf{U}_i = U_i H_i^{-1}.$$

The gain Q needs to stabilize the plant $(\mathcal{A}, \mathcal{B}, \mathcal{C})$. With $Q = -kI$ with stiffness k, the closed-loop for this pair is

$$J_0\ddot{\boldsymbol{\phi}} + D_0\dot{\boldsymbol{\phi}} + (v_0\Lambda_0 + kI)\boldsymbol{\phi} = 0,$$

which is stable for sufficiently large $k > 0$. We choose $k = 5 \times 10^{-4}$.

We simulate the closed-loop system with the nonlinear oscillator network as the pattern generator and treat the velocity of the center of mass as a variable instead of assuming a constant rate. The top figure in Figure 3.5 shows that with a nonlinear controller, the plant state $\phi_i(t), \forall i \in \mathbb{I}_5$ converges to the target pattern of a prescribed amplitude. The bottom indicates the velocity achieves the desired value which is set to be -0.15 m/s with a tolerable undulation.

□

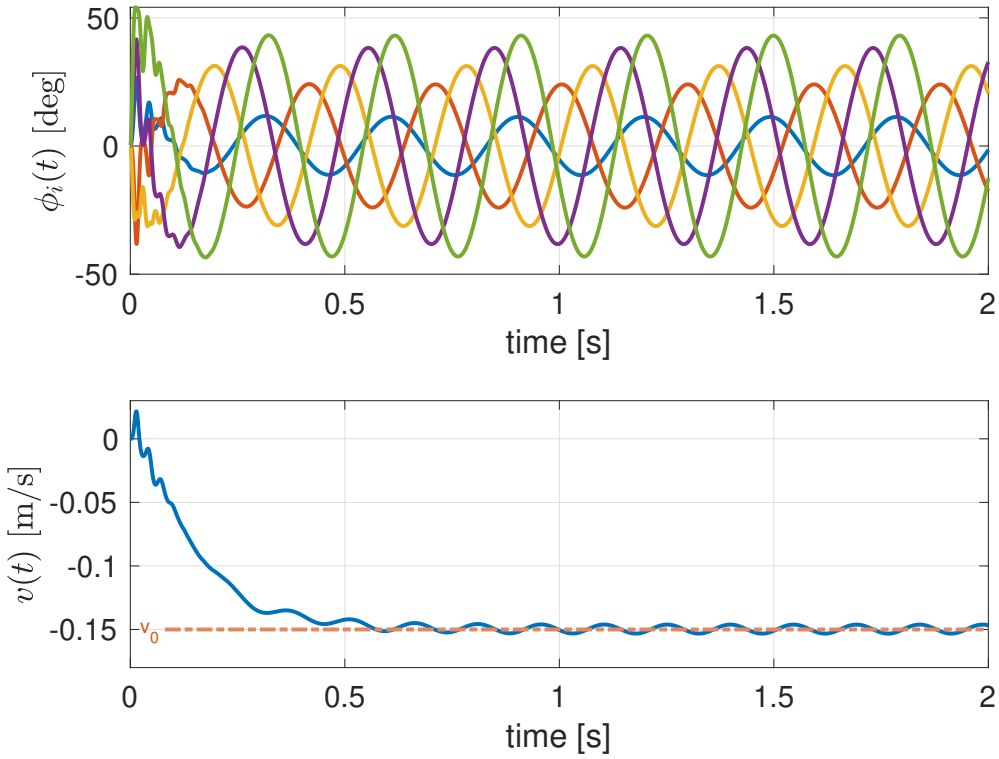

Figure 3.5: Nonlinear pattern formation for the flipper locomotor. Top: relative joint angles. Bottom: velocity of the center of mass.

Example 5 shows that by replacing the linear internal model in the controller with a nonlinear oscillator network, not only is the desired eigenstructure assigned, but also the amplitude of the target oscillation is stabilized. This motivates us to investigate the design of coupled nonlinear oscillators that has the target oscillation as its stable limit cycle. In addition, we may want to have a pattern formation controller for the flipper locomotor that is able to switch gaits for different situations. Therefore, though coupled AHO design is already possible by the existing results, it would be beneficial to be able to design a distributed network oscillator with multiple limit cycles. The following chapters are focused on the design of such network oscillators.

CHAPTER 4

Network of Linearly Coupled Oscillators

4.1 Problem Formulation

In Section 3.2.2, we have shown the potential of pattern formation control with AHO network as the reference generator. We would like to investigate a more general oscillator model that preserves all the merits the AHO network exhibits and in addition admits multiple limit cycles with stability.

4.1.1 Problem Statement

We consider the design of a nonlinear oscillator such that multiple periodic solutions are embedded in the state space as locally stable limit cycles, where the desired period, amplitudes, phases, and temporal shapes are prescribed for each solution. In particular, consider a nonlinear dynamical system

$$\dot{\mathbf{x}} = \mathfrak{f}(\mathbf{x}), \quad \mathbf{y} = \mathfrak{h}(\mathbf{x}), \quad \mathbf{x}(t) \in \mathbb{R}^{\mathfrak{n}}, \quad \mathbf{y}(t) \in \mathbb{R}^{n}, \tag{4.1}$$

assume that a target oscillation $\boldsymbol{\eta}(t) \in \mathbb{R}^n$ has frequency $\omega \in \mathbb{R}$, phase $\boldsymbol{\varphi} \in \mathbb{R}^n$, and temporal shape as well as amplitude characterized by a 2π-periodic function $\mathfrak{s}_i : \mathbb{R} \mapsto \mathbb{R}, i \in \mathbb{I}_m$. Then the target oscillation can be described by

$$\eta_i(t) = \mathfrak{s}_i(\omega t + \varphi_i), \quad i \in \mathbb{I}_m. \tag{4.2}$$

For example, $\mathfrak{s}_i(\theta_i) := \alpha_i \sin\theta_i$ for $i \in \mathbb{I}_n$ makes $\eta_i(t)$ sinusoidal with amplitude α_i. The phase variable φ_i can be absorbed into the shape function $\mathfrak{s}_i$, but we keep this redundant

description for design flexibility.

The problem is to find functions $\mathfrak{f}$ and $\mathfrak{h}$ so that system (4.1) has a periodic solution $\mathbf{x} = \boldsymbol{\xi}$ that yields $\mathbf{y} = \boldsymbol{\eta}$, and convergence to the periodic orbit is locally guaranteed. The convergence property follows the notion of orbital stability defined in [HC94] and is precisely characterized as follows.

Definition 2 (orbital stabilty)**.** Let $\boldsymbol{\chi}(t) = \boldsymbol{\xi}(t) \in \mathbb{R}^{\mathfrak{n}}$ be a periodic solution to the autonomous system (4.1). The orbit of $\boldsymbol{\xi}(t)$ in state space is represented by a closed curve

$$\mathbb{O} := \{\, \boldsymbol{\xi}(t) \in \mathbb{R}^{\mathfrak{n}} : t \geq 0 \,\}.$$

Define the distance between the state $\boldsymbol{\chi}$ and the orbit $\mathbb{O}$ to be

$$\operatorname{dist}(\boldsymbol{\chi}, \mathbb{O}) := \inf_{\mathbf{o} \in \mathbb{O}} ||\boldsymbol{\chi} - \mathbf{o}||.$$

Then $\boldsymbol{\xi}$ is said to be **orbitally stable** if for any $\varepsilon > 0$, there exists a $\delta > 0$ such that if $\operatorname{dist}(\boldsymbol{\chi}(0), \mathbb{O}) < \delta$, $\operatorname{dist}(\boldsymbol{\chi}(t), \mathbb{O}) < \varepsilon$ for all $t \geq 0$. $\boldsymbol{\xi}$ is said to be **asymptotically orbitally stable** if $\boldsymbol{\xi}$ is orbitally stable and there exists a $\delta > 0$ such that if $\operatorname{dist}(\boldsymbol{\chi}(0), \mathbb{O}) < \delta$,

$$\lim_{t \to \infty} \operatorname{dist}(\boldsymbol{\chi}(t), \mathbb{O}) = 0.$$

$\boldsymbol{\xi}$ is said to be **exponentially orbitally stable** if $\boldsymbol{\xi}$ is asymptotically orbitally stable and there exist $\delta > 0, c > 0, \sigma > 0$ such that if $\operatorname{dist}(\boldsymbol{\chi}(0), \mathbb{O}) < \delta$,

$$\operatorname{dist}(\boldsymbol{\chi}(t), \mathbb{O}) \leq c e^{-\sigma t}, \quad \forall t \geq 0.$$

□

Throughout this dissertation, we will use the term **orbital stability** to implicitly refer to the notion of **exponential orbital stability** for conciseness.

With the definition of orbital stability, we now formally state the problem.

Problem 3 (multiple limit cycle design)**.** Consider a nonlinear dynamical system given by (4.1). Let $\mathfrak{m}$ periodic functions $\boldsymbol{\eta}^k(t) \in \mathbb{R}^n, k \in \mathbb{I}_\mathfrak{m}$ be prescribed as in (4.2). Find functions $\mathfrak{f}(\cdot)$ and $\mathfrak{h}(\cdot)$ such that the system has $\mathfrak{m}$ periodic solutions $\mathbf{x}(t) = \boldsymbol{\xi}^k(t)$ as its orbitally stable limit cycles that yield $\mathfrak{y}(t) = \boldsymbol{\eta}^k(t)$ for all $k \in \mathbb{I}_\mathfrak{m}$. □

The single limit cycle design problem is a special case when of Problem 3 when there is only one such periodic solution of interest. Or conversely, Problem 3 is an extension of single limit cycle design problem. Without loss of generality, we describe our methods in terms of the single limit cycle design problem in the subsection that follows.

4.1.2 Approach

Our approach can be outlined as follows. First, note that any piecewise continuous temporal profile $\mathfrak{s}_i$ in (4.2) can be approximated by a finite Fourier series

$$\mathfrak{s}_i(\theta_i) \approx \sum_{l=0}^{\ell} \Re[c_{li} e^{jl\theta_i}], \quad c_{li} \in \mathbb{C}, \quad i \in \mathbb{I}_n \tag{4.3}$$

with arbitrary accuracy by taking a sufficiently large number of terms ℓ. This motivates us to consider a nonlinear oscillator with complex state variables of dimension n, same as that of the target oscillation $\boldsymbol{\eta}$,

$$\dot{\mathbf{z}} = f(\mathbf{z}), \quad \mathbf{z}(t) \in \mathbb{C}^n, \tag{4.4}$$

having an orbitally stable limit cycle $\mathbf{z} = \boldsymbol{\zeta}$ with

$$\zeta_i(t) = e^{j(\omega t + \varphi_i)}, \quad i \in \mathbb{I}_m. \tag{4.5}$$

The desired oscillation $\eta_i(t)$ in (4.2) can then be approximately generated as the real part (or equivalently, the imaginary part) of a polynomial of $\zeta_i(t)$ with coefficients c_{li}. We now relate system (4.4) to (4.1) by defining $\mathbf{z} =: \mathbf{x} + j\mathbf{y}$ with $\mathbf{x}, \mathbf{y} \in \mathbb{R}^n$. Then we have $\mathfrak{n} := 2n$,

and

$$\mathfrak{f}(\mathbf{x}) := \begin{bmatrix} \Re[f(\mathbf{x}+j\mathbf{y})] \\ \Im[f(\mathbf{x}+j\mathbf{y})] \end{bmatrix}, \quad \boldsymbol{\mathfrak{x}} := \begin{bmatrix} \mathbf{x} \\ \mathbf{y} \end{bmatrix},$$

$$\mathfrak{h} = \mathrm{col}(\mathfrak{h}_1, \ldots, \mathfrak{h}_n), \quad \mathfrak{h}_i(\mathbf{x}) := \sum_{l=1}^{\ell} \Re[c_{li}(x_i + jy_i)^l].$$

The complex system (4.4) having an orbitally stable limit cycle $\mathbf{z} = \boldsymbol{\zeta}$ is equivalent to the above real system having an orbitally stable limit cycle $\boldsymbol{\mathfrak{x}} = \boldsymbol{\xi} \in \mathbb{R}^{2n}$ with

$$\boldsymbol{\xi}(t) = \begin{bmatrix} \cos(\omega t + \boldsymbol{\varphi}) \\ \sin(\omega t + \boldsymbol{\varphi}) \end{bmatrix}, \quad \boldsymbol{\varphi} \in \mathbb{R}^n,$$

which yields $\mathbf{y}(t) = \boldsymbol{\eta}(t)$ approximately, with the error being the higher order terms in the Fourier series beyond frequency $\ell\omega$. Therefore, the original problem is reduced to embedding an orbitally stable limit cycle $\mathbf{z}(t) = \boldsymbol{\zeta}(t)$ defined in (4.5) into the complex oscillator (4.4).

We are going to exploit the technique of Floquet theory to address Problem 3. The idea is presented in the following lemma [HC94].

Lemma 10. *Consider the dynamical system* $\dot{\mathbf{z}} = f(\mathbf{z}), \quad \mathbf{z}(t) \in \mathbb{C}^n$ *with a periodic solution* $\mathbf{z}(t) = \boldsymbol{\zeta}(t) \in \mathbb{C}^n$. $\boldsymbol{\zeta}$ *is orbitally stable if and only if the Floquet multipliers of the linearized system*

$$\dot{\mathbf{q}} = A(t)\mathbf{q}, \quad A(t) := \frac{\partial f}{\partial \mathbf{z}}(\boldsymbol{\zeta}(t))$$

lie strictly inside the unit circle on the complex plane except for one at 1. □

As such, the orbital stability is determined the values of the Floquet multipliers of the linearized system around the target limit cycle.

4.2 Single Oscillator

4.2.1 Complex Oscillator with Orbital Stability

Let us start with the simplest case where $z(t)$ in (4.4) and (4.5) is a scalar variable, i.e., $n = 1$. In this case, the phase φ_i in (4.5) is irrelevant and can be set to zero without loss of generality since the orbits of $e^{j(\omega t+\varphi_i)}$ and $e^{j\omega t}$ are the same for any φ_i. We thus consider the design of $\dot{z} = f(z)$ with $z(t) \in \mathbb{C}$ such that $z = e^{j\omega t}$ is an orbitally stable limit cycle.

The idea is simple. Note that the linear oscillator $\dot{z} = j\omega z$ has solutions $z = \gamma e^{j\omega t}$ parametrized by arbitrary amplitude $\gamma \in \mathbb{R}$. To stabilize the amplitude at $\gamma = 1$, we may add a nonlinear mechanism as follows:

$$\dot{z} = (1 - |z|^2)z + j\omega z, \tag{4.6}$$

where z is attracted toward the origin when $|z| > 1$ and repelled away when $|z| < 1$, thus achieving $|z(t)| \to 1$. This is in fact the complex form of the Andronov-Hopf oscillator (AHO)

$$\begin{bmatrix} \dot{x}_1 \\ \dot{x}_2 \end{bmatrix} = \begin{bmatrix} 1 - x_1^2 - x_2^2 & -\omega \\ \omega & 1 - x_1^2 - x_2^2 \end{bmatrix} \begin{bmatrix} x_1 \\ x_2 \end{bmatrix},$$

where x_1 and x_2 are real variables and (4.6) is obtained by defining $z := x_1 + jx_2$. It can readily be shown [Kha96] that every nontrivial solution of (4.6) globally converges to the orbit of $z = e^{j\omega t}$.

We extend this idea to achieve multiple limit cycles with local stability. Consider the general nonlinear oscillator of the form

$$\dot{z} = \phi(|z|)z, \qquad z(t) \in \mathbb{C}, \quad \phi : \mathbb{R}_+ \mapsto \mathbb{C}, \tag{4.7}$$

where the real and imaginary parts of ϕ are continuously differentiable. The AHO is a special case with

$$\phi(r) := \mu(\gamma^2 - r^2) + j\omega, \tag{4.8}$$

where $\omega, \gamma \in \mathbb{R}_+$ are prescribed frequency and amplitude, and $\mu \in \mathbb{R}_+$ is a parameter to adjust the convergence rate. The following result gives a condition for the general system to have $z = \gamma e^{j\omega t}$ as an orbitally stable limit cycle.

Theorem 7. *Consider the complex nonlinear system (4.7). Let $\omega, \gamma \in \mathbb{R}_+$ be given and suppose*

$$\phi(\gamma) = j\omega, \quad \Re[\phi'(\gamma)] < 0. \tag{4.9}$$

Then $z(t) = \gamma e^{j\omega t}$ is an orbitally stable limit cycle. □

Proof. With the coordinate transformation $z = re^{j\theta}$, the system can be described by

$$\dot{r} = \Re[\phi(r)]r, \quad \dot{\theta} = \Im[\phi(r)].$$

It can readily be verified that $r(t) = \gamma$ and $\theta(t) = \omega t$ is a solution since $\phi(\gamma) = j\omega$. Linearizing the system around the solution, we have

$$\begin{bmatrix} \dot{\rho} \\ \dot{\vartheta} \end{bmatrix} = \begin{bmatrix} \gamma\Re[\phi'(\gamma)] & 0 \\ \Im[\phi'(\gamma)] & 0 \end{bmatrix} \begin{bmatrix} \rho \\ \vartheta \end{bmatrix} \qquad \begin{aligned} \rho &:= r - \gamma, \\ \vartheta &:= \theta - \omega t. \end{aligned}$$

By the supposition, the eigenvalues of the coefficient matrix are negative and zero. Hence one of the Floquet multipliers is at 1 and the other is inside the unit circle, and we conclude the orbital stability of $z = \gamma e^{j\omega t}$. ■

The orbital stability in Theorem 7 is local, and convergence to the orbit is guaranteed only when the initial state is sufficiently close to the orbit. If desired, convergence can be made global as in the AHO with the additional property:

$$(r - \gamma)\Re[\phi(r)] < 0, \quad \forall\, r \neq \gamma. \tag{4.10}$$

In particular, consider the Lyapunov function

$$\begin{aligned} V(r) &= \tfrac{1}{2}(r - \gamma)^2 > 0, \\ \dot{V}(r) &= (r - \gamma)\Re[\phi(r)]r < 0, \end{aligned}$$

where the inequalities hold for all $r > 0$ not equal to γ. Hence, $r(t)$ converges to γ with arbitrary $r(0) > 0$, and every nontrivial trajectory converges to the orbit of $z = \gamma e^{j\omega t}$.

4.2.2 Examples

Example 6. Consider the system in (4.7) with

$$\phi(r) = j\omega r/\gamma + \gamma - r,$$

Clearly, the function satisfies condition (4.9) with $\Re[\phi'(\gamma)] = -1$ and hence $z = \gamma e^{j\omega t}$ is an orbitally stable limit cycle. In fact, condition (4.10) is also satisfied and thus convergence to the orbit is global except for $z(0) = 0$. The presence of the factor r/γ in the imaginary part of $\phi(r)$ is unimportant for these stability properties, but is added here just for illustrative purposes. This factor makes the oscillation frequency low/high when the amplitude is small/large. Any periodic signal of an arbitrary temporal shape can be generated as an output $\mathtt{y}$ that depends polynomially on z using the shape function in (4.3). For example,

$$\mathtt{y}(t) = \sin(\omega t) + 5\cos(2\omega t) - 3\sin(3\omega t), \quad \omega = 5,$$

is given by

$$\mathtt{y} = \Re[-jz + 5z^2 + 3jz^3], \quad z = \gamma e^{j\omega t}, \quad \gamma = 1.$$

The system is simulated with the initial condition $z(0) = \gamma/10$, and the result is shown in Figure 4.1. The real and imaginary parts of $z(t)$ converge to sinusoids, and output $\mathtt{y}$ converges to the nonsinusoidal signal of the specified shape.

□

With local stability, it is possible to embed multiple limit cycles $\zeta_k(t) = \gamma_k e^{j\omega_k t}$ with $k \in \mathbb{I}_m$, into oscillator (4.7) by choosing ϕ such that

$$\phi(\gamma_k) = j\omega_k, \quad \Re[\phi'(\gamma_k)] < 0, \quad \forall\ k \in \mathbb{I}_m,$$

where m is the number of limit cycles to be embedded. In this case, the function $\Re[\phi(r)]$ passes through zero multiple times at $r = \gamma_k$ with negative slopes. By continuity, the function

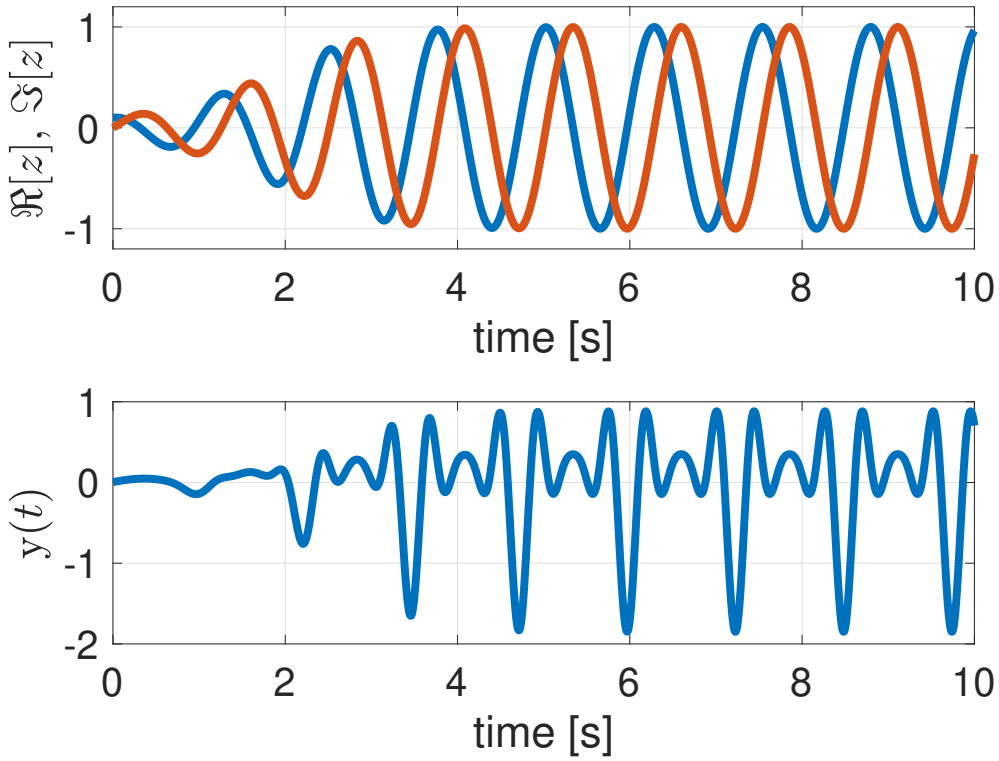

Figure 4.1: Complex oscillator with arbitrary temporal shape.

has to pass through zero with positive slopes at some values $r = \varrho_k \in (\gamma_k, \gamma_{k+1})$, assuming that γ_k are ordered as $0 < \gamma_1 < \ldots < \gamma_m$. Then the system (4.7) has periodic solutions $z = \varrho_k e^{j\varpi_k t}$ with $\varpi_k := \Im[\phi(\varrho_k)]$. Each solution $z = \varrho_k e^{j\varpi_k t}$ is an unstable limit cycle and forms the boundary between the domains of attraction for stable limit cycles $z = \gamma_k e^{j\omega_k t}$ and $z = \gamma_{k+1} e^{j\omega_{k+1} t}$.

Example 7. Consider the system in (4.7) with

$$\phi(r) = \phi_r(r) + j\phi_i(r),$$
$$\phi_r(r) = a(r - \gamma_1)(r - \varrho_1)(r - \gamma_2),$$
$$\phi_i(r) = (r - \gamma_1)(\omega_2 - \omega_1)/(\gamma_2 - \gamma_1) + \omega_1,$$

where $a < 0$ and $0 < \gamma_1 < \varrho_1 < \gamma_2$. Choosing

$$\gamma_1 = 1, \quad \gamma_2 = 3, \quad \varrho_1 = 2,$$
$$\omega_1 = 2\pi, \quad \omega_2 = \pi, \quad a = -5,$$

the function $\phi(r)$ is plotted in Figure 4.2 (top). Since $\phi_r(r)$ intersects the horizontal axis three times, the system embeds three limit cycles $z = r_o e^{\phi_i(r_o)t}$ with r_o being the intercepts γ_1, γ_2, or ϱ_1. Each solution is orbitally stable when the slope at the intersection $\phi_r'(r_o)$ is negative. Hence, the system has two stable limit cycles $z = \gamma_i e^{j\omega_i t}$, $i = 1, 2$ and one unstable limit cycle $z = \varrho_1 e^{j\varpi_1 t}$ with $\varpi_1 := \phi_i(\varrho_1) = 3\pi/2$. The system is simulated with two initial conditions $z(0) = 2 \pm 10^{-6}$, and the result is shown in Figure 4.2 (middle, bottom). If $z(0)$ is slightly inside/outside the unstable limit cycle orbit $z = \varrho_1 e^{j\varpi_1 t}$, then the trajectories (blue/red) stay near the orbit for a while but eventually diverge away and converge to the stable limit cycle orbits of smaller/larger radius. The unstable orbit forms the boundary between the domains of attraction for the two stable orbits.

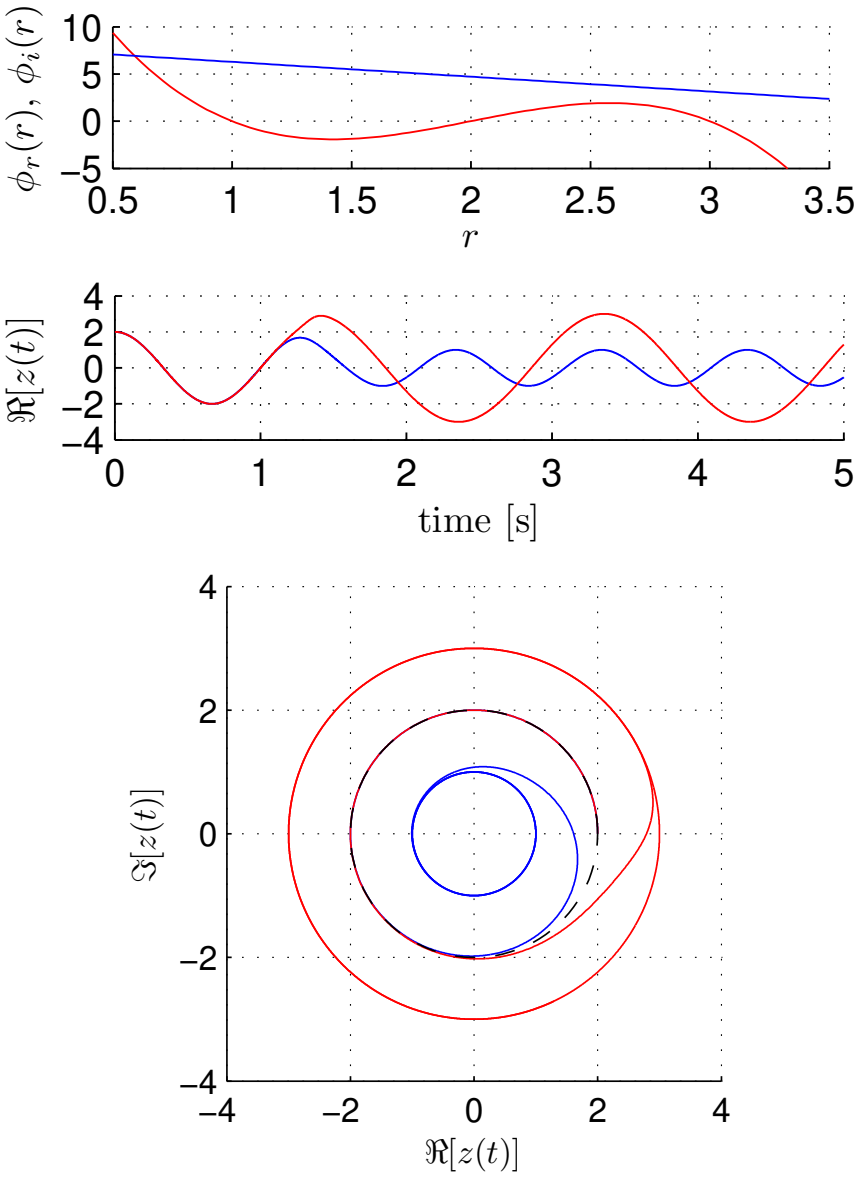

Figure 4.2: Complex oscillator with 3 limit cycles.

□

4.3 Oscillator Network

4.3.1 Single Limit Cycle

We now consider the problem of designing a nonlinear system (4.4) so that the periodic solution $\mathbf{z} = \boldsymbol{\zeta}$ in (4.5) is an orbitally stable limit cycle of the system. The problem is slightly modified by allowing for specification of the amplitude $\gamma \in \mathbb{R}$ to set the target oscillation as $\zeta_i(t) := \gamma e^{j(\omega t + \varphi_i)}$. We will achieve the design by an interconnected network formed by n complex oscillators from the previous section. In this network, each oscillator is an agent. Without any communication between the agents, an individual oscillator would converge to an oscillation of the prescribed common frequency and magnitude, but the phase relationship is undetermined. We aim to achieve a coordination between agents by properly designing the structure of the network. Moreover, we study the case where the coupling between agents is linear. Thus, the connectivity of the network and the nonlinearity of the dynamics of an oscillator are of interest. Specifically, the problem is formulated as follows.

Problem 4. Suppose a network of n coupled nonlinear oscillators (4.7) is given by

$$\begin{aligned} &\dot{\mathbf{z}} = \Phi(|\mathbf{z}|)\mathbf{z} + M\mathbf{z}, \qquad \mathbf{z} \in \mathbb{C}^n, \quad M \in \mathbb{C}^{n\times n}, \\ &\Phi(|\mathbf{z}|) := \operatorname{diag}(\phi(|z_1|), \ldots, \phi(|z_n|)), \quad \phi : \mathbb{R}_+ \mapsto \mathbb{C}, \end{aligned} \tag{4.11}$$

with $\mathbf{z} := \begin{bmatrix} z_1 & \ldots & z_n \end{bmatrix}^\mathsf{T}$. We look for the conditions on M, which is a matrix specifying the coupling of individual subsystems $\dot{z}_i = \phi(|z_i|)z_i$ with $i \in \mathbb{I}_n$, and ϕ so that the state trajectories of system (4.11) locally converge to the periodic solution

$$\begin{aligned} &\boldsymbol{\zeta}(t) := \gamma e^{j(\omega t + \boldsymbol{\varphi})} \in \mathbb{C}^n, \\ &\gamma \in \mathbb{R}_+, \quad \omega \in \mathbb{R}_+, \quad \boldsymbol{\varphi} \in \mathbb{R}^n \end{aligned} \tag{4.12}$$

with orbital stability. □

The following result reduces the design problem to an eigenvalue problem through linearization.

Lemma 11. *Consider the nonlinear system (4.11) and a target oscillation described in (4.12). Without coupling ($M = 0$), each subsystem $\dot{z}_i = \phi(|z_i|)z_i$ has a solution $z_i = \zeta_i$ if and only if ϕ satisfies $\phi(\gamma) = j\omega$. Under this condition, system (4.11) has a solution $\mathbf{z} = \boldsymbol{\zeta}$ if and only if M satisfies $Me^{j\boldsymbol{\varphi}} = 0$. In this case, the solution is orbitally stable if and only if the real matrix*

$$\mathcal{M} = \begin{bmatrix} \kappa I + M_r & -M_i \\ \tau I + M_i & M_r \end{bmatrix} \quad \begin{array}{l} \kappa + j\tau := \gamma\phi'(\gamma), \\ M_r + jM_i := \Psi^* M \Psi, \end{array} \tag{4.13}$$

has eigenvalues in the open left half plane except for one at the origin, where $\Psi := \mathrm{diag}(e^{j\boldsymbol{\varphi}})$. □

Proof. It can be verified through direct substitutions that $\mathbf{z} = \boldsymbol{\zeta}$ is a solution of the differential equations if and only if the stated conditions are satisfied. To prove the orbital stability condition, we linearize the system (4.11) around its target limit cycle $\boldsymbol{\zeta}(t)$. Define the perturbation variable $\mathbf{p} := \mathbf{z} - \boldsymbol{\zeta}$ and note the approximations

$$\begin{aligned} |z_i| &= \sqrt{(p_i + \zeta_i)^*(p_i + \zeta_i)} \\ &\cong \sqrt{\gamma^2 + 2\Re[\zeta_i^* p_i]} \cong \gamma + \Re[\zeta_i^* p_i]/\gamma, \\ \phi(|z_i|)z_i &\cong \Big(\phi(\gamma) + \phi'(\gamma)\Re[\zeta_i^* p_i]/\gamma\Big)(\zeta_i + p_i) \\ &\cong j\omega(\zeta_i + p_i) + \phi'(\gamma)\zeta_i \Re[\zeta_i^* p_i]/\gamma. \end{aligned}$$

Then the linearized system is given by

$$\dot{\mathbf{p}} = (j\omega I + M)\mathbf{p} + (\phi'(\gamma)/\gamma)\ \boldsymbol{\zeta} \cdot \Re[\bar{\boldsymbol{\zeta}} \cdot \mathbf{p}]. \tag{4.14}$$

Therefore, $\boldsymbol{\zeta}$ is an orbitally stable limit cycle if and only if the linearized system (4.14) has one Floquet multiplier at 1 with the rest having magnitude less than 1. Further consider the coordinate transformation $\mathbf{p} \leftrightarrow \mathbf{q}$ defined by $\mathbf{p} = \boldsymbol{\zeta} \cdot \mathbf{q}$. Then the system can be expressed as

$$\dot{\mathbf{q}} = (\Psi^* M \Psi)\mathbf{q} + \gamma\phi'(\gamma)\Re[\mathbf{q}].$$

Defining the real state variables $\boldsymbol{\rho}, \boldsymbol{\vartheta} \in \mathbb{R}^n$ by $\mathbf{q} = \boldsymbol{\rho} + j\boldsymbol{\vartheta}$, the system is described by

$$\begin{bmatrix} \dot{\boldsymbol{\rho}} \\ \dot{\boldsymbol{\vartheta}} \end{bmatrix} = \begin{bmatrix} \kappa I + M_r & -M_i \\ \tau I + M_i & M_r \end{bmatrix} \begin{bmatrix} \boldsymbol{\rho} \\ \boldsymbol{\vartheta} \end{bmatrix}. \tag{4.15}$$

Since the linear periodic system (4.14) and the linear time-invariant system (4.15) are related by a Lyapunov transformation, they share the same set of Floquet multipliers, which are given by $e^{\lambda_i T}$ for $i \in \mathbb{I}_n$, where $T := 2\pi/\omega$ and λ_i are the eigenvalues of M. ■

Remark 5. Condition $Me^{\boldsymbol{\varphi}} = 0$ in Lemma 11 means that the coupling is diffusive and vanishes on the target orbit. In particular, for the special case of synchronization, we have $\boldsymbol{\varphi} = 0$ and $M\mathbf{1} = 0$. Since the row sum is zero for M, each oscillator dynamics can be written as

$$\dot{z}_i = \phi(|z_i|)z_i + \sum_{j=1}^{n} m_{ij}(z_j - z_i), \quad i \in \mathbb{I}_m,$$

where m_{ij} is the $(i,j)^{\text{th}}$ entry of M. Clearly, the coupling term is zero when synchronized ($z_j = z_i$). □

Based on Lemma 11, the stability analysis boils down to the eigenvalue assignment of M.

Lemma 12. *Let real matrices $M_r, M_i \in \mathbb{R}^{n\times n}$ and real scalars $\kappa, \tau \in \mathbb{R}$ be given and consider*

$$\mathsf{M} := \begin{bmatrix} \kappa I + M_r & -M_i \\ \tau I + M_i & M_r \end{bmatrix}, \quad M_0 := M_r + jM_i.$$

Let the eigenvalues of M_0 be denoted by λ_i with $i \in \mathbb{I}_n$ and suppose $\lambda_n = 0$ and $M_0\mathbf{1} = 0$. Then, with $|\kappa + j\tau|$ sufficiently small, the eigenvalues of M are at 0, κ, and in the neighborhood of λ_i and $\bar{\lambda}_i$ for $i \in \mathbb{I}_{n-1}$. □

Proof. Let $H \in \mathbb{R}^{n\times(n-1)}$ be such that $\mathbf{1}^{\mathsf{T}}H = 0$ and $H^{\mathsf{T}}H = I$, and define an invertible matrix

$$T = \begin{bmatrix} \kappa\mathbf{1} & -\tau\mathbf{1} & H & 0 \\ \tau\mathbf{1} & \kappa\mathbf{1} & 0 & H \end{bmatrix} \in \mathbb{R}^{2n\times 2n}.$$

Then, noting that the bottom row blocks of T^{-1} are given by $\mathrm{diag}(H^\mathsf{T}, H^\mathsf{T})$, it can be shown that

$$\mathsf{M}T = T\Lambda, \tag{4.16}$$

holds where

$$\Lambda := \begin{bmatrix} \kappa & -\tau & U \\ 0 & 0 & V \\ 0 & 0 & W+E \end{bmatrix}, \quad E := \begin{bmatrix} \kappa I & 0 \\ \tau I & 0 \end{bmatrix},$$

$$W := \begin{bmatrix} W_r & -W_i \\ W_i & W_r \end{bmatrix}, \quad \begin{aligned} W_r &:= H^\mathsf{T} M_r H, \\ W_i &:= H^\mathsf{T} M_i H. \end{aligned}$$

Since Λ is block triangular, we see that the eigenvalues of M are κ, 0, and those of $W+E$. Since the eigenvalues of $W+E$ depend continuously on (κ, τ), and E vanishes when $\kappa = \tau = 0$, the result follows if we show that the eigenvalues of W coincide with λ_i and $\bar{\lambda}_i$ for $i \in \mathbb{I}_{n-1}$. Denote the matrix $\mathcal{M}$ with $\kappa = \tau = 0$ by $\mathcal{M}_0$. Letting $\kappa = \tau = 0$ in (4.16) shows that M_0 has two eigenvalues at 0 and shares the other $2(n-1)$ eigenvalues with W. By Lemma 19 in the appendix, the eigenvalues of M_0 are λ_i and $\bar{\lambda}_i$ for $i \in \mathbb{I}_n$. This completes the proof. ■

Combining the previous two lemmas, we immediately have the following result.

Theorem 8. *Consider system (4.11) with target oscillation (4.12). Suppose the following holds.*

(i) $Me^{j\boldsymbol{\varphi}} = 0$, *and the eigenvalues of* M *are in the open left half plane except for one at the origin.*

(ii) $\phi(\gamma) = j\omega$, $\Re[\phi'(\gamma)] < 0$, *and* $|\phi'(\gamma)|$ *is sufficiently small.*

Then $\mathbf{z} = \boldsymbol{\zeta}$ *is an orbitally stable limit cycle of system (4.11).* □

Proof. The result follows from Lemma 11 and Lemma 12 once we notice that M_0 and M are related by a similarity transformation and hence share the set of eigenvalues, and $Me^{j\boldsymbol{\varphi}} = 0$ is equivalent to $M_0\mathbf{1} = 0$. ■

Remark 6. The orbital stability property is guaranteed when the slope $|\phi'(\gamma)|$ is sufficiently small. In this case, convergence of the amplitude may be slow. In view of the proof of Lemma 12, however, the limit cycle is orbitally stable even for a large $|\phi'(\gamma)|$ as long as the eigenvalues of $W + E$ have negative real parts. □

4.3.2 Multiple Limit Cycles

This section will extend the result of the previous section to embed multiple limit cycles within the state space of the coupled complex oscillators (4.11). In particular, we aim to obtain the conditions on ϕ and $M \in \mathbb{C}^{n\times n}$ such that

$$\boldsymbol{\zeta}_k(t) = \gamma_k e^{j(\omega_k t+\boldsymbol{\varphi}_k)} \in \mathbb{C}^n, \quad k \in \mathbb{I}_m, \tag{4.17}$$

are m orbitally stable limit cycles for (4.11), where $\gamma_k, \omega_k \in \mathbb{R}$ and $\boldsymbol{\varphi}_k \in \mathbb{R}^n$ are prescribed amplitude, frequency, and phase of the k^{th} limit cycle.

The extension is not straightforward. The diffusive coupling condition $Me^{j\boldsymbol{\varphi}_k} = 0$ for $k \in \mathbb{I}_m$ implies that M has at least m eigenvalues at the origin. Hence, condition *(i)* in Theorem 8 will not hold. Therefore, we need new conditions for the case with multiple limit cycles.

Let us first extend Lemma 11 and reduce the multi-oscillation problem to an eigenvalue problem.

Lemma 13. *Consider the nonlinear system (4.11) and target oscillations (4.17). Without coupling ($M = 0$), each subsystem $\dot{z}_i = \phi(|z_i|)z_i$ has a solution $z_i = \zeta_{k,i}$ if and only if ϕ satisfies $\phi(\gamma_k) = j\omega_k$. Under this condition, system (4.11) has a solution $\mathbf{z} = \boldsymbol{\zeta}_k$ if and only if M satisfies $Me^{j\boldsymbol{\varphi}_k} = 0$. In this case, the solution is orbitally stable if and only if the real*

matrix

$$\mathcal{M}_k = \begin{bmatrix} M_R & -M_I \\ M_I & M_R \end{bmatrix} + \begin{bmatrix} C_k & -S_k \\ S_k & C_k \end{bmatrix} \begin{bmatrix} \kappa_k I \\ \tau_k I \end{bmatrix} \begin{bmatrix} C_k & S_k \end{bmatrix} \tag{4.18}$$

has eigenvalues in the open left half plane except for one at the origin, where

$$M_R + jM_I := M, \qquad C_k := \operatorname{diag}(\cos \boldsymbol{\varphi}_k),$$
$$\kappa_k + j\tau_k := \gamma_k \phi'(\gamma_k) \quad S_k := \operatorname{diag}(\sin \boldsymbol{\varphi}_k).$$

□

Proof. The result follows directly from Lemma 11 by noting that

$$\mathbf{M} = \omega_k^{\mathsf{T}} \mathcal{M}_k \omega_k, \quad \omega_k := \begin{bmatrix} C_k & -S_k \\ S_k & C_k \end{bmatrix}$$

when $(\kappa, \tau, \boldsymbol{\varphi})$ in (4.13) coincides with $(\kappa_k, \tau_k, \boldsymbol{\varphi}_k)$. ■

For the single orbit case ($m = 1$), Lemma 13 reduces to Lemma 11 as a special case where the matrix $\mathcal{M}_k$ and $\mathbf{M}$ are related by a similarity transformation. The complication due to multiple orbits is that we require $Me^{j\boldsymbol{\varphi}_k} = 0$ for $k \in \mathbb{I}_m$ and hence M has m eigenvalues at the origin, which in turn implies that $\mathcal{M}_k$ has $2m$ eigenvalues at the origin. For the single orbit case ($m = 1$), one of the two eigenvalues at the origin can be moved to the left by a sufficiently small $|\kappa_k + j\tau_k|$ with $\kappa_k < 0$ due to Lemma 11. For the multiple orbit case ($m > 1$), we need to move $2m - 1$ out of the $2m$ eigenvalues at the origin.

The following result is useful for obtaining a condition under which the eigenvalues of $\mathbf{M}_k$ have negative real parts except for one at the origin.

Lemma 14. *Let matrices $A, B \in \mathbb{R}^{\mathfrak{n}\times\mathfrak{n}}$ be given. Suppose A has a semisimple eigenvalue at the origin with multiplicity r and the other $\mathfrak{n} - r$ eigenvalues are nonzero. Let $X, Y^{\mathsf{T}} \in \mathbb{R}^{\mathfrak{n}\times r}$ be full column rank matrices such that*

$$AX = 0, \quad Y^{\mathsf{T}} A = 0, \quad Y^{\mathsf{T}} X = I.$$

Suppose further that B satisfies $BXe = 0$ for some nonzero vector $e \in \mathbb{R}^r$. Then, for sufficiently small $\varepsilon > 0$, one of the eigenvalues of $A + \varepsilon B$ stays at the origin, $\mathfrak{n} - r$ of them are in the neighborhood of the nonzero eigenvalues of A, and the other $r-1$ eigenvalues have negative real parts if the eigenvalues of $Y^\mathsf{T} BX$, except for one at the origin, have negative real parts. □

Proof. Let the eigenvalues of $A + \varepsilon B$ for $\varepsilon \geq 0$ be denoted by $\lambda_i(\varepsilon) \in \mathbb{C}$ for $i \in \mathbb{I}_\mathfrak{n}$, which depend continuously on ε. Suppose the eigenvalues are ordered so that $\lambda_i(0) = 0$ for $i \in \mathbb{I}_r$. Note that $A+\varepsilon B$ has an eigenvalue at the origin with eigenvector Xv for any ε, and designate this as $\lambda_r(\varepsilon) = 0$. Then, from [OW88, Lemma 3.1], the one-sided derivatives of $\lambda_i(\varepsilon)$ for $i \in \mathbb{I}_r$ at $\varepsilon = 0$ are given by the eigenvalues of $Y^\mathsf{T} BX$. The derivative of $\lambda_r(\varepsilon)$ is zero, corresponding to the zero eigenvalue of $Y^\mathsf{T} BX$. If the other eigenvalues of $Y^\mathsf{T} BX$ have negative real parts, then $\Re[\lambda_i(\varepsilon)] < 0$, $i \in \mathbb{I}_{r-1}$, for sufficiently small $\varepsilon > 0$. ■

The following is the main result of this section.

Theorem 9. *Let m target oscillations be given by (4.17). Assume that, for each $k \in \mathbb{I}_m$, vectors $\mathbf{1}$, $\mathbf{c}_{hk}$, and $\mathbf{s}_{hk}$ with $h \in \mathbb{I}_m \setminus \{k\}$, are linearly independent, where*

$$\mathbf{c}_{hk} = \cos(\boldsymbol{\varphi}_h - \boldsymbol{\varphi}_k), \quad \mathbf{s}_{hk} = \sin(\boldsymbol{\varphi}_h - \boldsymbol{\varphi}_k).$$

Consider system (4.11) and suppose the following holds.

(i) The coupling matrix is given by $M = N\Lambda N^\dagger$, where $\Lambda \in \mathbb{C}^{(n-m)\times(n-m)}$ is an arbitrary Hurwitz matrix, and $N \in \mathbb{C}^{n\times(n-m)}$ is a full-rank matrix such that

$$X^* N = 0, \quad X := \begin{bmatrix} e^{j\boldsymbol{\varphi}_1} & \dots & e^{j\boldsymbol{\varphi}_m} \end{bmatrix} \in \mathbb{C}^{n\times m}.$$

(ii) For each $k \in \mathbb{I}_m$, function ϕ satisfies $\phi(\gamma_k) = j\omega_k$, and $\phi'(\gamma_k)$ is real negative with sufficiently small magnitude.

Then $z = \boldsymbol{\zeta}_k$ for $k \in \mathbb{I}_m$ are orbitally stable limit cycles of system (4.11). □

Proof. Fix $k \in \mathbb{I}_m$. Since $MX = 0$ and $\phi(\gamma_k) = j\omega_k$, we see from Lemma 13 that $z = \boldsymbol{\zeta}_k$ is a solution of (4.11). The solution is orbitally stable if the eigenvalues of $\mathcal{M}_k$ in (4.18) have negative real parts except for one at the origin, where $\tau_k := \Im[\gamma_k \phi'(\gamma_k)]$ is zero due to the supposition. By definition, $MX = 0$ and $MN = N\Lambda$ hold. From Lemma 19 in the appendix, these conditions are equivalent to

$$\mathcal{M} \begin{bmatrix} \mathcal{X} & \mathcal{N} \end{bmatrix} = \begin{bmatrix} \mathcal{X} & \mathcal{N} \end{bmatrix} \begin{bmatrix} 0 & 0 \\ 0 & \mathcal{L} \end{bmatrix} \tag{4.19}$$

where $\mathcal{M}$, $\mathcal{X}$, $\mathcal{N}$, and $\mathcal{L}$ are real matrices defined from the real and imaginary parts of M, X, N, and Λ, respectively, as in (A.1). Now, $\mathcal{M}_k$ in (4.18) can be written as

$$\mathcal{M}_k = \mathcal{M} + \kappa_k E_k^{\mathsf{T}} E_k, \quad E_k := \begin{bmatrix} C_k & S_k \end{bmatrix}.$$

Note that the linear independence assumption for $\mathbf{1}$, c_{hk} and s_{hk} is equivalent to $\operatorname{rank}(E_k\mathcal{X}) = 2m - 1$ since

$$E_k\mathcal{X} = \begin{bmatrix} \mathbf{c}_{1k} & \dots & \mathbf{c}_{mk} & \mathbf{s}_{1k} & \dots & \mathbf{s}_{mk} \end{bmatrix}.$$

The assumption implies that X has full column rank because otherwise $\operatorname{rank}(X) \leq m - 1$ and, from Lemma 19, $\operatorname{rank}(E_k\mathcal{X})$ is at most $2m - 2$. It can then readily be verified using Lemma 19 that $\operatorname{rank}(\mathcal{X}) = 2m$, $\operatorname{rank}(\mathcal{N}) = 2(n - m)$, $\mathcal{X}^{\mathsf{T}}\mathcal{N} = 0$, and $\mathcal{L}$ is Hurwitz because $\operatorname{rank}(X) = m$, $\operatorname{rank}(N) = n - m$, $X^*N = 0$, and Λ is Hurwitz, respectively. Hence, (4.19) gives a spectral decomposition of $\mathcal{M}$, showing that $\mathcal{M}$ has a semisimple eigenvalue at the origin with multiplicity $2m$, and the other $2(n - m)$ eigenvalues have negative real parts. Noting that the inverse of $[\mathcal{X} \;\; \mathcal{N}]$ is given by $\operatorname{col}(\mathcal{X}^\dagger, \mathcal{N}^\dagger)$, Lemma 14 assures that all the eigenvalues of $\mathcal{M}_k$, except for one at the origin, have negative real parts for $\kappa_k < 0$ of sufficiently small magnitude if the eigenvalues of $\Delta_k := \mathcal{X}^\dagger E_k^{\mathsf{T}} E_k \mathcal{X}$, except for one at the origin, have positive real parts. Note that Δ_k and $\mathcal{X}^{\mathsf{T}} E_k^{\mathsf{T}} E_k \mathcal{X}$ are related by similarity and congruence transformations:

$$T^{-1}\Delta_k T = T\mathcal{X}^{\mathsf{T}} E_k^{\mathsf{T}} E_k \mathcal{X} T, \quad T := (\mathcal{X}^{\mathsf{T}}\mathcal{X})^{-1/2}.$$

Since $\operatorname{rank}(E_k\mathcal{X}) = 2m-1$, matrix $\mathcal{X}^\intercal E_k^\intercal E_k \mathcal{X}$ has $2m-1$ positive real and one zero eigenvalues, and this property is shared by Δ_k. This completes the proof. ■

Remark 7. The linear independence assumption on $\boldsymbol{\varphi}_k$ ensures that the phases of the target oscillations are not redundant. For example, if $e^{j\boldsymbol{\varphi}_m}$ can be expressed as a linear combination of $e^{j\boldsymbol{\varphi}_k}$ with $k \in \mathbb{I}_{m-1}$, then the assumption would be violated. Hence, this assumption does not introduce difficulty for practical purposes. □

Example 8. Consider system (4.11) with $\phi(r)$ given by (4.8). We will embed in the state space multiple stable limit cycles $\mathbf{z} = \boldsymbol{\zeta}_k$ of the form (4.17). With the choice of $\phi(r)$ from the AHO, $\Re[\phi(r)] = 0$ has only one solution in the domain $r > 0$, and hence the frequency and amplitude of the targeted limit cycles cannot be specified by different values. However, design of the network connectivity M allows to specify different phase values. We consider the case where there are five oscillators, and two limit cycles $\boldsymbol{\zeta}_k(t) = \gamma e^{j(\omega t + \boldsymbol{\varphi}_k)}$, $k = 1, 2$, are to be embedded. The parameters are chosen as

$$\omega = 2\pi, \quad \boldsymbol{\varphi}_1 = \operatorname{col}(0,0,0,0,0),$$
$$\gamma = 1, \quad \boldsymbol{\varphi}_2 = \operatorname{col}(0,1,3,6,10)(\pi/10),$$

where $\boldsymbol{\zeta}_1$ is synchronized oscillations, while $\boldsymbol{\zeta}_2$ is traveling-wave oscillations. The system is designed to achieve these oscillations using Theorem 9. The assumption requires linear independence of $\mathbf{1}$, $\cos\boldsymbol{\varphi}_2$, and $\sin\boldsymbol{\varphi}_2$, which is satisfied. The orbital stability is guaranteed when $\Re[\phi'(\gamma)] = -2\mu\gamma$ is negative with sufficiently small magnitude. It turns out that $\mu = 1$ is small enough to give the stability. The coupling matrix M is designed as described in statement *(i)* of Theorem 9 using N whose columns form an orthonormal basis for the null space of X^*, and

$$\Lambda = \operatorname{diag}(0, 0, -1+2j, -3+4j, -5+6j).$$

The system is simulated with two initial conditions

$$z(0) = \gamma_0 e^{j\boldsymbol{\varphi}_0}, \quad \gamma_0 = \gamma/10, \quad \boldsymbol{\varphi}_0 = a\boldsymbol{\varphi}_1 + (1-a)\boldsymbol{\varphi}_2,$$

with $a = 0.6$ and 0.4; the former is considered closer to the $\boldsymbol{\zeta}_1$ orbit and the latter would be closer to the $\boldsymbol{\zeta}_2$ orbit. The result is shown in Figure 4.3. As expected, each initial condition leads to convergence to the nearby limit cycle.

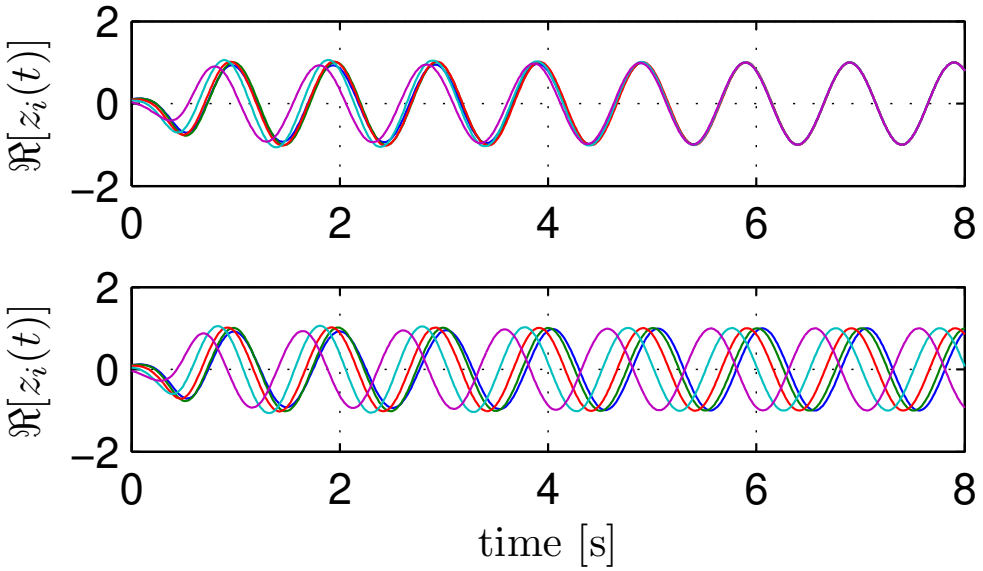

Figure 4.3: Coupled oscillators with 2 limit cycles.

□

4.3.3 Limitations

The conditions in Theorem 9 do not tie the amplitude and frequency with the phase in the sense the conditions are given in terms of the amplitude/frequency or the phase individually. Specifically, condition *(i)* determines the coupling matrix solely by the phase, while in condition *(ii)* the relationship between the amplitude and frequency is decided by the function $\phi(\cdot)$, which does not involve the phase. This introduces additional stable limit cycles which are a combination of amplitude/frequency pair and phase. We show this issue via the example below.

Example 9. Consider an oscillator network of 3 oscillators and 2 limit cycles to be embedded. The frequencies, amplitudes, and phases of the limit cycles are specified by

$$\begin{aligned}
&\omega_1 = 2\pi, \quad \gamma_1 = 1, \quad \boldsymbol{\varphi}_1 = \mathrm{col}(0,0,0),\\
&\omega_2 = \pi, \quad \gamma_2 = 2, \quad \boldsymbol{\varphi}_2 = \mathrm{col}(1,2,3)(\pi/3).
\end{aligned}$$

$\phi(r)$ is designed to be $\phi(r) = \phi_r(r) + j\phi_i(r)$, where $\phi_r(r) := -\mu(r-\gamma_1)(r-\gamma_0)(r-\gamma_2)$ with $\gamma_0 := (\gamma_1+\gamma_2)/2$, $\mu > 0$, and $\phi_i(r)$ is constructed as follows:

$$\begin{aligned}
&\phi_i(r) = a\left(\frac{1}{3}r^3 - \gamma_0 r^2 + \gamma_1\gamma_2 r\right) + b,\\
&a := \frac{\omega_1 - \omega_2}{c_1 - c_2}, \quad b := \omega_1 - c_1 a,\\
&c_1 := \frac{1}{3}\gamma_1^3 - \gamma_0\gamma_1^2 + \gamma_1^2\gamma_2, \quad c_2 := \frac{1}{3}\gamma_2^3 - \gamma_0\gamma_2^2 + \gamma_1\gamma_2^2.
\end{aligned}$$

By tuning the initial conditions, we observed the convergence to the 2 desired limit cycles specified above as in Figure 4.4. We also observed the convergence to an additional undesired limit cycle with frequency ω_1, amplitude γ_1, and phase $\boldsymbol{\varphi}_2$, as shown in Figure 4.5.

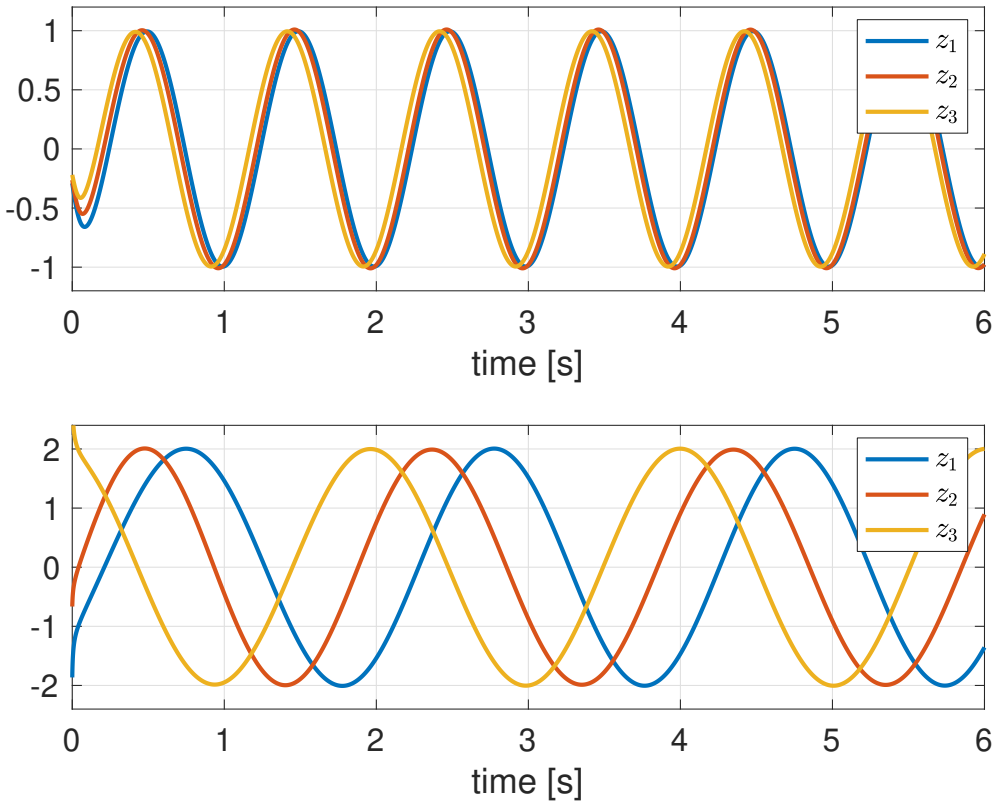

Figure 4.4: The 2 desired limit cycles.

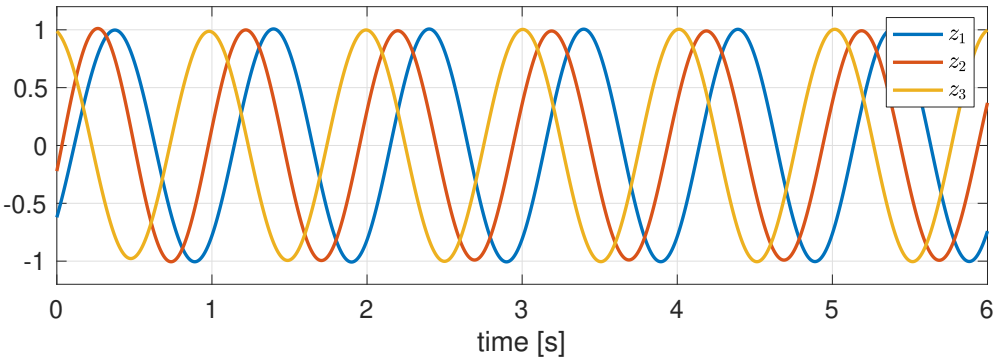

Figure 4.5: The additional undesired limit cycle.

□

This unpleasant introduction of extra limit cycle(s) is due to the linear coupling between oscillators. Thus we proceed with investigating nonlinear coupling in the subsequent chapter.

CHAPTER 5

Network of Nonlinearly Coupled Oscillators

5.1 Problem Formulation

Due to the limitations of linearly coupled oscillators discussed in Section 4.3.3, we consider a specific model of oscillator network similar to the one developed in the previous chapter but with nonlinear coupling in this chapter. Again, we start with the generalized nonlinear oscillator with complex state variable (4.7). With a slight modification, the dynamics of the oscillator is given by

$$\dot{z} = j\omega\phi(|z|)z, \qquad z(t) \in \mathbb{C}, \quad \phi : \mathbb{R}_+ \mapsto \mathbb{C}, \tag{5.1}$$

with

$$\phi(\gamma) = 1, \qquad \phi'(\gamma) = j\varepsilon, \quad \varepsilon > 0. \tag{5.2}$$

It is proved that the oscillator has an orbitally stable limit cycle $\zeta := \gamma e^{j\omega t}$. Without the nonlinear term $\phi(|z|)$, the oscillator becomes linear, having $\tilde{\gamma}e^{j\omega t}$ as its solution with arbitrary magnitude $\tilde{\gamma}$. The purpose of the nonlinearity is to fix the magnitude of the oscillation. This is achieved by the condition (5.2) imposed on the oscillator.

Inspired by the stability condition (5.2) for the limit-cycle oscillator (5.1), here we make the following assumption for the oscillator network.

Assumption 2. Consider a network of coupled nonlinear oscillators described in (5.3). Assume

$$\phi(\gamma) = 1, \qquad \phi'(\gamma) = j\varepsilon, \quad \varepsilon \in \mathbb{R}.$$

□

Moving forward, we consider a coordination problem of a network of such oscillators described in (5.1). In this network, each oscillator is an agent. Without any communication between the agents, an individual oscillator would converge to an oscillation of the prescribed common frequency and magnitude, but the phase relationship is undetermined. We aim to achieve a coordination between agents by properly designing the structure of the network. Moreover, we study the case where the coupling between agents is nonlinear. Thus, the connectivity of the network and the nonlinearity of the dynamics of an oscillator are of interest. Specifically, the problem is formulated as follows.

Problem 5. Suppose a network of n coupled nonlinear oscillators (5.1) is given by

$$\begin{aligned} &\dot{\mathbf{z}} = M\Phi(|\mathbf{z}|)\mathbf{z}, \qquad \mathbf{z} \in \mathbb{C}^n, \quad M \in \mathbb{C}^{n\times n}, \\ &\Phi(|\mathbf{z}|) := \operatorname{diag}(\phi(|z_1|), \ldots, \phi(|z_n|)), \quad \phi : \mathbb{R}_+ \mapsto \mathbb{C}, \end{aligned} \tag{5.3}$$

with $\mathbf{z} := \begin{bmatrix} z_1 & \ldots & z_n \end{bmatrix}^\mathsf{T}$. We look for the conditions on M and ϕ so that the state trajectories of system (5.3) locally converge to the periodic solution

$$\begin{aligned} &\boldsymbol{\zeta}(t) := \gamma e^{j(\omega t + \boldsymbol{\varphi})} \in \mathbb{C}^n, \\ &\gamma \in \mathbb{R}_+, \quad \omega \in \mathbb{R}_+, \quad \boldsymbol{\varphi} \in \mathbb{R}^n \end{aligned} \tag{5.4}$$

with orbital stability. □

5.2 Single Limit Cycle Design

5.2.1 An Equivalent Synchronization Problem

We proceed to address Problem 5 with only one limit cycle to stabilize. Before we linearize the system and apply Floquet theory, we observe that a coordinate transformation helps further simplifying the problem. Since our goal is for every state in $\mathbf{z}$,

$$z_k(t) \to \zeta_k := \gamma e^{j(\omega t + \varphi_k)},$$

where ζ_k, φ_k are the k^{th} entry of $\boldsymbol{\zeta}$, $\boldsymbol{\varphi}$, respectively, this motivates us to consider the following coordinate transformation

$$p_k(t) := e^{-j(\omega t+\varphi_k)} z_k(t).$$

It then can be easily seen that z_k converges to ζ_k if and only if p_k converges to γ. Therefore in the new coordinate, the objective is to synchronize all the states. To that end, we derive the dynamics of $\mathbf{p} := (p_1, p_2, \ldots, p_n)^{\mathsf{T}}$ and the result is stated in the following lemma.

Lemma 15. *Consider system (5.3) with target periodic solution (5.4) and Assumption 2. Define*

$$\delta L + j\omega I := \Psi^* M \Psi, \quad \Psi := \operatorname{diag}(e^{j\boldsymbol{\varphi}}) \in \mathbb{C}^{n\times n}, \tag{5.5}$$

where δ is a real positive scalar, and consider the a system with dynamics given by

$$\dot{\mathbf{p}} = j\omega(\Phi(|\mathbf{p}|) - I)\mathbf{p} + \delta L \Phi(|\mathbf{p}|)\mathbf{p}, \quad \mathbf{p} \in \mathbb{C}^n. \tag{5.6}$$

Then (5.4) is an orbitally stable limit cycle to the original system (5.3) if and only if $\mathbf{p}$ in (5.6) converges to $c\mathbf{1}$, where $c \in \mathbb{C}$ and $|c| = \gamma$. □

Proof. Consider a coordinate transformation on the original state variable $\mathbf{z}$,

$$p_k(t) := e^{-j(\omega t+\varphi_k)} z_k(t), \quad k \in \mathbb{I}_n.$$

In the matrix form

$$\mathbf{p} = e^{-j\omega t}\Psi^* \mathbf{z},$$

where Ψ is defined in (5.6). We notice that p_k and z_k have identical magnitude, i.e.,

$$|p_k| = |z_k| \implies |\mathbf{z}| = |\mathbf{p}|.$$

Then,

$$\begin{aligned}
\dot{\mathbf{p}} &= e^{-j\omega t}\Psi^*\dot{\mathbf{z}} - j\omega e^{-j\omega t}\Psi^*\mathbf{z} \\
&= e^{-j\omega t}\Psi^* M\Phi(|\mathbf{z}|)\mathbf{z} - j\omega e^{-j\omega t}\Psi^*\mathbf{z} \\
&= (\Psi^* M\Phi(|\mathbf{z}|))\left(\Psi e^{-j\omega t}\Psi^*\right)\mathbf{z} - j\omega e^{-j\omega t}\Psi^*\mathbf{z} && (\text{since } \Psi^*\Psi = I) \\
&= \Psi^* M\Psi\Phi(|\mathbf{p}|)\mathbf{p} - j\omega\mathbf{p}. && (\mathbf{p} = e^{-\omega t}\Psi^*\mathbf{z};\ \Phi, \Psi \text{ commute})
\end{aligned}$$

Substituting the expression in (5.5) for $\Psi^* M\Psi$, we arrive at (5.6). The orbital stability suggests that $z_k \to \gamma e^{j(\omega t+\varphi_k+\varphi_c)}$ for some constant phase shift φ_c. This happens if and only if $p_k \to c$ with $c = \gamma e^{j\varphi_c}$. ■

Remark 8. With Lemma 15, the previous coordination problem, where the states have non-uniform phase on the target oscillation, has been converted to a synchronization problem, where the objective is the reach at a synchronized state (consensus) among oscillators (agents). □

Remark 9. As shown in (5.6), the dynamical equation is partitioned into two parts. To justify this partition, let us take a look at the dynamics of an agent,

$$\dot{p}_k = j\omega(\phi(|p_k|) - 1)p_k + \delta\sum_{i=1}^{n} l_{ki}\phi(|p_i|)p_i,$$

where l_{ki} is the $(k,i)^{\text{th}}$ entry of L. The first component would admit a harmonic solution with magnitude γ and frequency ω, but arbitrary phase, whereas the second part can be treated as the coupling between agents, imposing a phase relationship across agents. In addition, we put a δ in front to represent the coupling strength. □

5.2.2 Linearization

Lemma 15 gives an equivalent condition for the convergence to the target limit cycle of the original system (5.3). Now we only need to consider the convergence of system (5.6) to the synchronization subspace $c\mathbf{1}$, where $c \in \mathbb{C}$ and $|c| = \gamma$. Further, the convergence is examined

by a solution in that subspace, say $\gamma\mathbf{1}$. Since we need to embed $\gamma\mathbf{1}$ as a solution to the system (5.6), the coupling matrix must satisfy

$$L\mathbf{1} = 0. \tag{5.7}$$

The stability of the new target limit cycle $\gamma\mathbf{1}$ then can be determined by the linearization around it. Define $\mathbf{q}$ as a slight perturbation to the system (5.6) around the target solution, i.e.,

$$\mathbf{q} := \mathbf{p} - \gamma\mathbf{1}. \tag{5.8}$$

Then the dynamics of $\mathbf{q}$ will give us the linearization around the target solution. Before we present the result, we propose a new notion in terms of stability for linear time-invariant (LTI) systems.

Definition 3 (o-stability)**.** Consider an LTI system

$$\dot{\boldsymbol{x}} = \mathsf{A}\boldsymbol{x}, \quad \boldsymbol{x} \in \mathbb{R}^n.$$

The system is said to be **o-stable** if $\mathsf{A} \in \mathbb{H}_o$, where $\mathbb{H}_o$ is the set of matrices with all the eigenvalues in the open left half plane except for one at the origin. □

With the definition of o-stability, we now state the result in the lemma below.

Lemma 16. *Consider the system (5.6) with L and δ defined in (5.5). Let L_R, L_I be the real and imaginary part of L, respectively, i.e., $L_R + jL_I := L$. An LTI system is constructed upon L_R, L_I, δ, and ε, where ε is introduced in Assumption 2,*

$$\begin{bmatrix} \dot{\mathbf{x}} \\ \dot{\mathbf{y}} \end{bmatrix} = \mathsf{A} \begin{bmatrix} \mathbf{x} \\ \mathbf{y} \end{bmatrix}, \qquad \mathbf{x},\ \mathbf{y} \in \mathbb{R}^n, \tag{5.9}$$

$$\mathsf{A} := \delta \begin{bmatrix} L_R & -L_I \\ L_I & L_R \end{bmatrix} - \varepsilon\gamma \begin{bmatrix} \omega I + \delta L_I & 0 \\ -\delta L_R & 0 \end{bmatrix}. \tag{5.10}$$

Then $\mathbf{p}$ orbitally converges to $\gamma\mathbf{1}$ if and only if the LTI system (5.9) is o-stable. □

Proof. First, several approximations are useful for linearizing the system (5.6). Denote p_k and q_k, $k \in \mathbb{I}_n$ as the k^{th} element of $\mathbf{p}$ and $\mathbf{q}$, respectively. We have

$$\begin{aligned}
|p_k| &= |q_k + \gamma| = \sqrt{\overline{q}_k q_k + \gamma^2 + 2\gamma \Re[q_k]} \\
&\approx \gamma \sqrt{1 + \frac{2}{\gamma} \Re[q_k]} && (\overline{q}_k q_k \text{ is a higher order term}) \\
&\approx \gamma (1 + \frac{1}{\gamma} \Re[q_k]) && (\text{first order approximation of } \sqrt{1+x}) \\
&= \gamma + \Re[q_k].
\end{aligned}$$

Then

$$\begin{aligned}
\phi(|p_k|) &\approx \phi(\gamma + \Re[q_k]) \\
&\approx \phi(\gamma) + \phi'(\gamma) \Re[q_k] && (\text{first order approximation}) \\
&= 1 + j\varepsilon \Re[q_k]. && (\text{by Assumption 2})
\end{aligned}$$

Furthermore, using (5.7),

$$\begin{aligned}
\dot{\mathbf{q}} = \dot{\mathbf{p}} &= j\omega(\Phi(|\mathbf{p}|) - I)\mathbf{p} + \delta L \Phi(|\mathbf{p}|)\mathbf{p} \\
&\approx j\omega(j\varepsilon \operatorname{diag}(\Re[\mathbf{q}]))(\mathbf{q} + \gamma \mathbf{1}) \\
&\qquad + \delta L (I + j\varepsilon \operatorname{diag}(\Re[\mathbf{q}]))(\mathbf{q} + \gamma \mathbf{1}) \\
&\approx \delta L \mathbf{q} + (j\varepsilon\gamma\delta L - \varepsilon\gamma\omega I)\Re[\mathbf{q}].
\end{aligned} \tag{5.11}$$

Let $\mathbf{x} + j\mathbf{y} := \mathbf{q}$. Finally the dynamics of $\mathbf{q}$ can further be written in terms of real variables $\mathbf{x}$ and $\mathbf{y}$, which is given in (5.9) with A defined in (5.10). Thus we conclude that $\mathbf{p}$ orbitally converges to $\gamma\mathbf{1}$ if and only if the LTI system (5.9) is o-stable.

■

5.2.3 Sufficient Conditions

Notice that for the LTI system (5.9), the matrix A in (5.10) is jointly determined by γ, ω, ε, δ, and the matrix L, among which γ and ω and prescribed by the target oscillation.

Therefore, the stability conditions for (5.9) are supposed to be in terms of ε, δ, and L. The conditions further infer the stability of the original network of coupled oscillators (5.3). Combining the previous results, we present several sufficient conditions as follows.

Theorem 10. *Consider the network of coupled oscillators (5.3) with Assumption 2, and define L and δ as in (5.5). The system admits a periodic solution $\boldsymbol{\zeta}$ described in (5.4) if and only if $L\mathbf{1} = 0$. Under this condition, $\boldsymbol{\zeta}$ is exponentially orbitally stable*

(i) (Weak nonlinearity) if and only if $L \in \mathbb{H}_o$, given that $\varepsilon > 0$ is sufficiently small; or

(ii) (Weak coupling) if and only if $\Re[L] \in \mathbb{H}_o$, given that $\delta > 0$ is sufficiently small; or

(iii) (Decoupling) if and only if $L \in \mathbb{H}_o$, given that L is real and $\varepsilon > 0$;

where the set $\mathbb{H}_o$ is defined in Definition 3. □

Proof. We first derive the stability conditions for the LTI system (5.9). Let $Q \in \mathbb{R}^{n\times(n-1)}$ be such that $\mathbf{1}^\mathsf{T} Q = 0$ and $Q^\mathsf{T} Q = I$. It can be shown, with constraint (5.7), that

$$\mathsf{A} W = W \Lambda,$$

where A is defined in (5.10) and

$$W := \begin{bmatrix} \mathbf{1} & 0 & Q & 0 \\ 0 & \mathbf{1} & 0 & Q \end{bmatrix}, \qquad \Lambda := \begin{bmatrix} -\varepsilon\omega\gamma & 0 & * \\ 0 & 0 & * \\ 0 & 0 & T \end{bmatrix},$$

$$T := \mathsf{Q}^\mathsf{T} \mathsf{A} \mathsf{Q}, \quad \mathsf{Q} := \begin{bmatrix} Q & 0 \\ 0 & Q \end{bmatrix}.$$

Then two eigenvalues of A are $-\varepsilon\omega\gamma$ and 0, and hence o-stability holds if and only if T is Hurwitz and $\varepsilon > 0$. We proceed to explore the structure of T. Define

$$D := Q^\mathsf{T} L Q, \quad D_R + j D_I := D.$$

Substituting (5.10) for A in $T = \mathsf{Q}^\mathsf{T}\mathsf{A}\mathsf{Q}$, we obtain that T is Hurwitz if and only if

$$\mathcal{D} = \delta\mathsf{D} - \varepsilon\gamma \begin{bmatrix} \omega I + \delta D_I & 0 \\ -\delta D_R & 0 \end{bmatrix}$$

is Hurwitz, where

$$\mathsf{D} := \begin{bmatrix} D_R & -D_I \\ D_I & D_R \end{bmatrix}.$$

In the following argument, we show three conditions under which $\mathcal{D}$ is guaranteed to be Hurwitz.

- If D is Hurwitz and ε is sufficiently small, then $\mathcal{D}$ is Hurwitz due to continuity. This implies *(i)* due to Lemma 19.

- Rewrite $\mathcal{D}$ as

  $$\mathcal{D} = \mathcal{D}_A + \delta\mathcal{D}_B,$$

  where

  $$\mathcal{D}_A = \begin{bmatrix} -\gamma\varepsilon\omega I & 0 \\ 0 & 0 \end{bmatrix}, \quad \mathcal{D}_B = \mathsf{D} - \gamma\varepsilon \begin{bmatrix} D_I & 0 \\ -D_R & 0 \end{bmatrix}.$$

  Define

  $$Y_1^* = \begin{bmatrix} 0_n & I_n \end{bmatrix}, \quad X_1 = \begin{bmatrix} 0_n \\ I_n \end{bmatrix}.$$

  Note that $Y_1^*\mathcal{D}_A X_1 = 0$ and $Y_1^*\mathcal{D}_B X_1 = D_R$. Applying Lemma 20, $\mathcal{D}$ is Hurwitz if D_R is Hurwitz and $\delta > 0$ is sufficiently small, which is guaranteed if *(ii)* holds.

- L being real means $L_I = 0$, $L = L_R$. Further we have $D_I = 0$ and $D = D_R$. $\mathcal{D}$ then becomes

  $$\mathcal{D} = \begin{bmatrix} \delta D - \varepsilon\gamma\omega I & 0 \\ \varepsilon\gamma\delta D & \delta D \end{bmatrix}.$$

  Thus, $\mathcal{D}$ is Hurwitz if and only if D is Hurwitz and $\varepsilon < 0$, which is equivalent to *(iii)*.

Having the conditions for the LTI system (5.9) to be o-stable, the rest of the proof readily follows Lemma 15 and Lemma 16. ■

Remark 10. Since ε is associated with the derivative of ϕ at the target amplitude by definition in Assumption 2, the magnitude of ε represents how 'strong' the nonlinear effect can be. An extreme case is $\varepsilon = 0$, which means ϕ can be treated as a constant, more specifically, $\phi = 1$, around the target oscillation, rendering the system (5.3) linear. □

Remark 11. With the definition for the matrix L, (5.5), the network of coupled oscillators (5.3) can be written as

$$\dot{z}_i = j\omega\phi(|z_i|)z_i + \delta \sum_{k=1}^{n} \ell_{ik} e^{j(\varphi_i - \varphi_k)} \phi(|z_k|) z_k, \quad i, k \in \mathbb{I}_n, \tag{5.12}$$

where ℓ_{ik} is the $(i,k)^{\text{th}}$ entry of L. It can be seen that δ governs the coupling strength between oscillators. □

Remark 12. Under condition *(iii)*, the LTI system (5.9) can be decoupled through a coordinate transformation. To see this, let P be a permutation matrix such that

$$\boldsymbol{\xi} = P \begin{bmatrix} \mathbf{x} \\ \mathbf{y} \end{bmatrix}, \quad \boldsymbol{\xi} := \begin{bmatrix} x_1 & y_1 & \dots & x_n & y_n \end{bmatrix}^{\mathsf{T}}.$$

With L being real, the dynamical equation of $\boldsymbol{\xi}$ is given by

$$\begin{aligned} &\dot{\boldsymbol{\xi}} = A\boldsymbol{\xi}, \quad A := I \otimes E + \delta(L \otimes I)(I \otimes F), \\ &E := \begin{bmatrix} -\varepsilon\omega\gamma & 0 \\ 0 & 0 \end{bmatrix}, \quad F := \begin{bmatrix} 1 & 0 \\ \varepsilon\gamma & 1 \end{bmatrix}. \end{aligned} \tag{5.13}$$

The assembled dynamical system (5.13) can be decoupled into subsystems using master stability analysis [PC98],

$$\dot{\boldsymbol{\xi}}_k = (E + \lambda_k \delta F)\, \boldsymbol{\xi}_k, \qquad \boldsymbol{\xi}_k \in \mathbb{R}^2, \quad k \in \mathbb{I}_n,$$

where λ_k is the k^{th} eigenvalue of L. It can be shown that with condition *(iii)*, all the subsystems are stabilized except for one converging to a constant, which corresponds to the rigid body mode. □

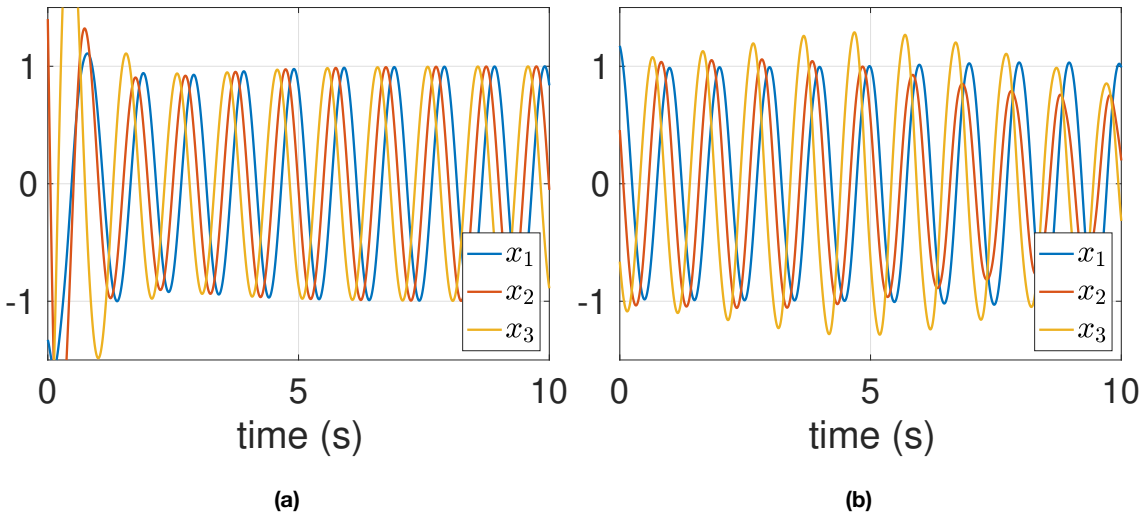

Figure 5.1: Stability with respect to the magnitude of ε. (a) $\varepsilon = 0.1$, A is o-stable; (b) $\varepsilon = 1$, A is unstable.

5.2.4 A Numerical Example

Example 10. Consider a network of three oscillators with target orbit $\boldsymbol{\zeta} = e^{j(\omega t + \boldsymbol{\varphi})}$, where $\omega = 2\pi$ and $\boldsymbol{\varphi} = \begin{bmatrix} 0 & \pi/3 & 2\pi/3 \end{bmatrix}^{\mathsf{T}}$. We examine the relationship between the magnitude of δ, ε and the stability of A defined in equation (5.10), also the stability of the network. First we set

$$L = L_R + jL_I,$$
$$L_R = \begin{pmatrix} -1 & 0 & 1 \\ 1 & -2 & 1 \\ 0 & 1 & -1 \end{pmatrix}, \quad L_I = \begin{pmatrix} -2 & 0 & 2 \\ -1 & -3 & 4 \\ 1 & 7 & -8 \end{pmatrix}.$$

Then $L \in \mathbb{H}_o$. The coupling matrix M is calculated through equation (5.5). In the first case, δ is fixed to be 1. When $\varepsilon = 0.1$, A is o-stable. A becomes unstable if we increase ε to 1. Simulations with two different values of ε is shown in Figure 5.1.

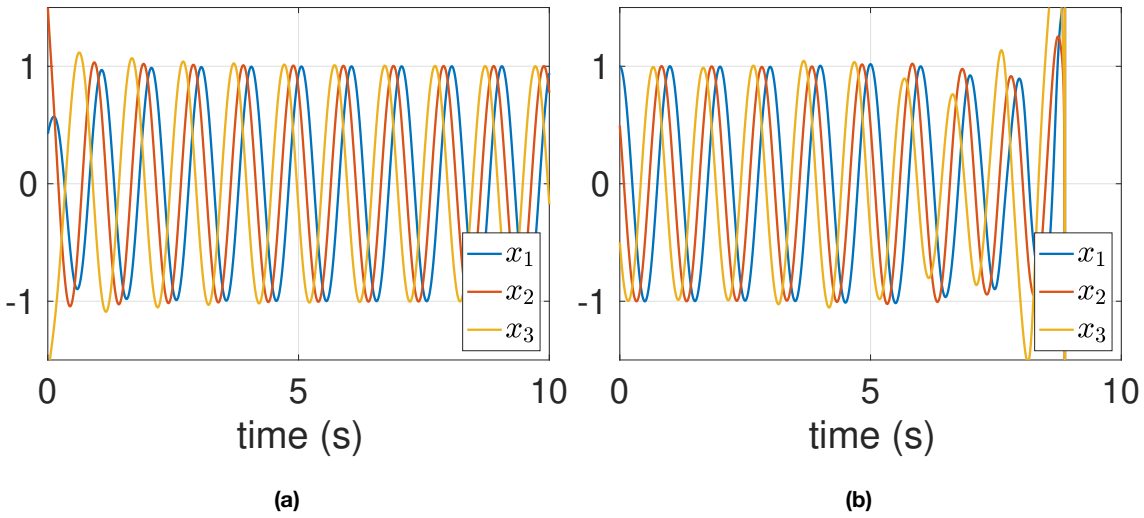

Figure 5.2: Stability with respect to the magnitude of δ. (a) $\delta = 0.1$, $\mathbf{A}$ is o-stable; (b) $\delta = 1$, $\mathbf{A}$ is unstable.

Then we set

$$L = L_R + jL_I,$$
$$L_R = \begin{pmatrix} -1 & 0 & 1 \\ 1 & -2 & 1 \\ 0 & 1 & -1 \end{pmatrix}, \quad L_I = \begin{pmatrix} -2 & 0 & 2 \\ -2 & 5 & -3 \\ 6 & 4 & -10 \end{pmatrix}.$$

Note that $\Re[L] \in \mathbb{H}_o$ while $\Im[L] \notin \mathbb{H}_o$. In this case, ε is fixed to be 1. When $\delta = 0.1$, $\mathbf{A}$ is o-stable. $\mathbf{A}$ becomes unstable if we increase δ to 1. Simulations with two different values of δ is shown in Figure 5.2. □

5.3 Multiple Limit Cycle Design

5.3.1 Limitation of the Single Limit Cycle Result

Suppose we want to embed multiple limit cycles into the coupled oscillator network (5.3). For each oscillation profile of a limit cycle, the associated L matrix is defined by (5.5) which we denote as L_k here. In addition, L_k must satisfy the eigenstructure condition (5.7). This

implies that, for the frequency and phase pair $(\omega_k, \boldsymbol{\varphi}_k)$ of the k^{th} limit cycle, it holds that

$$Me^{j\boldsymbol{\varphi}_k} = j\omega_k e^{j\boldsymbol{\varphi}_k}.$$

Moreover, the eigenvalues of L_k associated with that limit cycle must lie in the open left half plane except for a zero eigenvalue. This is equivalent to that M has all the eigenvalues in the open left half plane except for one at $j\omega_k$, which corresponds to the eigenvector $e^{j\boldsymbol{\varphi}_k}$. This is not possible since every limit cycle would impose such condition. M would have as many eigenvalues on the imaginary axis as the number of limit cycles. This contradicts the conditions in Theorem 10.

5.3.2 Linearization Around Multiple Orbits

Knowing that converting to a synchronization problem would not help to solve the multiple limit cycle problem, we backstep to the original coordinate, and attempt to solve a coordination problem instead. To that end, let us first assume there are m limit cycles given by

$$\begin{aligned} &\boldsymbol{\zeta}_k = \gamma e^{j(\omega_k t + \boldsymbol{\varphi}_k)} \in \mathbb{C}^n, \\ &\gamma \in \mathbb{R}_+, \quad \omega_k \in \mathbb{R}_+, \quad \boldsymbol{\varphi}_k \in \mathbb{R}^n, \quad k \in \mathbb{I}_m. \end{aligned} \tag{5.14}$$

Then for the k^{th} limit cycle we define a new state variable

$$\mathbf{w} := \Psi_k \mathbf{q}, \quad \Psi_k := \operatorname{diag}(e^{j\boldsymbol{\varphi}_k}), \tag{5.15}$$

where $\mathbf{q}$ is the perturbation variable defined in (5.8). This implies $\mathbf{w} = e^{-j\omega_k t}(\mathbf{z} - \boldsymbol{\zeta}_k)$. For each limit cycle, $\mathbf{w}$ no longer seeks to synchronize. Unlike the dynamics of $\mathbf{q}$ given by (5.11), the dynamics of $\mathbf{w}$ would depend on the oscillation profile of a specific limit cycle. The following lemma states the dynamics in the $\mathbf{w}$ coordinate.

Lemma 17. *Consider the network of coupled oscillators (5.3) with Assumption 2, and*

periodic functions $\boldsymbol{\zeta}_k, \forall k \in \mathbb{I}_m$ *in* (5.14). *Define*

$$M_R + jM_I := M, \quad \mathcal{M} := \begin{bmatrix} M_R & -M_I \\ M_I & M_R \end{bmatrix},$$

and

$$\mathcal{K}_k := \mathcal{M} - \omega_k \mathcal{I}, \quad \mathcal{I} := \begin{bmatrix} 0 & -I \\ I & 0 \end{bmatrix},$$

$$\mathbf{e}_k := \begin{bmatrix} \cos \boldsymbol{\varphi}_k \\ \sin \boldsymbol{\varphi}_k \end{bmatrix}.$$

Then $\mathbf{z} = \boldsymbol{\zeta}_k$ *is a solution to* (5.3) *if and only if*

$$\mathcal{K}_k \mathbf{e}_k = 0. \tag{5.16}$$

In this case, the linearization around $\mathbf{z} = \boldsymbol{\zeta}_k$ *can be described as*

$$\dot{\boldsymbol{w}} = (\mathcal{K}_k + \varepsilon\gamma \mathcal{I}\mathcal{M}\mathsf{G}_k)\boldsymbol{w}, \tag{5.17}$$

$$\boldsymbol{w} := \begin{bmatrix} \Re[\mathbf{w}] \\ \Im[\mathbf{w}] \end{bmatrix}, \quad \mathbf{w} := e^{-j\omega_k t}(\mathbf{z} - \boldsymbol{\zeta}_k),$$

where

$$\mathsf{G}_k := \begin{bmatrix} C_k \\ S_k \end{bmatrix} \begin{bmatrix} C_k & S_k \end{bmatrix}, \quad \begin{matrix} C_k := \operatorname{diag}(\cos \boldsymbol{\varphi}_k), \\ S_k := \operatorname{diag}(\sin \boldsymbol{\varphi}_k). \end{matrix} \tag{5.18}$$

□

Proof. First, (5.16) is a direct implication from the zero eigenvalue constraint (5.7) and Lemma 19. Then with the relationship between $\mathbf{w}$ and $\mathbf{q}$, (5.15), and noting that $\Psi_k = C_k + jS_k$, we obtain

$$\Re[\mathbf{q}] = C_k \Re[\mathbf{w}] + S_k \Im[\mathbf{w}].$$

Thus using the dynamical equations of $\mathbf{q}$, (5.11), and plugging in the relationship between L and M, (5.5), we have

$$\begin{aligned}\dot{\mathbf{w}} &= \Psi_k \dot{\mathbf{q}} \\ &= (M - j\omega_k I)\mathbf{w} + j\varepsilon\gamma M(C_k + jS_k)(C_k\Re[\mathbf{w}] + S_k\Im[\mathbf{w}]).\end{aligned}$$

Using Lemma 19, we arrive at

$$\begin{aligned}\begin{bmatrix}\Re[\dot{\mathbf{w}}] \\ \Im[\dot{\mathbf{w}}]\end{bmatrix} &= (\mathcal{M} - \omega_k\mathcal{I}) \begin{bmatrix}\Re[\mathbf{w}] \\ \Im[\mathbf{w}]\end{bmatrix} \\ &\qquad + \varepsilon\gamma\mathcal{I}\mathcal{M} \begin{bmatrix}C_k & -S_k \\ S_k & C_k\end{bmatrix} \begin{bmatrix}C_k\Re[\mathbf{w}] + S_k\Im[\mathbf{w}] \\ 0\end{bmatrix} \\ &= (\mathcal{M} - \omega_k\mathcal{I}) \begin{bmatrix}\Re[\mathbf{w}] \\ \Im[\mathbf{w}]\end{bmatrix} + \varepsilon\gamma\mathcal{I}\mathcal{M} \begin{bmatrix}C_k \\ S_k\end{bmatrix} \begin{bmatrix}C_k & S_k\end{bmatrix} \begin{bmatrix}\Re[\mathbf{w}] \\ \Im[\mathbf{w}]\end{bmatrix} \\ \iff \dot{\boldsymbol{w}} &= (\mathcal{K}_k + \varepsilon\gamma\mathcal{I}\mathcal{M}\mathsf{G}_k)\boldsymbol{w}.\end{aligned}$$

■

Remark 13. Define $K_k := M - j\omega_k I$. Using Lemma 19, we see that

$$\mathcal{K}_k = \begin{bmatrix}K_R & -K_I \\ K_I & K_R\end{bmatrix}, \quad K_R + jK_I := K_k.$$

Solving this equation for M in terms of K_k, the original system (5.3) is now described as

$$\dot{\mathbf{z}} = j\omega_k\Phi(|\mathbf{z}|)\mathbf{z} + K_k\Phi(|\mathbf{z}|)\mathbf{z}.$$

With $K_k = 0$, this system is a set of uncoupled oscillators having a periodic solution $z_i = \gamma e^{j\omega_k t}$ for all $i \in \mathbb{I}_n$, which is orbitally stable if $\Im[\phi'(\gamma)] > 0$. Hence, K_k can be thought of as the coupling matrix. □

5.3.3 Condition for Multi-Stability

The orbital stability of a specific limit cycle is guaranteed if the linearization around that limit cycle leads to an o-stable system. In this section, we show that, with constraints

on the eigenstructure of the coupling matrix M of the system (5.3) imposed jointly by the oscillation profiles of the limit cycles, along with constraints on the nonlinearity of the nonlinear oscillators, the system (5.3) is capable of exhibiting multiple limit cycles with orbital stability ensured. We state the results first and provide the proof thereafter.

Theorem 11. *Consider system (5.3) with Assumption 2. Let m target oscillations be given by*

$$\boldsymbol{\zeta}_k(t) = \gamma e^{j(\omega_k t + \boldsymbol{\varphi}_k)} \in \mathbb{C}^n, \quad k \in \mathbb{I}_m,$$

where $\gamma, \omega_k \in \mathbb{R}_+$ and $\boldsymbol{\varphi}_k \in \mathbb{R}^n$ are prescribed constants. Suppose the following holds.

(i) $MV = V\Lambda$, *where*

$$V := \begin{bmatrix} e^{j\boldsymbol{\varphi}_1} & e^{j\boldsymbol{\varphi}_2} & \dots & e^{j\boldsymbol{\varphi}_m} \end{bmatrix},$$

$$\Lambda := j \begin{bmatrix} \omega_1 & & & \\ & \omega_2 & & \\ & & \ddots & \\ & & & \omega_m \end{bmatrix};$$

(ii) $\mathrm{eig}(M) \setminus \{j\omega_k\} \in \mathrm{OLHP}$;

(iii) ε *is positive and sufficiently small.*

Then $z = \boldsymbol{\zeta}_k, \forall k \in \mathbb{I}_m$ are orbitally stable limit cycles of system (5.3). □

Proof. Starting from Lemma 17, the linearized dynamics around each limit cycle are given by (5.17) under condition (5.16), which is satisfied due to condition *(i)*. Thus equivalently we need to prove that the LTI system (5.17) is o-stable for all $k \in \mathbb{I}_m$. Without loss of generality, we prove the case of one of the limit cycles, and thereby drop the sub/superscript k for simplicity. The dynamics of (5.17) can be divided into two parts, $\mathcal{K}$ and $\varepsilon\gamma\mathcal{I}\mathcal{M}\mathbb{G}$. The latter matrix can be regarded as a perturbation on $\mathcal{K}$. We will first prove that all the

eigenvalues of $\mathcal{K}$ are either on the imaginary axis, or in the OLHP, and then argue that all the eigenvalues on the imaginary axis, except for one at the origin, will be perturbed and moved towards left by the effect of $\varepsilon\gamma\mathcal{I}\mathcal{M}\mathsf{G}$.

First notice that $M\mathbf{v}_i = j\omega_i\mathbf{v}_i, \mathbf{v}_i := e^{j\boldsymbol{\varphi}_i}$ for all $i \in \mathbb{I}_m$. Denote by $\mathbf{u}_i$ the left eigenvalue of M associated with $j\omega_i$, that is,

$$\mathbf{u}_i^* M = j\omega_i \mathbf{u}_i^*, \quad \mathbf{u}_i^* \mathbf{v}_i = 1.$$

Also, we have

$$K\mathbf{v}_i = j(\omega_i - \omega)\mathbf{v}_i, \quad \mathbf{u}_i^* K = j(\omega_i - \omega)\mathbf{u}_i,$$

where $K := M - j\omega I$, and ω is the frequency of the limit cycle of linearization. Immediately it comes to our notice that M and $\mathcal{M}$, also K and $\mathcal{K}$ can be related through Lemma 19. Then

$$\begin{aligned} \mathcal{M}\mathcal{V}_i &= \omega_i \mathcal{V}_i \mathcal{J}, & \mathcal{U}_i\mathcal{M} &= \omega_i \mathcal{J}\mathcal{U}_i, \\ \mathcal{K}\mathcal{V}_i &= (\omega_i - \omega)\mathcal{V}_i\mathcal{J}, & \mathcal{U}_i\mathcal{K} &= (\omega_i - \omega)\mathcal{J}\mathcal{U}_i, \end{aligned}$$

for all $i \in \mathbb{I}_m$, where

$$\mathcal{V}_i := \begin{bmatrix} \mathbf{v}_i & \overline{\mathbf{v}}_i \\ -j\mathbf{v}_i & j\overline{\mathbf{v}}_i \end{bmatrix} \in \mathbb{C}^{2n\times 2},$$

$$\mathcal{U}_i := \begin{bmatrix} \mathbf{u}_i^* & j\mathbf{u}_i^* \\ \mathbf{u}_i^\mathsf{T} & -j\mathbf{u}_i^\mathsf{T} \end{bmatrix} \in \mathbb{C}^{2\times 2n}, \quad \mathcal{J} := \begin{bmatrix} j & \\ & -j \end{bmatrix} \in \mathbb{C}^{2\times 2}.$$

As can be seen, $\mathcal{K}$ has $2m$ eigenvalues on the imaginary axis which show up as conjugate pairs, including two at the origin, and the corresponding left/right eigenvectors are well defined. We shall then see how $\varepsilon\gamma\mathcal{I}\mathcal{M}\mathsf{G}$ is going to affect those eigenvalues of $\mathcal{K}$ on the imaginary axis. First we consider the non-zero eigenvalues. Without loss of generality, we analyze one eigenvalue of a conjugate pair, $j(\omega_i - \omega)$, with the associated right and left eigenvalue $\begin{bmatrix} \mathbf{v}_i \\ -j\mathbf{v}_i \end{bmatrix}$

and $\begin{bmatrix} \mathbf{u}_i^* & j\mathbf{u}_i^* \end{bmatrix}$, respectively. In light of Lemma 20, the right and left eigenvectors, along with the perturbation term, will altogether determine the direction the associated eigenvalue moves towards given the perturbation is small. Thus, using the definition of G in (5.18), the matrix

$$\begin{aligned}
\mathcal{N}_i &= \begin{bmatrix} \mathbf{u}_i^* & j\mathbf{u}_i^* \end{bmatrix} \varepsilon\gamma \mathcal{I}\mathcal{M}\mathsf{G} \begin{bmatrix} \mathbf{v}_i \\ -j\mathbf{v}_i \end{bmatrix} \\
&= \varepsilon\gamma \begin{bmatrix} \mathbf{u}_i^* & j\mathbf{u}_i^* \end{bmatrix} \mathcal{M}\mathcal{I} \begin{bmatrix} C \\ S \end{bmatrix} \begin{bmatrix} C & S \end{bmatrix} \begin{bmatrix} \mathbf{v}_i \\ -j\mathbf{v}_i \end{bmatrix} \\
&= j\varepsilon\omega\gamma \begin{bmatrix} \mathbf{u}_i^* & j\mathbf{u}_i^* \end{bmatrix} \begin{bmatrix} 0 & -I \\ I & 0 \end{bmatrix} \begin{bmatrix} C \\ S \end{bmatrix} \begin{bmatrix} C & S \end{bmatrix} \begin{bmatrix} \mathbf{v}_i \\ -j\mathbf{v}_i \end{bmatrix} \\
&= -\varepsilon\omega_i\gamma \mathbf{u}_i^*(C + jS)(C - jS)\mathbf{v}_i \\
&= -\varepsilon\omega_i\gamma \mathbf{u}_i^*\mathbf{v}_i \\
&= -\varepsilon\omega_i\gamma
\end{aligned}$$

decides how the eigenvalue $j(\omega_i - \omega)$ is perturbed if ε is sufficiently small. $\mathcal{N}_i$ has to be negative if we are to move the eigenvalue to the left of the imaginary axis. By definition, ω_i and γ are positive numbers. Therefore, the condition boils down to simply $\varepsilon > 0$. The same conclusion is valid for its complex conjugate $j(\omega - \omega_i)$.

We then consider the two zero eigenvalues. Since the zero eigenvalue is repeated, all the associated eigenvector should be incorporated in the analysis. Denote by $\mathbf{v}_o$ and $\mathbf{u}_o$ the right and left eigenvectors of M corresponding to $j\omega$, respectively. I.e.,

$$\begin{aligned}
&M\mathbf{v}_o = j\omega\mathbf{v}_o, \quad \mathbf{v}_o := e^{j\boldsymbol{\varphi}}. \\
&\mathbf{u}_o^* M = j\omega\mathbf{u}_o^*, \quad \mathbf{u}_o^*\mathbf{v}_o = 1.
\end{aligned}$$

Therefore, by Lemma 19, we arrive at

$$\begin{aligned}
&\mathcal{M}\mathcal{V}_o = \omega\mathcal{I}\mathcal{V}_o, \quad \mathcal{U}_o\mathcal{M} = \omega\mathcal{U}_o\mathcal{I}, \\
&\mathcal{K}\mathcal{V}_o = 0, \qquad\quad \mathcal{U}_o\mathcal{K} = 0,
\end{aligned}$$

where

$$\mathcal{V}_o := \begin{bmatrix} \mathbf{c} & -\mathbf{s} \\ \mathbf{s} & \mathbf{c} \end{bmatrix} \in \mathbb{R}^{2n\times 2}, \quad \begin{aligned} \mathbf{c} &:= \cos\boldsymbol{\varphi}, \\ \mathbf{s} &:= \sin\boldsymbol{\varphi}, \end{aligned}$$

$$\mathcal{U}_o := \begin{bmatrix} \Re[\mathbf{u}_o]^\mathsf{T} & \Im[\mathbf{u}_o]^\mathsf{T} \\ -\Im[\mathbf{u}_o]^\mathsf{T} & \Re[\mathbf{u}_o]^\mathsf{T} \end{bmatrix} \in \mathbb{R}^{2\times 2n}.$$

Then the matrix

$$\begin{aligned} \mathcal{N}_o &= \mathcal{U}_o\varepsilon\gamma\mathcal{I}\mathcal{M}\mathsf{G}\mathcal{V}_o = \varepsilon\gamma\mathcal{U}_o\mathcal{M}\mathcal{I}\mathsf{G}\mathcal{V}_o = -\varepsilon\omega\gamma\mathcal{U}_o\mathsf{G}\mathcal{V}_o \\ &= -\varepsilon\omega\gamma\mathcal{U}_o \begin{bmatrix} C \\ S \end{bmatrix} \begin{bmatrix} C & S \end{bmatrix} \begin{bmatrix} \mathbf{c} & -\mathbf{s} \\ \mathbf{s} & \mathbf{c} \end{bmatrix} \\ &= \begin{bmatrix} -\varepsilon\omega\gamma & 0 \\ 0 & 0 \end{bmatrix} \end{aligned} \tag{5.19}$$

needs to have all the eigenvalues on the OLHP except for a zero. This is accomplished by $\varepsilon > 0$.

A similar deduction would yield where the eigenvalues of $\mathcal{K}$, other than those on the imaginary axis, are located. Consider an eigenvalue of M, λ, in the OLHP. Then $\lambda - j\omega$ would be an eigenvalue of K. Further, $\mathcal{K}$ will have $\lambda - j\omega$ and $\overline{\lambda} + j\omega$ as its eigenvalues, which are also in the OLHP. They will remain in the OLHP under small perturbation due to continuity.

As such, we have proved that $\mathcal{K}$ is o-stable, and this holds for all limit cycles. Then this theorem is concluded due to Lemma 17. ■

Remark 14. The results of Theorem 11 actually resemble those of a linear system. Let us consider the case where the nonlinearity is removed. Then the corresponding linear system is described by

$$\dot{\mathbf{z}} = M\mathbf{z}, \qquad \mathbf{z} \in \mathbb{C}^n, \quad M \in \mathbb{C}^{n\times n}.$$

This linear system exhibits exactly m oscillatory modes $\boldsymbol{\zeta}_k(t) = \tilde{\gamma}e^{j(\omega_k t + \boldsymbol{\varphi}_k)}$ if and only if condition *(i)* and *(ii)* in Theorem 11 hold for all $k \in \mathbb{I}_m$, where $\tilde{\gamma}$ is dependent on the

initial conditions. Two issues would emerge without the nonlinearity term. One is that the amplitude of the oscillation is undetermined, while the other issue being all modes are not orbitally stable. That means the state of the linear system converges to a superposition of several oscillatory modes, with amplitude depending on the initial conditions. With the aid of the nonlinear dynamics, we manage to fix the amplitude and stabilize the orbit. □

5.3.4 A Numerical Example

Example 11. Let us take a look at a simple design example as shown in Figure 5.3. A network is consist of 3 oscillators and admits 2 limit cycles. The amplitude of the oscillations is set uniformly to be $\gamma = 1$. The two phase profiles are

$$\boldsymbol{\varphi}_1 = \begin{bmatrix} 0 & 0 & 0 \end{bmatrix}^\mathsf{T}, \quad \boldsymbol{\varphi}_2 = \begin{bmatrix} 0 & \pi/3 & 2\pi/3 \end{bmatrix}^\mathsf{T}.$$

And the frequencies are chosen to be

$$\omega_1 = 2\pi, \quad \omega_2 = \pi.$$

First V is given by $V = \begin{bmatrix} e^{j\boldsymbol{\varphi}_1} & e^{j\boldsymbol{\varphi}_2} \end{bmatrix}$, and $\Lambda = j\mathrm{diag}(\omega_1, \omega_2)$. Let U be the orthogonal complement of V and define $T := \begin{bmatrix} V & U \end{bmatrix}$. Let $\Omega = j\mathrm{diag}(\Lambda, \lambda)$ where $\lambda \in \mathbb{C}$ can be any complex number with negative real part. Here we choose $\lambda = -2 + j1$. Finally, M is constructed by $M = T\Omega T^{-1}$, which yields

$$M = \begin{pmatrix} 0.69 + j3.97 & 0.97 + j0.92 & -1.66 + j1.39 \\ 1.32 + j2.25 & -1.20 + j2.49 & -0.12 + j1.55 \\ 1.26 + j0.70 & 0.23 + j1.62 & -1.49 + j3.97 \end{pmatrix}.$$

The weights of the coupling between two oscillators are decided by the matrix M. Figure 5.4 illustrates the two orbitally stable limit cycles this network admits.

□

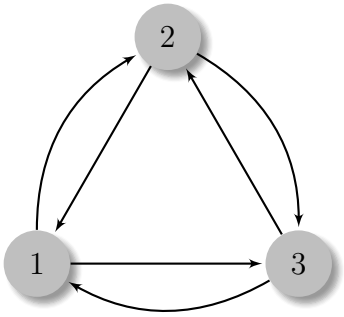

Figure 5.3: An example of a network with 3 oscillators.

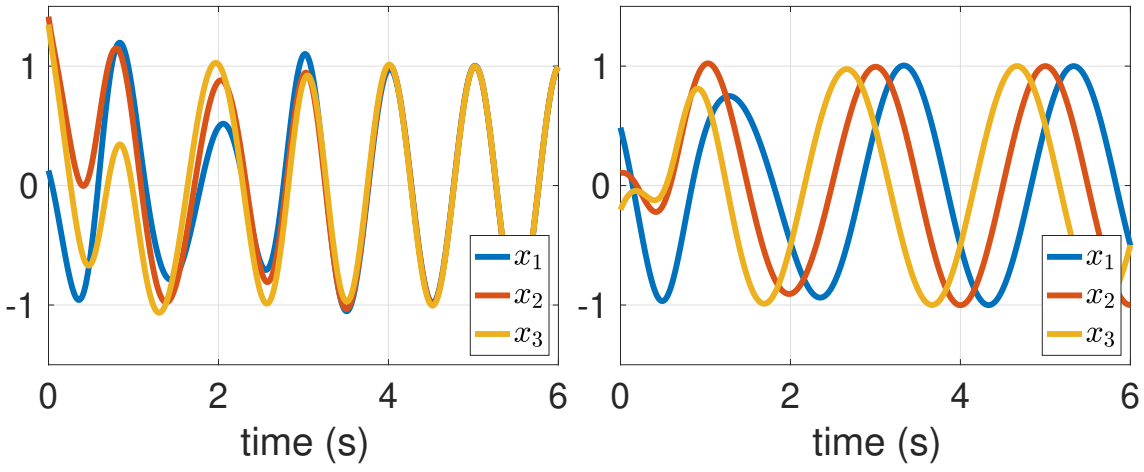

Figure 5.4: Two limit cycles of the network depicted in Figure 5.3 depending on the initial condition.

5.4 Distributed Network

The design procedures for the oscillator networks in the previous sections do not impose any constraints on the connectivity of the oscillators. Hence the network is unstructured. However it is not always possible to specify the communication between the oscillators arbitrarily. Or, sometimes it is preferable to have the connectivity in a certain form than another. We thereby discuss the design of a distributed network in this section. In the formulation (5.3), the connectivity of the network is determined by the coupling matrix M. Thus the design problem with connectivity constraints boils down to designing a network with structured M.

5.4.1 Single Limit Cycle

It is straightforward to find the conditions for distributed network with one limit cycle based on Theorem 10. Since the network can be written in the form of (5.12), it is immediately noticed that L determines the topology of the network. A critical design constraint on L is the diffusive coupling (5.7). This coincides with the property of a Laplacian matrix in graph theory. Suppose the topology of the network is represented by a connected directed graph $\mathcal{G}(\mathcal{V}, \mathcal{E})$, with vertices $\mathcal{V}$, edges $\mathcal{E} \subseteq \mathcal{V} \times \mathcal{V}$, weights a_{ij}, and associated Laplacian matrix L. L is known to have a zero eigenvalue and corresponding eigenvector $\mathbf{1}$, i.e., $L\mathbf{1} = 0$. Moreover, L belongs to the set $\mathbb{H}_o$, which is a necessary condition in statement *(i)* and *(iii)* of Theorem 10, if and only if the directed graph contains a spanning tree with nonnegative weights [RB05, Lemma 3.3]. The definition of a spanning tree and the proof of the statement is referred to [LI17, Lemma 4].

Example 12. An example is illustrated in Figure 5.5(a). There are four vertices in the network. The red edges along with the vertices connected form a spanning tree with vertex

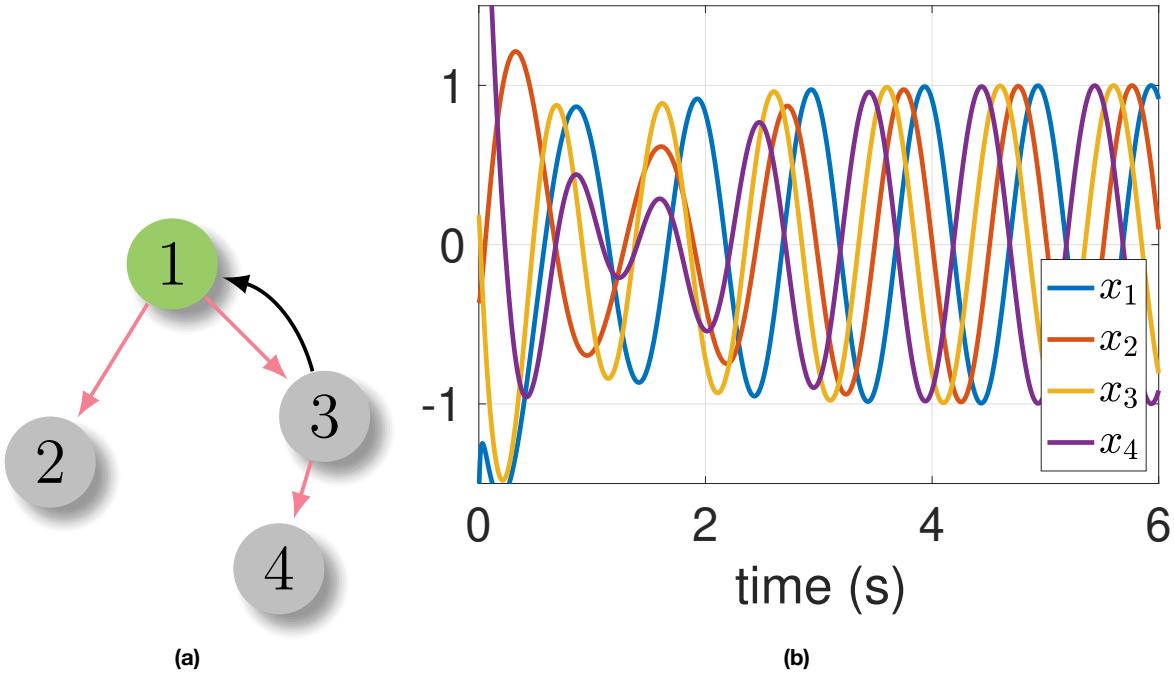

Figure 5.5: Spanning tree structure.

1 being the root. The Laplacian is given by

$$L = \begin{pmatrix} -1 & 0 & 1 & 0 \\ 1 & -1 & 0 & 0 \\ 1 & 0 & -1 & 0 \\ 0 & 0 & 1 & -1 \end{pmatrix}.$$

We consider a target limit cycle with phase $\varphi = \begin{bmatrix} 0 & \pi/3 & 2\pi/3 & \pi \end{bmatrix}^\mathsf{T}$, frequency $\omega = 2\pi$ and amplitude $\gamma = 1$. The coupling matrix M is obtained through equation (5.5) where we set $\delta = 1$. Figure 5.5(b) shows the simulation result.

□

5.4.2 Network Design via Eigenstructure Assignment

We rely on a result in [WI17] for the multiple limit cycle design. In [WI17], a strategy to design a distributed feedback controller to achieve pattern formation of a group of linear systems via eigenstructure assignment is proposed.

Consider n LTI plants

$$\dot{\mathbf{x}}_k = A_k\mathbf{x}_k + B_k\mathbf{u}_k, \quad k \in \mathbb{I}_n.$$

Suppose Λ is a known square matrix with eigenvalues in the closed right half plane. For each $k \in \mathbb{I}_n$, we are given a matrix X_k, and the matrix U_k which satisfies

$$A_kX_k + B_kU_k = X_k\Lambda.$$

Then K_k and J_k are chosen such that the matrix

$$\Omega_k := A_k + B_kK_k - X_kJ_k$$

is Hurwitz. Further, a matrix N_k is calculated such that

$$\Lambda N_k - N_k\Omega_k = J_k.$$

Finally, the matrix Γ_k is formed to be

$$\Gamma_k := \begin{bmatrix} N_kB_k & I - N_kX_k \end{bmatrix}.$$

Let $\mathbb{L}$ be the set of real Laplacian matrices for digraphs containing a spanning tree with positive weights. That is, $L \in \mathbb{L}$ if and only if L has the following properties: *1*) the row sum is equal to zero, *2*) all the off-diagonal entries are nonpositive, and *3*) at least one of the cofactors is nonzero. Let $\mathbb{L}_\Lambda$ be the set of $L \in \mathbb{L}$ such that the smallest real-part of the nonzero eigenvalues of L is greater than the largest real part of the eigenvalues of Λ.

Consider the distributed control

$$\mathbf{v} = -\mathcal{L}\boldsymbol{\eta}, \quad \mathcal{L} := L \otimes I_m, \quad L \in \mathbb{L}_\Lambda,$$
$$\begin{bmatrix} \boldsymbol{\eta}_k \\ \mathbf{u}_k \\ \dot{\boldsymbol{\xi}}_k \end{bmatrix} = \begin{bmatrix} I \\ U_k \\ \Lambda \end{bmatrix} \boldsymbol{\xi}_k + \begin{bmatrix} N_k \\ K_k \\ J_k \end{bmatrix} (\mathbf{x}_k - X_k \boldsymbol{\xi}_k) + \begin{bmatrix} 0 & 0 \\ I & 0 \\ 0 & I \end{bmatrix} \Gamma_k^\dagger \mathbf{v}_k.$$

The closed-loop system is given by

$$\begin{bmatrix} \dot{\mathbf{x}} \\ \dot{\boldsymbol{\xi}} \end{bmatrix} = M \begin{bmatrix} \mathbf{x} \\ \boldsymbol{\xi} \end{bmatrix},$$
$$M := \begin{bmatrix} A + BK - BG\mathcal{L}N & B(\mathcal{U} - K\mathcal{X}) - BG\mathcal{L}(I - N\mathcal{X}) \\ J - H\mathcal{L}N & \boldsymbol{\Lambda} - J\mathcal{X} - H\mathcal{L}(I - N\mathcal{X}) \end{bmatrix}$$

where A, B, K, J, N, $\mathcal{U}$, $\mathcal{X}$, $\boldsymbol{\Lambda}$, G and H are block diagonal matrices with A_k, B_k, K_k, J_k, N_k, U_k, X_k, λ, G_k and H_k on the diagonal, respectively, and G_k and H_k are defined by $\Gamma_k^\dagger = \mathrm{col}(G_k, H_k)$.

Define $X := \mathrm{col}(X_1, \ldots, X_n)$, $\mathrm{J} := \mathrm{col}(I_m, \ldots, I_m)$, and $\mathcal{V} := \mathrm{col}(X, \mathrm{J})$. Suppose that (X, Λ) is observable, and Γ_k has a full row rank. Then the system satisfies

$$M\mathcal{V} = \mathcal{V}\Lambda, \quad \mathrm{eig}(M) \setminus \mathrm{eig}(\Lambda) \subset \mathbb{C}_-.$$

where M is the coefficient matrix of the above closed-loop system, and we note that

$$\mathcal{L}\mathrm{J} = 0, \quad \boldsymbol{\Lambda}\mathrm{J} = \mathrm{J}\Lambda, \quad \mathcal{U}\mathrm{J} = U, \quad \mathcal{X}\mathrm{J} = X.$$

As can be seen, we managed to assign the desired eigenstructure onto the coefficient matrix M under a topological constraint described by L. We apply this design strategy to our network of coupled oscillators by extending the result to the case where the matrices are relaxed to be complex-valued. The result for eigenstructure assignment is stated below.

Lemma 18. *Consider*

$$M := \begin{bmatrix} K - \mathcal{X}\mathcal{L}N & \mathcal{X}\boldsymbol{\Lambda} - K\mathcal{X} - \mathcal{X}\mathcal{L}(I - N\mathcal{X}) \\ J - \mathcal{L}N & \boldsymbol{\Lambda} - J\mathcal{X} - \mathcal{L}(I - N\mathcal{X}) \end{bmatrix},$$
$$\mathcal{L} := L \otimes I_m, \quad L \in \mathbb{L}_\Lambda,$$

where K, J, N, and $\mathcal{X}$ are block diagonal complex matrices with K_k, J_k, N_k, and X_k, for $k \in \mathbb{I}_n$, on the diagonal, respectively, $\boldsymbol{\Lambda}$ is the block diagonal complex matrix with Λ repeated n times on the diagonal, and L is an $n \times n$ real matrix. Suppose $\Lambda \in \mathbb{C}^{m\times m}$ is a matrix with eigenvalues in the closed right half plane, $\Omega_k := K_k - X_k J_k$ has all eigenvalues in the open left half plane, and $\Lambda N_k - N_k \Omega_k = J_k$. Define $X := \mathrm{col}(X_1, \ldots, X_n)$, $\mathsf{J} := \mathrm{col}(I_m, \ldots, I_m)$, and $\mathcal{V} := \mathrm{col}(X, \mathsf{J})$. Then we have

$$M\mathcal{V} = \mathcal{V}\Lambda, \quad \mathrm{eig}(M) \setminus \mathrm{eig}(\Lambda) \subset \mathbb{C}_-.$$

□

Proof. First, $M\mathcal{V} = \mathcal{V}\Lambda$ can be verified through direct calculations by noting that $\mathcal{L}\mathsf{J} = 0, \mathcal{X}\mathsf{J} = X$, and $\boldsymbol{\Lambda}\mathsf{J} = \mathsf{J}\Lambda$. Next consider the similarity transformation

$$\begin{bmatrix} I & -\mathcal{X} \\ N & I - N\mathcal{X} \end{bmatrix} M \begin{bmatrix} I - \mathcal{X}N & \mathcal{X} \\ -N & I \end{bmatrix} = \begin{bmatrix} K - \mathcal{X}J & 0 \\ * & \boldsymbol{\Lambda} - \mathcal{L} \end{bmatrix}, \tag{5.20}$$

where $*$ indicates the immaterial entry. From the proof of Lemma 6 in [WI17], the eigenvalues of $\boldsymbol{\Lambda} - \mathcal{L}$ are give by $\lambda_i - \mu_j$ where $\lambda_i, i \in \mathbb{I}_m$ and $\mu_j, j \in \mathbb{I}_n$ are eigenvalues of $\Lambda \in \mathbb{C}^{m\times m}$ and $L \in \mathbb{R}^{n\times n}$, respectively. Since $L \in \mathbb{L}_\Lambda$, it has an eigenvalue at the origin ($\mu_n = 0$), and the other eigenvalues satisfy $\Re(\mu_j) > \Re(\lambda_i)$ for all $j \in \mathbb{I}_{n-1}$ and $i \in \mathbb{I}_m$. ■

Remark 15. The result essentially follows from Corollary 1 of [WI17] as a special case where

$$A_k = 0, \quad B_k = I,$$
$$U_k = X_k\Lambda, \quad G_k = X_k, \quad H_k = I, \quad k \in \mathbb{I}_m.$$

However, the above choice of $\mathrm{col}(G_k, H_k)$ is not exactly aligned with $\Gamma_k^\dagger$ in Corollary 1 of [WI17] since it is a pseudo-inverse but not necessarily the Moore-Penrose inverse. Also, the matrices in Lemma 18 are complex while those in Corollary 1 of [WI17] are real. The above proof justifies the statement in Lemma 18, and Corollary 1 of [WI17] provided the construction of M. □

5.4.3 Multiple Limit Cycles

For the network of coupled oscillators design with m limit cycles, we choose $\Lambda = j\Omega$ with Ω being the diagonal matrix with frequencies $\omega_k, k \in \mathbb{I}_m$, on the diagonal. For simplicity, x_k may be chosen to be a scalar variable, and (part of) the stability condition is a scalar inequality $K_k < X_k J_k$, where X_k is an m dimensional row vector specifying the phase of the k^{th} segmental oscillator for each of the m limit cycles: $X_{kq} = e^{j\varphi_{kq}}, q \in \mathbb{I}_m$.

Theorem 12. *Given m target oscillations*

$$\boldsymbol{\zeta}_i(t) = \gamma e^{j(\omega_i t + \boldsymbol{\varphi}_i)} \in \mathbb{C}^n, \quad i \in \mathbb{I}_m,$$

where $\gamma, \omega_i \in \mathbb{R}_+$ and $\boldsymbol{\varphi}_i \in \mathbb{R}^n$ are prescribed constants. Consider a network of n segmental oscillators whose dynamics is characterized by

$$\dot{\mathbf{x}}_k = P_k \Phi(|\mathbf{x}_k|)\mathbf{x}_k, \quad \mathbf{x}_k \in \mathbb{C}^{m+1},$$
$$P_k \in \mathbb{C}^{(m+1)\times(m+1)}, \quad k \in \mathbb{I}_n,$$

where $\Phi(\cdot)$ is defined in (5.3) with condition (5.2). Suppose the connectivity between the segmental oscillators is given by the Laplacian $L \in \mathbb{R}^{n\times n}$. Then the dynamics of the network can be captured by

$$\dot{\mathbf{x}}_k = P_k \Phi(|\mathbf{x}_k|)\mathbf{x}_k - \sum_{l=1}^{n} \ell_{kl} Q_{kl} \Phi(|\mathbf{x}_l|)\mathbf{x}_l, \quad k, l \in \mathbb{I}_n, \tag{5.21}$$

where ℓ_{kl} is the $(k,l)^{\text{th}}$ entry of L, and $Q_{kl} \in \mathbb{C}^{(m+1)\times(m+1)}$ is the additional interactive matrix between the segmental oscillators. Define E to be the $m \times m$ matrix whose $(i,k)^{\text{th}}$ entry is given by

$$E_{ik} = e^{j2\pi(ik/m)}, \quad i, k \in \mathbb{I}_m.$$

Then it can be verified that $E^*E = mI$. Let $\mathbf{x}_k$ be partitioned into

$$\mathbf{x}_k =: \begin{bmatrix} x_k & \boldsymbol{\xi}_k^{\mathsf{T}} \end{bmatrix}^{\mathsf{T}}, \quad x_k \in \mathbb{C}, \quad \boldsymbol{\xi}_k \in \mathbb{C}^m,$$

and define

$$\mathbf{z} := \begin{bmatrix} x_1, \ldots, x_n \end{bmatrix}^{\mathsf{T}}.$$

Then the network has m limit cycles, on which $\mathbf{z}$ converges to $\boldsymbol{\zeta}_i, i \in \mathbb{I}_m$, if P_k and Q_{kl} are constructed as

$$\begin{aligned} P_k &= \mathsf{E} \begin{bmatrix} K_k & X_k\Lambda - K_k X_k \\ J_k & \Lambda - J_k X_k \end{bmatrix} \mathsf{E}^{-1}, \\ Q_{kl} &= \mathsf{E} \begin{bmatrix} X_k \\ I \end{bmatrix} \begin{bmatrix} N_l & I - N_l X_l \end{bmatrix} \mathsf{E}^{-1}, \end{aligned} \tag{5.22}$$

respectively, where

$$\mathsf{E} := \mathrm{diag}(I, E), \quad \Lambda := j\mathrm{diag}(\omega_1, \ldots, \omega_m) \in \mathbb{C}^{m\times m};$$

$X_k \in \mathbb{C}^{1\times m}$ is the k^{th} row of

$$X := \begin{bmatrix} e^{j\boldsymbol{\varphi}_1} & \ldots & e^{j\boldsymbol{\varphi}_m} \end{bmatrix};$$

$K_k \in \mathbb{C}, J_k \in \mathbb{C}^m$ are such that

$$\Omega_k := K_k - X_k J_k$$

is Hurwitz; $N_l \in \mathbb{C}^m$ is determined by the Sylvester equation

$$\Lambda N_l - N_l \Omega_l = J_l.$$

□

Proof. With the above partition of $\boldsymbol{\chi}_k$ and choices of P_k, Q_{kl}, each segmental oscillator can be written as

$$\begin{aligned} \begin{bmatrix} \dot{x}_k \\ \dot{\boldsymbol{\xi}}_k \end{bmatrix} &= \mathsf{E} \begin{bmatrix} K_k & X_k\Lambda - K_k X_k \\ J_k & \Lambda - J_k X_k \end{bmatrix} \mathsf{E}^{-1} \begin{bmatrix} \phi(|x_k|)x_k \\ \Phi(|\boldsymbol{\xi}_k|)\boldsymbol{\xi}_k \end{bmatrix} \\ &\quad - \textstyle\sum_{l=1}^{n} \ell_{kl} \mathsf{E} \begin{bmatrix} X_k \\ I \end{bmatrix} \begin{bmatrix} N_l & I - N_l X_l \end{bmatrix} \mathsf{E}^{-1} \begin{bmatrix} \phi(|x_l|)x_l \\ \Phi(|\boldsymbol{\xi}_l|)\boldsymbol{\xi}_l \end{bmatrix}, \\ k &\in \mathbb{I}_n. \end{aligned}$$

Defining $\mathbf{x} = \mathrm{col}(x_k)$ and $\boldsymbol{\xi} = \mathrm{col}(\boldsymbol{\xi}_k)$, we have

$$\begin{bmatrix} \dot{\mathbf{x}} \\ \dot{\boldsymbol{\xi}} \end{bmatrix} = \mathcal{A} \begin{bmatrix} \Phi(|\mathbf{x}|)\mathbf{x} \\ \Phi(|\boldsymbol{\xi}|)\boldsymbol{\xi} \end{bmatrix}, \quad \mathcal{A} = FMF^{-1},$$
$$M := \begin{bmatrix} K - \mathcal{X}\mathcal{L}N & \mathcal{X}\Lambda - K\mathcal{X} - \mathcal{X}\mathcal{L}(I - N\mathcal{X}) \\ J - \mathcal{L}N & \Lambda - J\mathcal{X} - \mathcal{L}(I - N\mathcal{X}) \end{bmatrix},$$

where $\mathcal{L} := L \otimes I_m$, $F := \mathrm{diag}(I, E, \ldots, E)$ with E repeated n times on the diagonal, K, J, N, and $\mathcal{X}$ are block diagonal complex matrices with K_k, J_k, N_k, and X_k, for $k \in \mathbb{I}_n$, on the diagonal, respectively, Λ is the block diagonal complex matrix with Λ repeated n times on the diagonal. Application of Lemma 18 gives the eigenstructure of M. Since $\mathcal{A}$ is related to M by a similarity transformation, we have

$$\mathcal{A}W = W\Lambda, \quad W = \mathrm{col}(X, E, \ldots, E).$$

Thus all entries of W have magnitude one while the eigenvalues are preserved. At last, applying Theorem 11, the proof is completed. ■

Remark 16. Note that the network has the distributed structure specified by the directed graph associated with the Laplacian matrix L. Each decoupled subsystem admits a decomposition similar to (5.20) — just set $\mathcal{L} = 0$ and add subscript k, indicating that the eigenvalues are from $K_k - X_k J_k$ and Λ, with the eigenvectors for the latter given by $\mathrm{col}(X_k, E)$. Each segmental oscillator has multiple stable limit cycles specified by $x_k = e^{j(\omega_i t + \varphi_{ki})}$ and $\boldsymbol{\xi}_k = E_i, i \in \mathbb{I}_m$, where E_i is the i^{th} column of E. Notice that $E^{-1}E_i = e_i$, where e_i is the i^{th} column of the identity matrix I. That is, under a coordinate transformation E, the i^{th} auxiliary oscillator of a segmental oscillator is activated, and others are at rest. This holds true for every segmental oscillator. □

Based on Theorem 12, we provide Algorithm 1 for designing a distributed network with multiple limit cycles.

Remark 17. In the event that the number of limit cycle m is 1, $\Lambda = j\omega$ and $X_k = e^{j\varphi_k}, k \in \mathbb{I}_n$ reduce to scalars, where φ_k is the k^{th} entry of $\boldsymbol{\varphi}$. It is then possible to choose $K_k = \Lambda$ for all

Algorithm 1: Construct a distributed network with multiple limit cycles

Input : m target oscillations

$$\boldsymbol{\zeta}_i(t) = \gamma e^{j(\omega_i t + \boldsymbol{\varphi}_i)} \in \mathbb{C}^n, \quad i \in \mathbb{I}_m,$$

and graph Laplacian L.

Output: A network composed of n segmental oscillators, each of which has $m+1$ dimensional state.

construct $X := \begin{bmatrix} e^{j\boldsymbol{\varphi}_1} & \dots & e^{j\boldsymbol{\varphi}_m} \end{bmatrix}$, let $X_k \in \mathbb{C}^{1\times m}, k \in \mathbb{I}_n$ be the k^{th} row of X;

construct $\Lambda := j\text{diag}(\omega_1, \dots, \omega_m)$;

for $k \in \mathbb{I}_n$ **do**

  choose K_k and J_k, such that $\Omega_k := K_k - X_k J_k$ is Hurwitz;

  calculate N_k by solving the Sylvester equation $\Lambda N_k - N_k \Omega_k = J_k$;

end for

for $k, l \in \mathbb{I}_n$ **do**

  construct P_k and Q_{kl} as in (5.22);

end for

construct the oscillator network as in (5.21);

$k \in \mathbb{I}_n$ so that $X_k\Lambda - K_k X_k = 0$ and N_l such that $1 - N_l X_l = 0$, and thereby x_k is decoupled from $\boldsymbol{\xi}_k$. In this case the dynamics of x_k is given by

$$\dot{x}_k = j\omega\phi(|x_k|)x_k + \sum_{l=1}^{n} \ell_{kl} e^{j(\varphi_k - \varphi_l)} \phi(|x_l|)x_l, \quad l \in \mathbb{I}_n.$$

This is aligned with the statement *(iii)* of Theorem 10 since $L \in \mathbb{R}^{n\times n}$. □

Remark 18. If the oscillators are to be synchronized, and we choose $J_k = 0, M_k = 0$ for all $k \in \mathbb{I}_n$, the network becomes

$$\begin{bmatrix} \dot{\mathbf{x}} \\ \dot{\boldsymbol{\xi}} \end{bmatrix} = \begin{bmatrix} K & \mathcal{X}(\Lambda - \mathcal{L}) - K\mathcal{X} \\ 0 & \Lambda - \mathcal{L} \end{bmatrix} \begin{bmatrix} \Phi(|\mathbf{x}|)\mathbf{x} \\ \Phi(|\boldsymbol{\xi}|)\boldsymbol{\xi} \end{bmatrix}.$$

We can see that the dynamics of $\boldsymbol{\xi}$ is decoupled from $\mathbf{x}$. Furthermore, since K is diagonal, there is no direct communication between x_i and x_k, where $i, k \in \mathbb{I}_n$ and $i \neq k$. □

5.5 Example: Human Gaits Generator

In this section we demonstrate a design example following Algorithm 1. We obtained human motion data from [GEB20], which contains the kinematic data for the hip joint, knee joint, and ankle joint for both legs during a period of human motion. Here we pick two sets of gait data, one for running at 2.6 m/s, another walking at 1.6 m/s. The original data is shown in Figure 5.6.

Let ω be the frequency of a joint angle $y(t)$. The Fourier coefficients $c_l \in \mathbb{C}, l = 1, 2, \ldots$ for $y(t)$ are obtained using Fast Fourier Transform (FFT) such that

$$y(t) = \sum_{l=1}^{\ell} \Re[c_l \zeta^l],$$

where $\zeta := e^{j\omega t}$. We define the phase of this signal φ by the phase of its first-order coefficient c_1,

$$\varphi := \angle c_1.$$

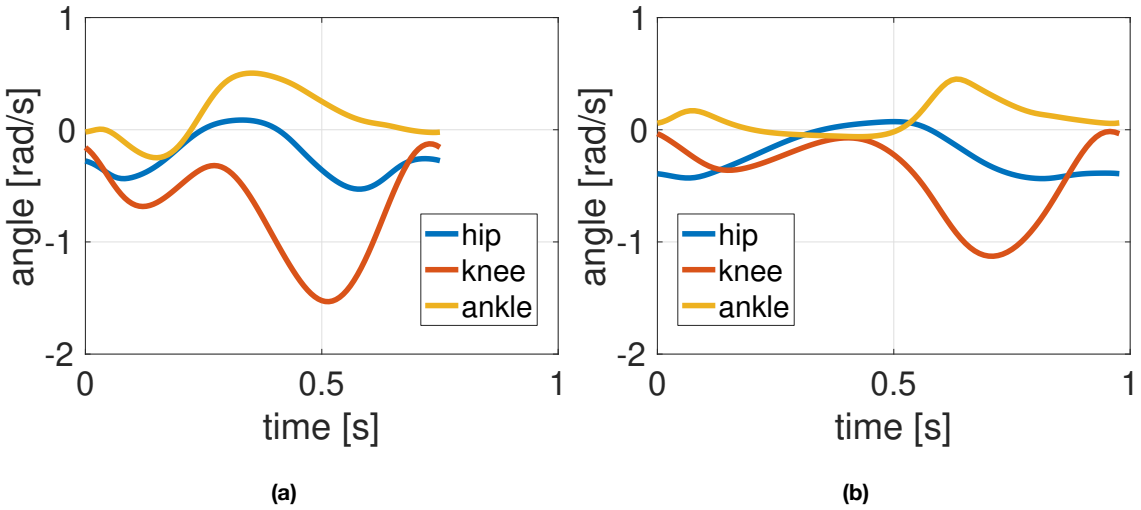

Figure 5.6: Two gaits. (a) running at 2.6 m/s; (b) walking at 1.6 m/s.

Then in order to obtain the coefficients for the signal with zero phase, we scale the coefficients as follows:

$$\tilde{c}_l = c_l(\frac{|c_1|}{c_1})^l.$$

Note that the new first-order coefficient $\tilde{c}_1 = |c_1|$ has zero phase.

Since there are 6 signals of interest, we place 6 segmental oscillators. In each segmental oscillator, the number of auxiliary oscillators is decided by the number of limit cycles (gaits), which is 2. The topology follows the skeleton of human legs. Figure 5.7 illustrates the structure of the oscillator network. The Laplacian associated with the graph in Figure 5.7 is given by

$$L = \begin{pmatrix} 1 & -1 & 0 & 0 & 0 & 0 \\ -1 & 2 & -1 & 0 & 0 & 0 \\ 0 & -1 & 2 & -1 & 0 & 0 \\ 0 & 0 & -1 & 2 & -1 & 0 \\ 0 & 0 & 0 & -1 & 2 & -1 \\ 0 & 0 & 0 & 0 & -1 & 1 \end{pmatrix}.$$

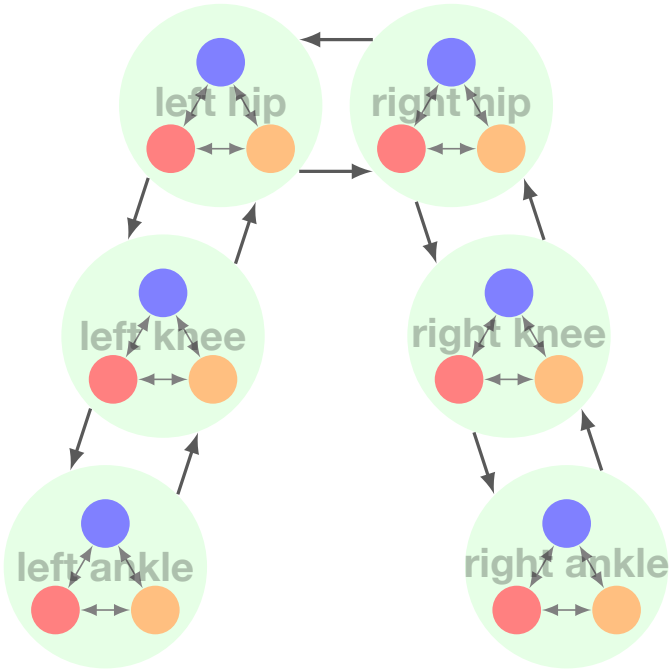

Figure 5.7: The network to produce human motion data.

We set the phase of the segmental oscillator corresponding to the left hip joint to be 0. The phase of other segmental oscillators are the difference between the phase of the corresponding joint and that of the left hip joint. Note that we assume the human leg motion is symmetric between left and right legs, so that the phase of a joint of the right leg is out of phase of the corresponding left joint. The connectivity is designed based on Algorithm 1, where we choose $K_k = -10, J_k = \begin{bmatrix} 1 & 1 \end{bmatrix}^\mathsf{T}$ for all $k \in \mathbb{I}_m$. Figure 5.8 shows the convergence to different gaits starting from different initial condition. For the gait of running at 2.6km/s, $\mathbf{x} := \begin{bmatrix} x_1 & \dots & x_6 \end{bmatrix}^\mathsf{T}$ is illustrated in Figure 5.9.

The transition between two gaits can be achieved by perturbing the state x at some time point. This is demonstrated in Figure 5.10(a). To better show the transition, we inspect the auxiliary oscillators in the first segmental oscillator as shown in Figure 5.10(b).

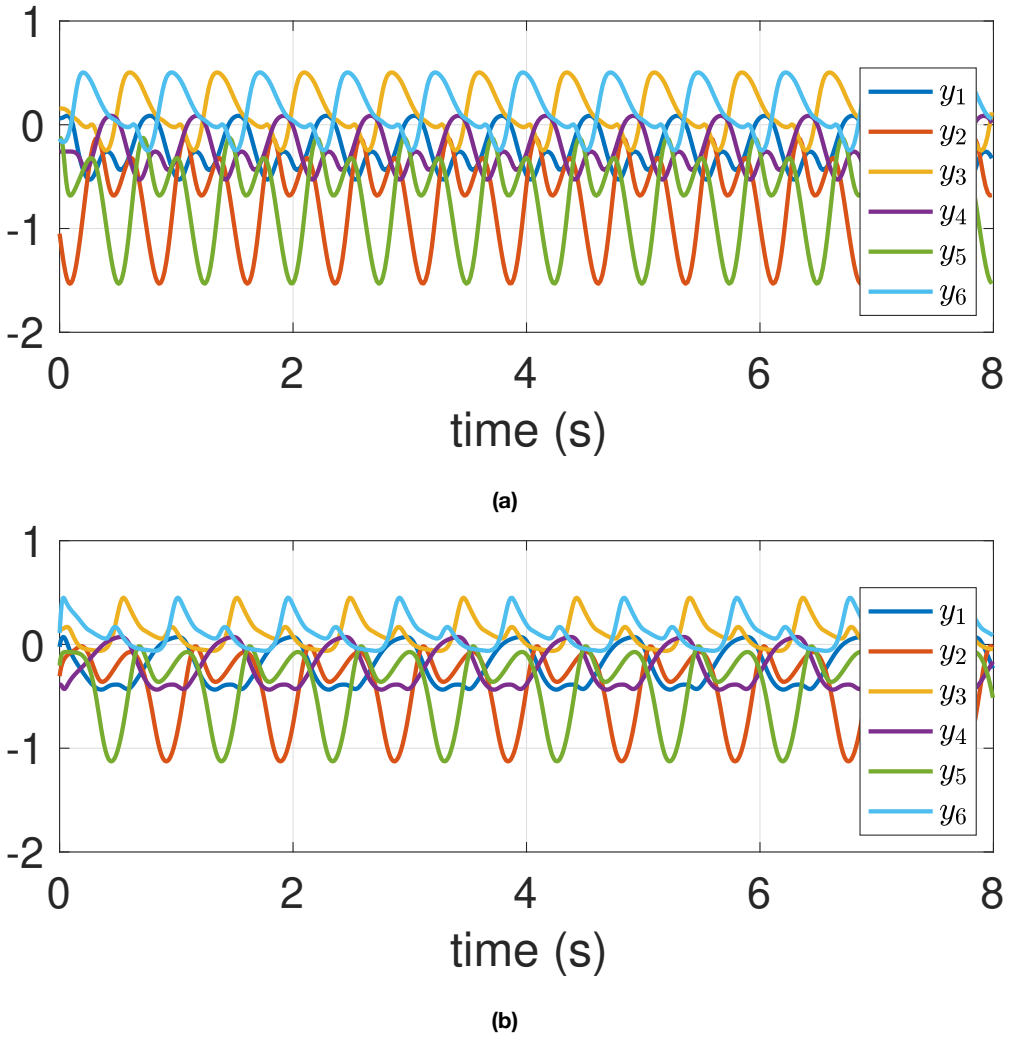

Figure 5.8: Oscillator networks converge to two gaits. (a) running at 2.6 m/s; (b) walking at 1.6 m/s.

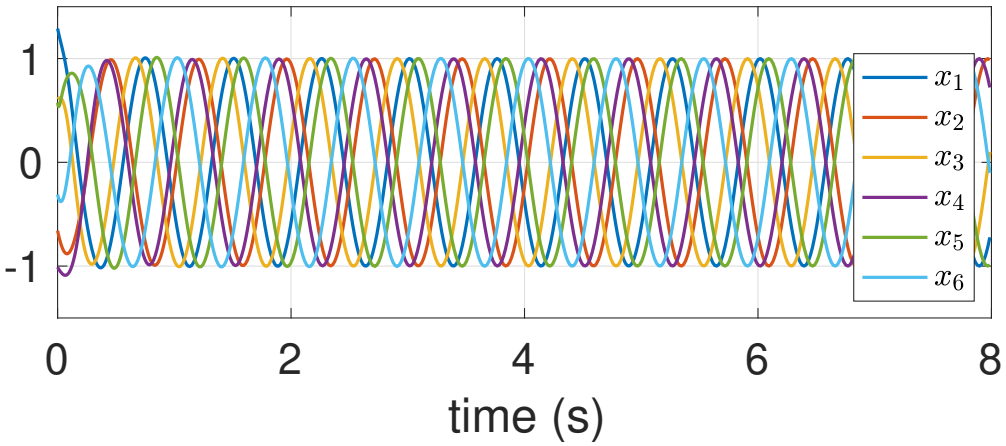

Figure 5.9: $\mathbf{x} := \begin{bmatrix} x_1 & \dots & x_6 \end{bmatrix}^\mathsf{T}$ for the gait of running at 2.6 m/s.

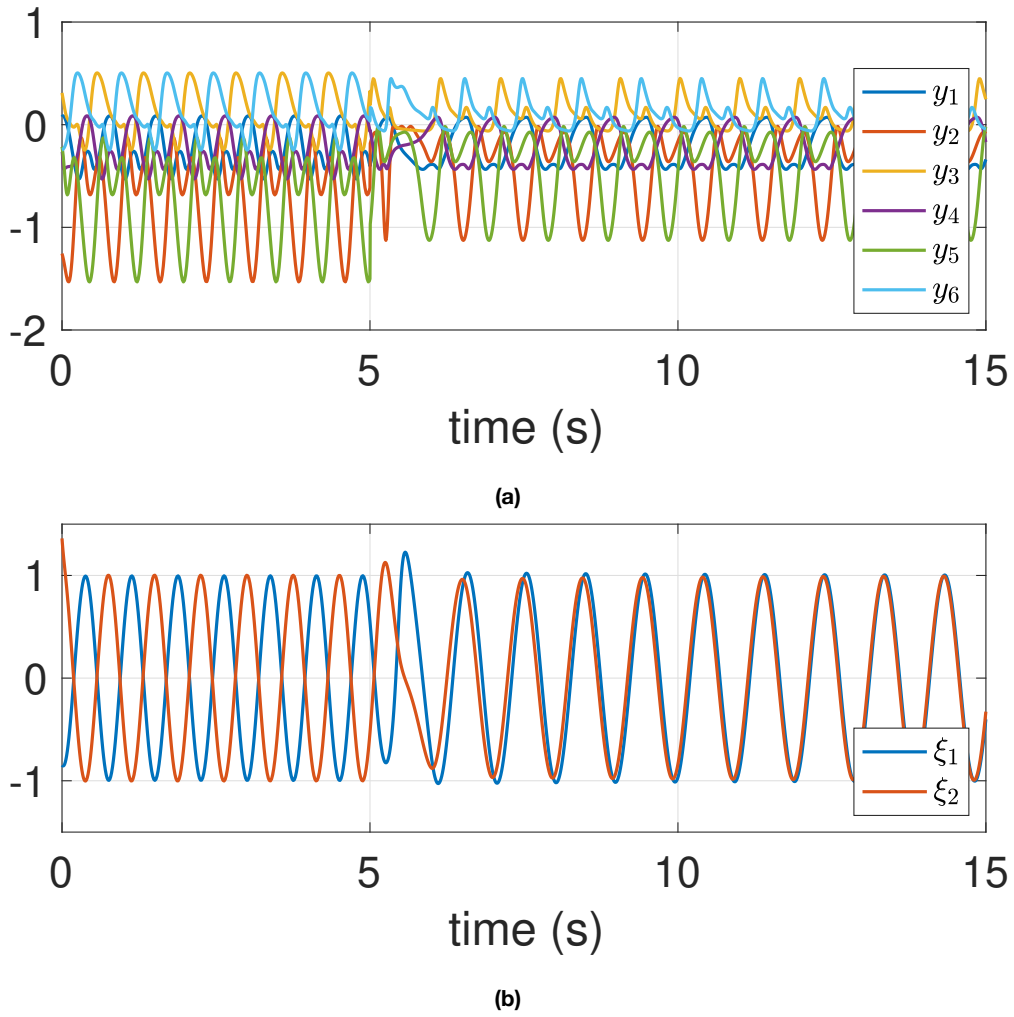

Figure 5.10: The transition between two gaits. (a) the output; (b) the auxiliary oscillators in the first segmental oscillator.

CHAPTER 6

Conclusion

We considered the distributed control synthesis for a class of continuous time, finite dimensional, linear time-invariant systems with local measurements and actuation in Chapter 2. We proposed a controller architecture in which the individual control unit takes partial measurements of the plant and exert on part of the plant, and the control units are interconnected by a strongly connected directed graph. We showed the distributed controller can be parametrized based on a centralized controller and the graph Laplacian so that the input-output mapping converges to that of the centralized controller in the sense of system norms with sufficiently large coupling strength between control units. Likewise, the closed-loop performance with the distributed controller is proved to be arbitrarily close to its centralized counterpart. We then applied our methods to a wide variety of classical control problems including observer, LQG control. Next, we showed how to reduce the communication between control units over network by formulating an iterative convex programming with LMI constraints.

In addition to the application to stabilizing control, we investigated the distributed control for eigenstructure assignment problems in Chapter 3. It was shown that the eigenstructure condition as well as the stability requirement can be met with a finite coupling strength. We proceeded to specialize our result to multi-agent systems with spatially distributed structure and local observability. By exploring the structure of multi-agent systems, we gave an observer based distributed controller for which local observers process local measurements and the information exchange only happens between the internal model of each control unit.

Then, by replacing the internal model by a nonlinear oscillator network, the potential of nonlinear control to achieve pattern formation was illustrated by a numerical example in which the oscillation amplitudes are stabilized.

Inspired by the numerical example with nonlinear oscillator network as the pattern generator, we modeled a network of linearly coupled oscillators in Chapter 4. We first formulated the general design problem of a dynamical system which embeds stable limit cycle(s) with desired attributes, such as frequency, amplitude, and phase. Then we provided an approach to capture the shape of a limit cycle by applying Fourier series on a sinusoidal signal with a frequency of the limit cycle. Next we considered specializing our dynamical system to be a network of coupled oscillators. To that end, we generalized the AHO and propose a nonlinear oscillator with a scalar complex variable z. A condition was derived for the complex oscillator to have a harmonic solution $z = \gamma e^{j\omega t}$ to which local convergence is guaranteed. We have shown how to embed multiple limit cycles into a single complex oscillator with a theoretical guarantee for local orbital stability. The use of the complex state variables makes it easy to produce arbitrary, not necessarily sinusoidal, periodic signals by simply defining the outputs as polynomials with Fourier coefficients. The oscillator contains a static nonlinearity $\phi(|z|)$, and its crossing of the imaginary axis determines the frequency ω and amplitude γ. We then constructed a general network of complex oscillators coupled through a constant interconnection matrix M, and analyzed orbital stability of a targeted limit cycle via linearization around the orbit. We provided a condition on the coupling matrix M and the nonlinearity of the oscillator ϕ such that the oscillator network achieves desired coordination. It was shown that the stability is guaranteed by a property of the eigenvalues of the coupling matrix. Moreover, we showed that multiple stable limit cycles can be embedded in the network of coupled complex oscillators, under a linear independence condition on the target phases, which appears to be generically satisfied. Numerical examples illustrated the single complex oscillator as well as their networks.

In Chapter 5, we considered the network of nonlinearly coupled oscillators with multiple

limit cycles to overcome the limitations of the model in Chapter 4. We first derived the conditions on the stability of single limit cycle to be embedded in the oscillator network, and showed the equivalence between this problem and a synchronization problem. We exploited Floquet theory for local stability and linearization was performed near the desired limit cycle. We gave a necessary and sufficient condition for the stability. Further with some assumptions on the coupling matrix, we also provided some sufficient conditions for these special cases. The results was illustrated by a numerical simulation. We then extended the development to multiple limit cycle case. We started by explaining where the difficulty lies for this case compared to the single limit cycle case, and formulated a coordination problem instead of a synchronization problem. The same linearization technique was applied with respect to every limit cycle. Then we derived the conditions under which every linearized system is stable. Upon this we gave a sufficient condition for the stability of the coupled oscillator network. An example with multiple limit cycles as an application of this theoretical result was demonstrated. We also considered structured design in the event that some topological constraints are imposed on the interconnection of oscillators. We handled this by introducing augmented network with extra oscillators to form coupled segmental oscillators. That is, the network is composed of subsystems each consisting of multiple oscillators. We showed that we were able to achieve the design goal with the augmented network under the presence of the topological constraints. A comprehensive design example was given in the end where we are to reproduce the human locomotion data using our oscillator network. The spatial relationship between the joints of human legs naturally imposes some topological constraints on the connectivity of the oscillators. We showed how we can achieve two different gaits by one oscillator network under the connectivity constraints.

APPENDIX A

Lemmas

Lemma 19. *Let complex matrices A, B, and C be given. Define real matrices $\mathcal{A}$, $\mathcal{B}$, and $\mathcal{C}$ by*

$$\mathcal{A} := \begin{bmatrix} A_R & -A_I \\ A_I & A_R \end{bmatrix}, \quad A_R + jA_I := A, \tag{A.1}$$

and similarly for $\mathcal{B}$ and $\mathcal{C}$. Then

$$AB = C \quad \Leftrightarrow \quad \mathcal{A}\mathcal{B} = \mathcal{C}, \tag{A.2}$$

holds, provided the matrix dimensions are such that the equations are well defined. Moreover,

$$2\ \mathrm{rank}(A) = \mathrm{rank}(\mathcal{A}), \quad \mathrm{eig}(A) \cup \overline{\mathrm{eig}(A)} = \mathrm{eig}(\mathcal{A})$$

hold, where A is assumed square for the latter equality, and $\mathrm{eig}(\cdot)$ denotes the set of eigenvalues. □

Proof. The equivalence (A.2) follows from a direct calculation. Define the function F as the operation to obtain $\mathcal{A}$ from A as in (A.1), i.e. $\mathcal{A} = F(A)$. Consider the case where A is $n \times n$ square and note that, for $\lambda \in \mathbb{C}$ and $v \in \mathbb{C}^n$,

$$Av = \lambda v \quad \Leftrightarrow \quad \mathcal{A}\mathcal{V} = \mathcal{V}\Lambda,$$

where $\mathcal{V} := F(v)$ and $\Lambda := F(\lambda)$ are matrices with two columns. It can readily be verified that the eigenvalues of Λ are λ and $\bar{\lambda}$, and the two columns of matrix $\mathcal{V}$ are linearly independent whenever $v \neq 0$ since $\mathcal{V}^\mathsf{T}\mathcal{V} = \|v\|^2 I$. Hence, $\lambda \in \mathbb{C}$ is an eigenvalue of A if and only if λ and

$\bar{\lambda}$ are eigenvalues of $\mathcal{A}$. To show the rank property, consider the case where the dimensions of A are arbitrary. Noting that $\mathcal{A}^{\mathsf{T}}\mathcal{A} = F(AA)$, we see that the singular values of A are also those of $\mathcal{A}$, repeated twice. Thus, the rank of A is r if and only if the rank of $\mathcal{A}$ is $2r$. ■

Lemma 20. *Given A and $B \in \mathbb{R}^{n\times n}$, let $M(\varepsilon) = A + \varepsilon B$ where $\varepsilon \in \mathbb{R}$. Assume A has a semisimple eigenvalue $\lambda_0 = j\omega, \omega \in \mathbb{R}$ with multiplicity r, i.e., there are nonsingular matrices $X = \begin{bmatrix} X_1 & X_2 \end{bmatrix}, Y = \begin{bmatrix} Y_1 & Y_2 \end{bmatrix} \in \mathbb{C}^{n\times n}$ with $X_1, Y_1 \in \mathbb{C}^{n\times r}$ such that*

$$Y^*AX = \begin{bmatrix} \lambda_0 I_r & 0_{r\times(n-r)} \\ 0_{(n-r)\times r} & A_{22} \end{bmatrix},$$

$$Y^*X = I, \qquad \lambda_0 \notin \operatorname{eig}(A_{22}).$$

Let $\lambda_1(\varepsilon), \ldots, \lambda_r(\varepsilon)$ be continuous functions $\mathbb{R} \mapsto \mathbb{C}$ parametrizing r eigenvalues of $M(\varepsilon)$ with $\lambda_1(0) = \cdots = \lambda_r(0) = \lambda_0$. Then

$$\Re[\lambda_i(\varepsilon)] < 0 \text{ holds when } \varepsilon > 0 \text{ is sufficiently small}$$

for all $i \in \{1, \ldots, r\}$ if and only if

$$\nabla = Y_1^* B X_1$$

is Hurwitz [OW88]. □

REFERENCES

[ADL19] James Anderson, John C Doyle, Steven H Low, and Nikolai Matni. "System level synthesis." *Annual Reviews in Control*, **47**:364–393, 2019.

[BI04a] J. Buchli and A.J. Ijspeert. "Distributed central pattern generator model for robotics application based on phase sensitivity analysis." *BioADIT*, **3141**:333–349, 2004.

[BI04b] J. Buchli and A.J. Ijspeert. "A simple adaptive locomotion toy-system." In *From Animals to Animats 8: Proceedings of the Seventh [i.e. Eighth] International Conference on Simulation of Adaptive Behavior*, volume 8, pp. 153–162. MIT Press, 2004.

[BPD02] Bassam Bamieh, Fernando Paganini, and Munther A Dahleh. "Distributed control of spatially invariant systems." *IEEE Transactions on automatic control*, **47**(7):1091–1107, 2002.

[BRI06] Jonas Buchli, Ludovic Righetti, and Auke Jan Ijspeert. "Engineering entrainment and adaptation in limit cycle systems." *Biological Cybernetics*, **95**(6):645, 2006.

[BTS00] E. Bizzi, M.C. Tresch, P. Saltiel, and A. d'Avella. "New perspectives on spinal motor systems." *Nature reviews. Neuroscience*, **1**(2):101, 2000.

[CHR82] A.H. Cohen, P.J. Holmes, and R.H. Rand. "The nature of the coupling between segmental oscillators of the lamprey spinal generator for locomotion: a mathematical model." *J. Math. Biol.*, **13**:345–369, 1982.

[CW80] A.H. Cohen and P. Wallen. "The neuronal correlate of locomotion in fish: "Fictive swimming" induced in an in vitro preparation of the lamprey spinal cord." *Exp. Brain Res.*, **41**:11–18, 1980.

[DB14] F. Dorfler and F. Bullo. "Synchronization in complex networks of phase oscillators: A survey." *Automatica*, **50**:1539–1564, 2014.

[DBD99] I. Delvolvé, P. Branchereau, R. Dubuc, and J.-M. Cabelguen. "Fictive rhythmic motor patterns induced by NMDA in an in vitro brain stem–spinal cord preparation from an adult urodele." *Journal of Neurophysiology*, **82**(2):1074–1077, 1999.

[DD03] Raffaello D'Andrea and Geir E Dullerud. "Distributed control design for spatially interconnected systems." *IEEE Transactions on automatic control*, **48**(9):1478–1495, 2003.

[DFF00] M.H. Dickinson, C.T. Farley, R.J. Full, M. Koehl, R. Kram, and S. Lehman. "How animals move: an integrative view." *Science*, **288**(5463):100–106, 2000.

[EK84] G.B. Ermentrout and N. Kopell. "Frequency plateaus in a chain of weakly coupled oscillators, I." *SIAM J. Math. Anal.*, **15**(2):215–237, March 1984.

[FHB01] Maryam Fazel, Haitham Hindi, and Stephen P Boyd. "A rank minimization heuristic with application to minimum order system approximation." In *Proceedings of the 2001 American Control Conference.(Cat. No. 01CH37148)*, volume 6, pp. 4734–4739. IEEE, 2001.

[FK99] R.J. Full and D.E. Koditschek. "Templates and anchors: neuromechanical hypotheses of legged locomotion on land." *Journal of Experimental Biology*, **202**(23):3325–3332, 1999.

[GEB20] Martin Grimmer, Ahmed A Elshamanhory, and Philipp Beckerle. "Human lower limb joint biomechanics in daily life activities: a literature based requirement analysis for anthropomorphic robot design." *Frontiers in Robotics and AI*, 2020.

[Gri06] Sten Grillner. "Biological pattern generation: the cellular and computational logic of networks in motion." *Neuron*, **52**(5):751–766, 2006.

[GS03] M. Golubitsky and I. Stewart. *The symmetry perspective: from equilibrium to chaos in phase space and physical space*, volume 200. Springer Science & Business Media, 2003.

[HC94] J. Hauser and C. Chung. "Converse Lyapunov functions for exponentially stable periodic orbits." *Sys. Contr. Lett.*, **23**:27–34, 1994.

[HFK06] P. Holmes, R.J. Full, D. Koditschek, and J. Guckenheimer. "The dynamics of legged locomotion: Models, analyses, and challenges." *Siam Review*, **48**(2):207–304, 2006.

[HGL92] J. Hellgren, S. Grillner, and A. Lansner. "Computer simulation of the segmental neural network generating locomotion in lamprey by using populations of network interneurons." *Biological cybernetics*, **68**(1):1–13, 1992.

[HH52] A.L Hodgkin and A.F. Huxley. "A quantitative description of membrane currents and its application to conduction and excitation in nerve." *J. Physiol.*, **117**(4):500–544, 1952.

[HTI14] S. Hara, H. Tanaka, and T. Iwasaki. "Stability analysis of systems with generalized frequency variables." *IEEE Trans. Auto. Contr.*, **59**(2):313–326, 2014.

[HTW18] Weixin Han, Harry L Trentelman, Zhenhua Wang, and Yi Shen. "A simple approach to distributed observer design for linear systems." *IEEE Transactions on Automatic Control*, **64**(1):329–336, 2018.

[ICF14] T. Iwasaki, J. Chen, and W.O. Friesen. "Biological clockwork underlying adaptive rhythmic movements." *Proc. National Academy of Sciences of USA*, **111**(3):978–983, 2014.

[Ijs08] A.J. Ijspeert. "Central pattern generators for locomotion control in animals and robots: A review." *Neural Networks*, **21**:642–653, 2008.

[IK06] E.M. Izhikevich and Y. Kuramoto. "Weakly coupled oscillators." *Encyclopedia of Mathematical Physics, Elsevier*, **5**:448, 2006.

[Iwa08] T. Iwasaki. "Multivariable harmonic balance for central pattern generators." *Automatica*, **44**(12):4061–4069, 2008.

[Iwa12] T. Iwasaki. "Biological control mechanisms for oscillation and locomotion." *Proc. Chinese Control Conference*, pp. 27–30, 2012.

[IYA03] S. Inagaki, H. Yuasa, and T. Arai. "CPG model for autonomous decentralized multi-legged robot system – generation and transition of oscillation patterns and dynamics of oscillators." *Robotics and Autonomous Systems*, **44**(3-4):171–179, 2003.

[IZ06] T. Iwasaki and M. Zheng. "Sensory feedback mechanism underlying entrainment of central pattern generator to mechanical resonance." *Biological Cybernetics*, **94**(4):245–261, 2006.

[JCF05] W.B. Kristan Jr., R. Calabrese, and W.O. Friesen. "Neuronal control of leech behavior." *Prog. in Neurobiol.*, **76**:279–327, 2005.

[KEW91] N. Kopell, G.B. Ermentrout, and T.L. Williams. "On chains of oscillators forced at one end." *SIAM Journal on Applied Math.*, **51**(5):1397–1417, 1991.

[Kha96] H.K. Khalil. *Nonlinear Systems*. Prentice Hall, 1996.

[KS98] C. Koch and I. Segev. *Methods in Neuronal Modeling: From Ions to Networks*. MIT press, 1998.

[KSC16] Taekyoo Kim, Hyungbo Shim, and Dongil Dan Cho. "Distributed Luenberger observer design." In *2016 IEEE 55th Conference on Decision and Control (CDC)*, pp. 6928–6933. IEEE, 2016.

[KSS10] Hongkeun Kim, Hyungbo Shim, and Jin Heon Seo. "Output consensus of heterogeneous uncertain linear multi-agent systems." *IEEE Transactions on Automatic Control*, **56**(1):200–206, 2010.

[Kur75] Y. Kuramoto. "Self-entrainment of a population of coupled non-linear oscillators." *Int. Sympo. Math. Prob. in Theoretical Physics*, pp. 420–422, 1975.

[LCD04] Cédric Langbort, Ramu Sharat Chandra, and Raffaello D'Andrea. "Distributed control design for systems interconnected over an arbitrary graph." *IEEE Transactions on Automatic Control*, **49**(9):1502–1519, 2004.

[LI17] X. Liu and T. Iwasaki. "Design of coupled harmonic oscillators for synchronization and coordination." *IEEE Trans. Auto. Contr.*, **62**(8):3877–3889, 2017.

[LS98] W. Lohmiller and J.J.E. Slotine. "On contraction analysis for non-linear systems." *Automatica*, **34**(6):683–696, 1998.

[Mat85] K. Matsuoka. "Sustained oscillations generated by mutually inhibiting neurons with adaptation." *Biol. Cybern.*, **52**(6):367–376, 1985.

[Mat87] K. Matsuoka. "Mechanisms of frequency and pattern control in the neural rhythm generators." *Biol. Cybern.*, **56**(5-6):345–353, 1987.

[OM04] R. Olfati-Saber and R. Murray. "Consensus problems in networks of agents with switching topology and time-delays." *IEEE. Trans. Auto. Contr.*, **49**(9):1520–1533, 2004.

[OW88] M.L. Overton and R.S. Womersley. "On minimizing the spectral radius of a nonsymmetric matrix function: Optimality conditions and duality theory." *SIAM J. Matrix Anal. Appl.*, **9**(4):473–498, 1988.

[PC98] L.M. Pecora and T.L. Carroll. "Master stability functions for synchronized coupled systems." *Physical Review Letters*, **80**(10):2109–2112, 1998.

[PN01] A. Pogromsky and H. Nijmeijer. "Cooperative oscillatory behavior of mutually coupled dynamical systems." *IEEE Trans. Circuit and Systems – I: Fundamental Theory and Applications*, **48**(2):152–162, 2001.

[PPS18] Alexey Pavlov, Anton V Proskurnikov, Erik Steur, and Nathan van de Wouw. "Synchronization of networked oscillators under nonlinear integral coupling." *IFAC-PapersOnLine*, **51**(33):56–61, 2018.

[PS07] Q.C. Pham and J.J. Slotine. "Stable concurrent synchronization in dynamic system networks." *Neural Networks*, **20**:62–77, 2007.

[PSN02] Alexander Pogromsky, Giovanni Santoboni, and Henk Nijmeijer. "Partial synchronization: from symmetry towards stability." *Physica D: Nonlinear Phenomena*, **172**(1-4):65–87, 2002.

[RB05] Wei Ren and Randal W Beard. "Consensus seeking in multiagent systems under dynamically changing interaction topologies." *IEEE Transactions on automatic control*, **50**(5):655–661, 2005.

[RBI06] L. Righetti, J. Buchli, and A.J. Ijspeert. "Dynamic Hebbian learning in adaptive frequency oscillators." *Physica D: Nonlinear Phenomena*, **216**(2):269–281, 2006.

[RBM05] W. Ren, R. Beard, and T. McLain. "Coordination variables and consensus building in multiple vehicle systems." *Proceedings of the 2003 Block Island Workshop on Cooperative Control, Lecture Notes in Control and Information Sciences series*, pp. 439–442, 2005.

[Ren08] Wei Ren. "Synchronization of coupled harmonic oscillators with local interaction." *Automatica*, **44**(12):3195–3200, 2008.

[RIa] Kewei Ren and Tetsuya Iwasaki. "Distributed Synthesis of Linear Controllers." (In Preparation).

[RIb] Kewei Ren and Tetsuya Iwasaki. "A Network of Nonlinearly Coupled Oscillators with Multiple Limit Cycles." (In Preparation).

[RI06] L. Righetti and A.J. Ijspeert. "Programmable central pattern generators: an application to biped locomotion control." *IEEE Int. Conf. Robotics and Automation*, pp. 1585–1590, 2006.

[RI18] Kewei Ren and Tetsuya Iwasaki. "Design of Complex Oscillator Network with multiple Limit Cycles." In *2018 IEEE Conference on Decision and Control (CDC)*, pp. 115–120. IEEE, 2018.

[RL05] Michael Rotkowitz and Sanjay Lall. "A characterization of convex problems in decentralized control." *IEEE transactions on Automatic Control*, **50**(12):1984–1996, 2005.

[SAJ13] S Yusef Shafi, Murat Arcak, Mihailo Jovanović, and Andrew K Packard. "Synchronization of diffusively-coupled limit cycle oscillators." *Automatica*, **49**(12):3613–3622, 2013.

[SCS10] K. Seo, S.J. Chung, and J.J.E. Slotine. "CPG-based control of a turtle-like underwater vehicle." *Auton. Robot*, **28**(3):247–269, 2010.

[SH11] Youfeng Su and Jie Huang. "Cooperative output regulation of linear multi-agent systems." *IEEE Transactions on Automatic Control*, **57**(4):1062–1066, 2011.

[SJK90] G. Schöner, W.Y. Jiang, and J.A.S. Kelso. "A synergetic theory of quadrupedal gaits and gait transitions." *Journal of theoretical Biology*, **142**(3):359–391, 1990.

[SM11] Cristina P Santos and Vítor Matos. "Gait transition and modulation in a quadruped robot: A brainstem-like modulation approach." *Robotics and Autonomous Systems*, **59**(9):620–634, 2011.

[SRA16] Georg S Seyboth, Wei Ren, and Frank Allgöwer. "Cooperative control of linear multi-agent systems via distributed output regulation and transient synchronization." *Automatica*, **68**:132–139, 2016.

[SS09] L. Scardovi and R. Sepulchre. "Synchronization in networks of identical linear systems." *Automatica*, **45**:2557–2562, 2009.

[TBL93] HG Traven, L Brodin, A Lansner, O Ekeberg, P Wallén, and S Grillner. "Computer simulations of NMDA and non-NMDA receptor-mediated synaptic drive: sensory and supraspinal modulation of neurons and small networks." *Journal of neurophysiology*, **70**(2):695–709, 1993.

[WI17] A. Wu and T. Iwasaki. "Pattern formation via eigenstructure assignment: General theory and multi-agent applications." *IEEE Trans. Auto. Contr.*, **63**(7):1959–1972, 2017.

[WS05] W. Wang and J.J.E. Slotine. "On partial contraction analysis for coupled nonlinear oscillators." *Biol. Cyb.*, **92**(1):38–53, 2005.

[WSA11] P. Wieland, R. Sepulchre, and F. Allgower. "An internal model principle is necessary and sufficient for linear output synchronization." *Automatica*, **47**:1068–1074, 2011.

[YCC09] Wenwu Yu, Guanrong Chen, Ming Cao, and Jürgen Kurths. "Second-order consensus for multiagent systems with directed topologies and nonlinear dynamics." *IEEE Transactions on Systems, Man, and Cybernetics, Part B (Cybernetics)*, **40**(3):881–891, 2009.

[ZCM15] Lijun Zhu, Zhiyong Chen, and Richard H Middleton. "A general framework for robust output synchronization of heterogeneous nonlinear networked systems." *IEEE Transactions on Automatic Control*, **61**(8):2092–2107, 2015.

[ZFI07] M. Zheng, W.O. Friesen, and T. Iwasaki. "Systems-level modeling of neuronal circuits for leech swimming." *J. Computational Neuroscience*, **22**(1):21–38, 2007.

[ZI17] J. Zhao and T. Iwasaki. "Adaptive natural entrainment via Andronov-Hopf oscillator." *American Contr. Conf.*, pp. 1257–1262, 2017.